TU Delft

Delft University of Technology

Document Version
Final published version

Citation (APA)
Fu, A. (2024). *Self-organizing voltage regulation in the distribution networks: Insights into planning, operation and validation*. [Dissertation (TU Delft), Delft University of Technology]. https://doi.org/10.4233/uuid:0cd87b4b-ec59-4fcc-83aa-fbdda205f95d

Important note
To cite this publication, please use the final published version (if applicable).
Please check the document version above.

Copyright
In case the licence states “Dutch Copyright Act (Article 25fa)”, this publication was made available Green Open Access via the TU Delft Institutional Repository pursuant to Dutch Copyright Act (Article 25fa, the Taverne amendment). This provision does not affect copyright ownership.
Unless copyright is transferred by contract or statute, it remains with the copyright holder.

Sharing and reuse
Other than for strictly personal use, it is not permitted to download, forward or distribute the text or part of it, without the consent of the author(s) and/or copyright holder(s), unless the work is under an open content license such as Creative Commons.

Takedown policy
Please contact us and provide details if you believe this document breaches copyrights.
We will remove access to the work immediately and investigate your claim.

This work is downloaded from Delft University of Technology.

SELF-ORGANIZING VOLTAGE REGULATION IN THE DISTRIBUTION NETWORKS

INSIGHTS INTO PLANNING, OPERATION AND VALIDATION

SELF-ORGANIZING VOLTAGE REGULATION IN THE DISTRIBUTION NETWORKS

INSIGHTS INTO PLANNING, OPERATION AND VALIDATION

Dissertation

for the purpose of obtaining the degree of doctor
at Delft University of Technology,
by the authority of the Rector Magnificus Prof.dr.ir. T.H.J.J. van der Hagen,
Chair of the Board for Doctorates
to be defended publicly on
Tuesday 28 May 2024 at 10:00 o'clock

by

Aihui FU

Master of Science in Electrical Engineering, Shandong University, China
born in Shouguang, China.

The dissertation has been approved by the promotors.

Promotor: Prof. dr. P. Palensky
Copromotor: Dr. M. Cvetković

Composition of the doctoral committee:

Rector Magnificus,	chairperson
Prof. dr. P. Palensky,	Delft University of Technology, promotor
Dr. M. Cvetković,	Delft University of Technology, copromotor

Independent members:

Prof. dr. G. Hug,	Eidgenössische Technische Hochschule
Prof. dr. J.L. Hurink,	University of Twente
Prof. dr. J.E.J. Schmitz,	Delft University of Technology
Prof. dr. J.K. Kok,	Eindhoven University of Technology
Dr. K.N.D. Malamaki,	Independent Power Transmission Operator
Prof. dr. M. Zeman,	Delft University of Technology, Reserve member

This research is financially supported by China Scholarship Council (CSC).

Keywords: Self-organizing voltage regulation, multi-energy system, DRES penetration level, model predictive control, distributed cooperation.

Printed by: Proefschrift Specialist

Cover design by: Aihui Fu

Copyright © 2024 by Aihui Fu

ISBN 978-94-93391-00-0

An electronic version of this dissertation is available at
http://repository.tudelft.nl/.

Enjoy the journey,
not only destination.

Aihui Fu

NOTATION

List of Abbreviations

AC	Alternating Current
ADMM	Alternating Direction Method of Multipliers
AMI	Advanced Metering Infrastructure
ANM	Active Network Management
BESS	Battery Energy Storage System
DCS	Distributed Control System
DD	Dual Decomposition Algorithm
DHI	Diffused Horizontal Irradiance
DNI	Direct Normal Irradiance
DN	Distribution Network
DP	Dynamic Programming
DRES	Distributed Renewable Energy Sources
DSO	Distribution System Operator
ECS	Energy Community System
EMS	Energy Management System
EMT	Electromagnetic Transient
EOA	Evolutionary Optimization Algorithm
EV	Electric Vehicle
GA	Genetic Algorithm
GHI	Global Horizontal Irradiance
HIL	Hardware-In-Loop
HS	Hydrogen System
H2H	Hydrogen Recycling System
H2P	Hydrogen-to-Power System
ICT	Information and Communication Technologies
IED	Intelligent Electronic Device
IEA	The International Energy Agency
IPCC	The International Panel on Climate Change
IRENA	The International Renewable Energy Agency
LP	Linear Programming
LV	Low Voltage
MAS	Multi-Agent System
MINL	Mixed Integer Nonlinear
MPC	Model Predictive Control
MV	Medium Voltage
OPSD	Open Power System Data Platform

P2H2P	Power-to-Hydrogen-to-Power System
P2H	Power-to-Hydrogen System
PCC	Point of Common Coupling
PSO	Particle Swarm Optimization
PV	Photovoltaic
RasPi	Raspberry Pi
RMS	Root Mean Square
SOC	State of Charge
TSO	Transmission System Operator

CONTENTS

SUMMARY

Global energy trends are experiencing a significant shift characterized by a growing movement toward the integration of Distributed Renewable Energy Sources (DRES), such as wind and solar energy, into the power grid. Accelerated by technological advancements and supportive policy initiatives, this transition aims to reduce our reliance on fossil fuels, promote local energy generation, and improve energy security. However, the extensive penetration of DRES into the power grid presents its unique set of challenges.

A big challenge associated with the integration of DRES is their innate intermittency and unpredictability, which induce fluctuations in power availability and demand. Such fluctuations could lead to voltage instability, frequency deviations, and general power quality problems within the power grid. Moreover, the traditional power grid, which is largely unidirectional in design, cannot manage the bidirectional power flow resulting from DRES integration. As a result, ensuring the stability and reliability of the power grid becomes essential with the widespread integration of DRES. Furthermore, incorporating DRES requires innovative grid planning and operation methodologies to optimize resources and prevent potential congestion.

Motivated by these challenges, this thesis develops and implements the method on identifying the main barriers to increasing the integration of DRES in distribution networks (DN) and developing the solution that can enable high DRES penetration levels in power grids, thereby supporting the transition to a future 100% renewable energy system. This thesis provides a solution for three critical phases for future smart power grids: planning, operation, and validation.

Planning phase: The thesis introduces a stochastic simulation-based approach to assess DRES penetration levels and the capacity requirements for the central Battery Energy Storage System (BESS) in DNs while ensuring technical constraints. The stochastic method creates a wide range of scenarios under various conditions. For each scenario, my proposed approach calculates the maximum allowable DRES penetration level and the required BESS capacity with different DRES control logic. The maximum allowable DRES penetration level and the BESS capacity requirements are then determined by analyzing various simulation results. The unique contribution lies in equipping distribution system operators (DSO) with the ability to compare results and select the most appropriate voltage control and power smoothing methods. This helps address the challenges associated with voltage violation and intermittency issues arising from DRES-generated power, thus improving the overall resilience and reliability of the power grid. Moreover, data analysis techniques are utilized to compare the efficacy of various local voltage and BESS control methodologies, offering valuable insights for network planners.

Operation phase (DSO): Building on the foundational knowledge acquired in the planning phase about DRES high penetration level network, a novel algorithm is proposed to achieve optimal voltage regulation through the self-organizing actions of agents. This algorithm empowers distributed agents to coordinate and collaborate in real time

to regulate voltage in DNs with high DRES penetration. The proposed method can minimize the number of agents involved in the voltage regulation and the change of required power for voltage regulation, which together minimizes the need for re-dispatching, i.e., the impact of voltage regulation on the exchange of energy. Moreover, the proposed method performs online optimization, i.e., the value of the decision variable is physically implemented as a controller set-point at each iteration, which reduces the response time. The presented algorithm is benchmarked against the alternating direction method of multipliers (ADMM) algorithm and centralized optimization to validate its efficiency.

Operation phase (Energy community): While coordinating DRES strategies from the grid's viewpoint is vital, it's equally important to consider the energy management of energy communities. I propose a comprehensive four-stage energy management approach that employs receding-horizon optimization to stabilize power fluctuations in a residential energy community system. This system comprises a photovoltaic (PV) installation, a BESS, and a hydrogen system with an electrolyzer, a fuel cell, and a hydrogen storage. This innovative approach uniquely integrates four optimization stages, i.e., yearly, monthly, day-ahead, and intra-day. It blends long-term and short-term optimization techniques in EMS development to utilize hydrogen generated via electrolysis as seasonal storage. The introduced algorithm incorporates three modes with distinct objective functions for enhanced user adaptability. The approach is tested through simulations and operational analysis of an on-site PV–BESS–electrolyzer–fuel cell energy system field lab, including an in-depth analysis of system failure rates, system efficiency evaluation, and performance comparison across different modes of operation.

Validation Phase: To make our research more hands-on and highlight the challenges of DRES, I developed a practical simulation tool named The Illuminator. The Illuminator helps illustrate the challenges of DRES integration, acts as a sandbox for testing new research concepts in real and nonreal time, and allows real-world equipment simulations to check an algorithm before it is fully used. The Illuminator technology is primarily a modular software platform developed on a Raspberry Pi cluster. It is open-source, available on GitHub and developed in Python. The Illuminator comprises models of common energy technologies, such as PV panels, wind turbines, BESS, and hydrogen systems. The uniqueness of The Illuminator is in its modularity and flexibility to reconfigure scenarios and cases on the fly, even by non-experts in a plug-and-play fashion. I introduce The Illuminator and show its performance in two simple case studies.

This research improves the collective understanding of DRES integration by developing practical tools and methodologies that can significantly influence the design and operation of future power grids. Consequently, it paves the way for a cleaner, more efficient, and reliable energy system.

SAMENVATTING

Wereldwijde energietrends ondergaan een significante verschuiving, gekenmerkt door een groeiende beweging naar de integratie van Gedistribueerde Hernieuwbare Energiebronnen (DRES), zoals wind- en zonne-energie, in het elektriciteitsnet. Versneld door technologische vooruitgang en ondersteunende beleidsinitiatieven, streeft deze transitie ernaar om onze afhankelijkheid van fossiele brandstoffen te verminderen, lokale energieopwekking te bevorderen en de energiezekerheid te verbeteren. Echter, de uitgebreide penetratie van DRES in het elektriciteitsnet brengt unieke uitdagingen met zich mee.

Een grote uitdaging die gepaard gaat met de integratie van DRES is hun inherente intermitterendheid en onvoorspelbaarheid, die schommelingen in de beschikbaarheid en vraag van energie veroorzaken. Dergelijke schommelingen kunnen leiden tot spanningsinstabiliteit, frequentieafwijkingen en algemene problemen met de energiekwaliteit binnen het elektriciteitsnet. Bovendien kan het traditionele, voornamelijk unidirectionele ontwerp van het elektriciteitsnet de bidirectionele energiestroom die resulteert uit de integratie van DRES niet beheren. Als gevolg hiervan is het essentieel om de stabiliteit en betrouwbaarheid van het elektriciteitsnet te waarborgen met de wijdverbreide integratie van DRES. Verder vereist het incorporeren van DRES innovatieve netwerkplanning en operationele methodologieën om bronnen te optimaliseren en mogelijke congestie te voorkomen.

Gemotiveerd door deze uitdagingen, ontwikkelt en implementeert deze scriptie de methode voor het identificeren van de belangrijkste belemmeringen voor het verhogen van de integratie van DRES in distributienetwerken (DN) en het ontwikkelen van de oplossing die hoge penetratieniveaus van DRES in elektriciteitsnetten mogelijk kan maken, ter ondersteuning van de overgang naar een toekomstig 100% hernieuwbaar energiesysteem. Deze scriptie biedt een oplossing voor drie kritieke fasen voor toekomstige slimme elektriciteitsnetten: planning, operatie en validatie.

Planningsfase: De scriptie introduceert een op stochastische simulatie gebaseerde aanpak om de penetratieniveaus van DRES en de capaciteitsvereisten voor het centrale Batterij Energie Opslagsysteem (BESS) in DN's te beoordelen, waarbij technische beperkingen worden gewaarborgd. De stochastische methode creëert een breed scala aan scenario's onder verschillende omstandigheden. Voor elk scenario berekent mijn voorgestelde aanpak het maximaal toelaatbare penetratieniveau van DRES en de benodigde BESS-capaciteit met verschillende DRES-regellogica. Het maximaal toelaatbare penetratieniveau van DRES en de BESS-capaciteitsvereisten worden vervolgens bepaald door verschillende simulatieresultaten te analyseren. De unieke bijdrage ligt in het uitrusten van distributiesysteembeheerders (DSO) met de mogelijkheid om resultaten te vergelijken en de meest geschikte methoden voor spanningsregeling en vermogensafvlakking te selecteren. Dit helpt de uitdagingen aan te pakken die samenhangen met spanningsinbreuken en intermitterendheidsproblemen die voortkomen uit door DRES opgewekte

energie, waardoor de algehele veerkracht en betrouwbaarheid van het elektriciteitsnet wordt verbeterd. Bovendien worden data-analysetechnieken gebruikt om de effectiviteit van verschillende lokale spannings- en BESS-regelmethodologieën te vergelijken, wat waardevolle inzichten biedt voor netwerkplanners.

Operationele fase (DSO): Voortbouwend op de fundamentele kennis verworven in de planningsfase over netwerken met een hoog penetratieniveau van DRES, wordt een nieuw algoritme voorgesteld om optimale spanningsregulatie te bereiken door de zelforganiserende acties van agenten. Dit algoritme stelt gedistribueerde agenten in staat om in real-time samen te werken en samen te werken om de spanning in DN's met hoge DRES-penetratie te reguleren. De voorgestelde methode kan het aantal agenten dat betrokken is bij de spanningsregulatie minimaliseren en de verandering van de vereiste energie voor spanningsregulatie minimaliseren, wat samen de noodzaak voor herdispatch, d.w.z. de impact van spanningsregulatie op de energie-uitwisseling, minimaliseert. Bovendien voert de voorgestelde methode online optimalisatie uit, d.w.z. de waarde van de beslissingsvariabele wordt fysiek geïmplementeerd als een controller set-point bij elke iteratie, wat de responstijd vermindert. Het gepresenteerde algoritme wordt vergeleken met het algoritme voor afwisselende richtingsmethode van vermenigvuldigers (ADMM) en gecentraliseerde optimalisatie om zijn efficiëntie te valideren.

Operationele fase (Energiegemeenschap): Terwijl het coördineren van DRES strategieën vanuit het perspectief van het net essentieel is, is het even belangrijk om het energiebeheer van energiegemeenschappen te overwegen. Ik stel een uitgebreide vierfasige energiebeheerbenadering voor die terugwijkende-horizonoptimalisatie gebruikt om vermogensschommelingen in een residentieel energiegemeenschapssysteem te stabiliseren. Dit systeem omvat een fotovoltaïsche (PV) installatie, een BESS en een waterstofsysteem met een elektrolyzer, een brandstofcel en een waterstofopslag. Deze innovatieve aanpak integreert op unieke wijze vier optimalisatiefasen, d.w.z. jaarlijks, maandelijks, dag vooruit en intra-dag. Het combineert langetermijn- en kortetermijnoptimalisatietechnieken in EMS-ontwikkeling om waterstof geproduceerd via elektrolyse als seizoensopslag te gebruiken. Het geïntroduceerde algoritme omvat drie modi met verschillende doelfuncties voor verbeterde gebruikersaanpasbaarheid. De aanpak wordt getest door simulaties en operationele analyse van een ter plaatse PV-BESS-elektrolyzer-brandstofcelsysteem veldlab, inclusief een diepgaande analyse van systeemfoutpercentages, systeemefficiëntie-evaluatie en prestatievergelijking over verschillende modi van operatie.

Validatiefase: Om ons onderzoek praktischer te maken en de uitdagingen van DRES te benadrukken, heb ik een praktisch simulatiehulpmiddel ontwikkeld genaamd The Illuminator. The Illuminator helpt de uitdagingen van DRES-integratie te illustreren, fungeert als een sandbox voor het testen van nieuwe onderzoeksconcepten in real-time en niet-real-time, en laat real-world apparatuursimulaties toe om een algoritme te controleren voordat het volledig wordt gebruikt. The Illuminator-technologie is voornamelijk een modulair softwareplatform ontwikkeld op een Raspberry Pi-cluster. Het is open-source, beschikbaar op GitHub en ontwikkeld in Python. The Illuminator bestaat uit modellen van gangbare energietechnologieën, zoals PV-panelen, windturbines, BESS en waterstofsystemen. De uniciteit van The Illuminator ligt in zijn modulariteit en flexibiliteit om scenario's en gevallen on-the-fly te herconfigureren, zelfs door niet-experts

op een plug-and-play-manier. Ik introduceer The Illuminator en toon zijn prestaties in twee eenvoudige casestudy's.

1

INTRODUCTION

This introductory section provides a comprehensive overview of the research background, questions, and methodologies employed in this thesis. Energy systems worldwide are transitioning from fossil-based to renewable sources to combat climate change and ensure sustainable energy futures. This positions electricity as the dominant energy source in energy sectors. However, the integration of renewable sources has led to pressing issues in grid stability, particularly in systems with high levels of distributed renewable energy sources (DRES) penetration. For instance, in the Netherlands, rapid DRES adoption has strained the existing grid infrastructure, leading to operational challenges and necessitating substantial upgrades. Therefore, This thesis aims to identify the main barriers to increasing the integration of DRES in DNs and develop and verify solutions that enable high DRES penetration levels in power grids, thereby supporting the transition to a 100% renewable energy future. This chapter introduces the research questions that steer the project and the approaches and contributions made by the study. To aid readers in navigating this thesis, the final segment of this chapter outlines the structure and discusses the content of each subsequent chapter comprehensively.

1

1.1. RENEWABLE ENERGY INTEGRATION BACKGROUND AND CHALLENGES

Fossil fuels have long been the backbone of our energy landscape, but their extensive environmental impacts, particularly significant greenhouse gas emissions contributing to climate change, make them increasingly unsustainable [1, 2]. Consequently, a global shift towards sustainable and climate-resilient energy systems has become crucial. To support this transition, the International Energy Agency (IEA) has developed a detailed roadmap outlining key milestones for the global energy sector's progress toward achieving net-zero greenhouse gas emissions [3]. This roadmap forecasts a pivotal change in how we produce and consume energy, highlighting electricity as the main energy source to decrease reliance on fossil fuels. It sets an ambitious annual target of adding 1,020 GW of new electricity generation capacity from solar and wind sources by 2050. This initiative will significantly boost the proportion of renewable energy in the global energy mix. According to the roadmap, electricity is expected to represent nearly 50% of total energy consumption by 2050 [4]. In line with the goals of the Paris Agreement, which seeks to limit global warming to a maximum of 1.5 degrees Celsius above preindustrial levels, the International Renewable Energy Agency (IRENA) asserts that renewable energy should make up 90% of all energy production by 2050 [5], demanding a greater share of renewable sources. The Intergovernmental Panel on Climate Change (IPCC) also highlights the urgent need to quickly move towards distributed renewable energy sources (DRES) such as solar, wind, and green hydrogen, to lessen the severe effects of climate change and safeguard our planet for future generations [6]. Therefore, the global energy transition is focused on moving from fossil fuels to renewable energy, which is crucial for creating a sustainable energy future and enhancing resilience against climate change.

Integrating a large amount of Distributed Renewable Energy Sources (DRES) into the power grid poses significant challenges, mainly due to their variability and intermittency. Solar and wind power, for instance, heavily depend on weather conditions, which makes their energy output less predictable than that from traditional sources like coal, natural gas, or nuclear plants [7]. This unpredictability often results in a mismatch between electricity supply and demand. For example, excess electricity generated by DRES during low demand can lead to an oversupply if there aren't adequate storage solutions or demand response strategies in place. On the other hand, when there is not enough generation from DRES, the grid must depend on fossil fuels to meet the shortfall. The key challenges of high DRES penetration in the power grid include maintaining voltage regulation, controlling frequency, and managing increased complexity in operation and planning [8]. To address these issues, enhancements in grid flexibility are essential. This can involve the use of technologies such as batteries, demand response systems, hydrogen-based fuels, and hydropower. Moreover, renewable energy sources are typically installed at various, often remote, geographic locations and contribute to bidirectional power flows, which can strain the existing grid infrastructure [9]. Therefore, it is necessary to upgrade the grid to manage these flows and incorporate advanced monitoring and control technologies to integrate higher DRES penetration in the future power grid.

The Netherlands has been at the forefront of renewable energy adoption, with am-

bitious goals to increase the share of clean energy in its energy portfolio. However, the rapid integration of DRES has presented significant challenges to the Dutch power grid. Since 2021, cities such as Lelystad and Leeuwarden have faced difficulties accommodating additional renewable energy sources due to existing grid infrastructure constraints, leading to areas without the available capacity for electricity feed-in. These areas are highlighted in Figure 1.1, where the map shows areas of congestion investigated by the Transmission System Operator (TSO) in black shading. Areas shaded red indicate regions that, despite the use of congestion management, are unable to accommodate additional DRES. As of August 2023, there are only limited gray areas without any restrictions. To maintain the reliability of the power system and ensure a consistent electricity supply for consumers while continuing to support the integration of renewable energy, Alliander, one of the largest Dutch distribution system operators (DSO), has announced that more than 30% of the power grid in the Netherlands requires substantial upgrades and modifications [10], blocking the greater integration of renewable energy into existing power systems.

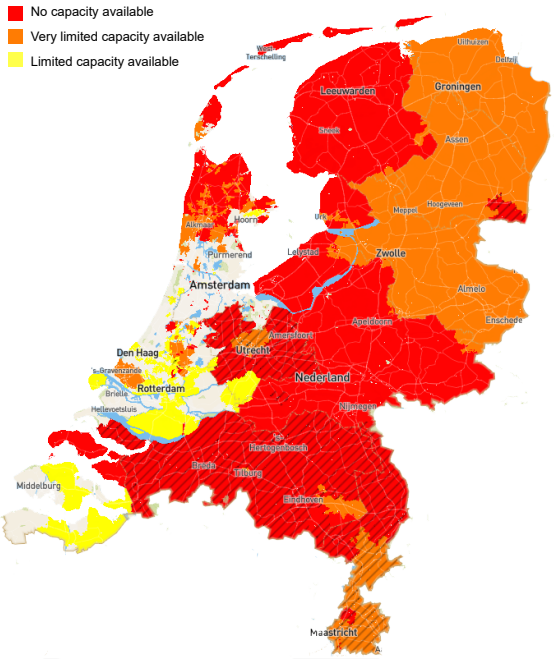

Figure 1.1: Available capacity for electricity feed-in in The Netherlands in August 2023 [11]

The adoption of DRES is pivotal for achieving a sustainable future energy system. As we transition towards a grid increasingly powered by renewable energy, it becomes crucial to address challenges such as the inherent variability and intermittency of DRES. Central to addressing these challenges is to advance the smart grid technology that not only adapts but also excels with high levels of DRES integration, without compromising

stability and reliability. This research aims to identify and address significant barriers to the integration of DRES in distribution networks (DN), and to enhance the level of DRES penetration. The main objectives of this study are outlined as follows:

Identifying the main barriers to increasing the integration of DRES in DNs and developing and verifying solutions that enable high DRES penetration levels in power grids, thereby supporting the transition to a future 100% renewable energy system.

1.2. RESEARCH SCOPE AND QUESTIONS

Integrating high penetration levels of DRES into power grids is essential for a sustainable energy transition. Yet, the inherent constraints of the technical limitations of power grids can pose challenges in accommodating as much renewable energy as desired [12]. The acceptable DRES penetration level for a power grid depends on various factors, including the existing infrastructure, load profile, renewable energy resource availability, etc [13]. The situation for each DN varies, making it essential to find a general method to identify the maximum DRES penetration level and the main factors limiting the DRES penetration level. On the one hand, DSOs face an urgent and pressing challenge: developing reliable methods and metrics to determine the feasibility and extent of integrating additional DRES into a network. This requires a detailed analysis of current infrastructures and their potential to handle increasing renewable energy sources without preserving the stability and reliability of the grid. Conversely, it's equally crucial to delve into and tackle the core challenges that limit DRES integration levels. DSO must identify the primary barriers to DRES integration and formulate effective solutions. These are crucial to integrating high DRES into the power grid to achieve a high-renewable energy landscape. Consequently, the first research question is

Q1: How to integrate a large amount of DRES into DNs?

This research question can be further divided into sub-questions:

1. What is the acceptable DRES penetration for a specific DN?
2. What are the main issues limiting the DRES penetration level?
3. How can we effectively deal with DRES-generated power fluctuations to ensure grid stability and reliability?

By addressing these research questions, this study aims to comprehensively understand the challenges and solutions associated with integrating high levels of renewable energy into power grids, ultimately contributing to a more sustainable and resilient energy future. DRES results in power injections that can raise voltages both locally and at nearby nodes. Considering that traditional networks typically measure voltage solely at secondary substations and considering the fluctuating and unpredictable nature of DRES, the increasing penetration of DRES raises voltage regulation challenges in DNs. This voltage regulation challenge is a direct barrier to increasing the integration of DRES [14]. According to the research of Gabdullin et al. [15], a 20% penetration of photovoltaic (PV) systems in residential grids will lead to voltage issues. Furthermore, the growing

popularity of electric vehicles (EV) in residential and commercial networks will aggravate voltage problems if peak demand is not adequately managed [16]. A One-day voltage profile of a radial DN with 18 nodes is shown in Figure 1.2, with one line representing one node. Different feeders radiate from a substation or a generating station in the radial DN and feed the distributors at one end. The voltage is expressed per unit, which denotes the deviation from the nominal values where one is nominal, and the typical tolerance limits to the voltage are marked by ±5% from the nominal [17]. In the DN operating without DRES, voltage drop is typically the primary concern. With the integration of EVs and DRES into the grid, voltage drop problems become more pronounced, and DNs also experience voltage increases, especially at noon when PV power generation peaks. Consequently, as the penetration level of PVs and EVs increase, DNs will face more significant challenges related to voltage rise during the day, voltage drop at night, and voltage deviations on cloudy days.

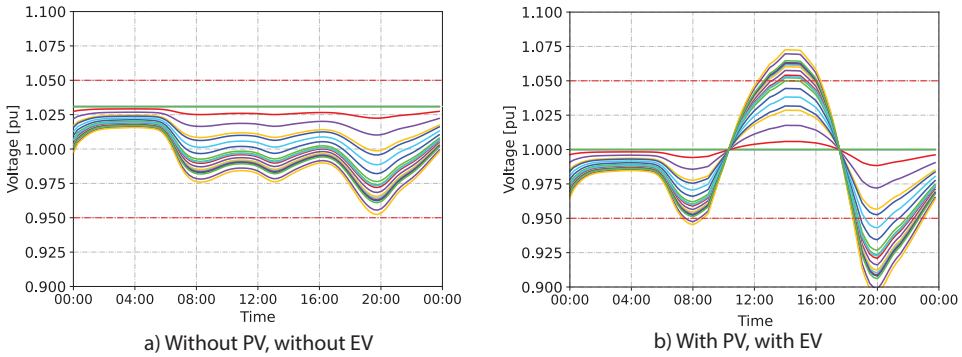

Figure 1.2: One-day voltage profile of DN with 18 nodes

PV power curtailment is a common solution to prevent over-voltage, but it results in losing cost-effective and clean renewable energy. In Germany, for example, residential PV systems must reduce their output to a fixed value (30% of their nominal capacity) when they generate excessive power [18]. However, increasing curtailment reduces the economic and environmental benefits of PV installations. DSOs must adapt to accommodate the growing PV penetration and maximize its advantages. These discussions highlight the need for control algorithms at the distribution level and DRES connection points. Furthermore, the power electronic components of DRES can contribute to voltage regulation in distributed networks. The IEEE 1547 standard has defined Q(V) and Q(P) modes [19], and the German grid code requires PV inverters to provide reactive power using the Q(P) mode [20]. Australian standards for PV grid-connected inverters (AS4777) specify their response to high or low grid voltages [21]. However, local voltage regulation methods tested in research question Q1 are insufficient to address future grids' voltage challenges. The installation of new infrastructures, such as batteries, introduces additional complexity to grid management, requiring sophisticated control algorithms and coordination between different grid components. Moreover, a new regu-

latory framework should be developed to address voltage issues. The intelligent voltage control approach can use the DRES and traditional voltage regulation devices to do the voltage regulation and make them cooperate with each other. In this thesis, the term "agent" is used to describe a voltage regulation resource provider, and its structure is illustrated in Figure 1.3. An agent comprises a combination of energy assets or devices connected at the same node within the power grid, including wind farms, PV systems, or energy storage systems. Each agent can tackle the unpredictability and variability of the primary energy sources via proper power smoothing control. Each agent is tasked with managing the energy distribution among its assets and providing the necessary active or reactive power to regulate voltage levels. By utilizing the capabilities of each agent, this approach aims to address the shortcomings of conventional local voltage regulation methods, thereby facilitating higher penetration of DRES in DNs. This leads to the formulation of the second research question.

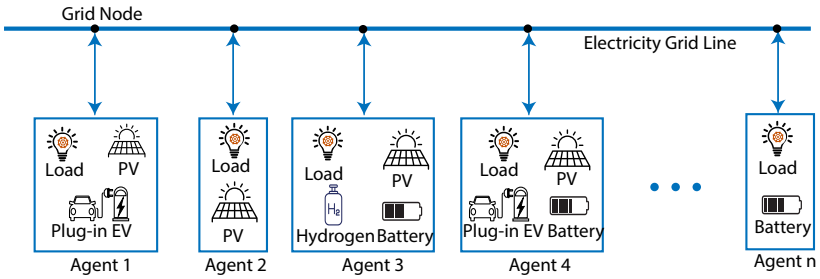

Figure 1.3: The structure of the voltage regulation resources provider

Q2: How can voltage regulation in future DNs be effectively managed to accommodate the increasing DRES penetration levels from the DSO side?

This research question can be further divided into sub-questions:

1. What is the distributed voltage control architecture, and how can it be conceptualized?

2. How can advanced control strategies be designed and integrated to achieve self-organizing voltage regulation in DNs with high penetration of DRES?

The research question Q2 can coordinate DRES strategies from the viewpoint of the grid operator, which is vital. However, It is also important to consider the energy management of energy communities. With the development of modern information and communication technologies (ICT) and the advanced metering infrastructure (AMI), new opportunities have been created to operate the power grid by controlling and accommodating the DRES. There has been a shift in the role of energy consumers from passive consumers to active participants in the energy system. This has been made possible by adopting smart grid concepts [22], which have transformed consumers into "prosumers" who actively engage in energy exchange mechanisms. For instance, the

UK has been working on Active Network Management (ANM) to increase renewable energy capacity [23]. In addition, DSOs are willing to provide incentives to consumers with DRES to become prosumers and provide ancillary services [24, 25]. To do so, prosumers are required to take an active role in controlling the output of their available DRES and setting consumption patterns, which means the prosumer should have an energy management system (EMS) that can dispatch its energy consumption and production. EMS gives prosumers greater control over their energy consumption, enabling them to make informed decisions and participate actively in grid operations. EMS can facilitate demand response strategies for the grid by adjusting energy consumption in response to grid conditions and price signals. This flexibility helps stabilize the grid and reduces the need for costly infrastructure investments or additional generation capacity. By actively managing local energy consumption and generation, local EMS can alleviate stress on the grid and maintain stability during periods of high demand or when faced with supply constraints. This reduces the risk of blackouts and enhances grid reliability. For the energy transition, local EMS can manage and optimize the operation of DRES, such as PV panels, wind turbines, and energy storage systems, ensuring efficient and reliable integration into the grid. The third research question emerges:

Q3: How to develop an EMS for energy communities that optimally synchronizes energy consumption and generation, facilitating self-organizing voltage regulation?

This research question can be further divided into the following sub-questions:

1. How can the EMS system be designed to enable seamless integration with various DRES?
2. How can the EMS algorithm be adapted for use by multiple agents in a power grid to achieve self-organizing voltage regulation?
3. How can the reliability of the self-organizing voltage regulation method be evaluated based on the performance of the EMS algorithms in the agents?

By answering the first three research questions, the penetration level of DRES can significantly increase. Although these methods can be tested through simulation and case studies, the on-site deployment of an algorithm requires real-time simulations to verify their validity and reliability. This initial step is crucial to identify potential pitfalls and unexpected issues that might arise when the algorithms are implemented in real-world DNs. Simulation insights are pivotal in optimizing the algorithms and proactively formulating solutions to anticipated complications.

It is also important to note that simulating certain infrastructures can be particularly challenging. In such cases, integrating actual hardware with digital simulations is crucial, leading to a method known as "hardware-in-the-loop (HIL)". This approach allows researchers and practitioners to more accurately reproduce real-world conditions by blending the physical properties of hardware with the flexibility and control of a digitally simulated environment. The hybrid approach enhances the reliability of simulations and accelerates the field implementation of algorithms, facilitating a smooth transition from digital test beds to real-world applications.

This discussion leads to the formulation of the fourth research question, which is central to enabling the practical application of intelligent grid control algorithms:

Q4: How can a flexible and extendable kit be developed to enable intelligent grid control algorithms from digital test fields to real-world applications?

This research question can be further divided into the following sub-questions:

1. What are the key components and architectural considerations required for developing a flexible and extendable energy system integration development kit?
2. What software and hardware tools are necessary to enable seamless integration and HIL testing within the development kit?
3. What steps are necessary to build an environment for testing intelligent grid control algorithms with flexibility and scalability?
4. How can the development kit be accessible to researchers and engineers with varying levels of expertise in power systems and simulation technologies?
5. How to manage time synchronization and interactions across the integrated energy assets?

Addressing this question will enable the effective testing of novel algorithms on large-scale grid operations and facilitate the practical application of developed algorithms to control physical assets.

Addressing these four research questions can provide valuable insights into the technical and regulatory challenges associated with the integration of high levels of DRES into power grids. The development of the solution includes the planning phase, the operation phase for the DSO and energy community, and the validation phase. They will contribute to overcoming these challenges and promoting a more sustainable and resilient energy future. By enhancing our collective understanding of DRES integration and developing practical tools and technologies, this research holds the potential to significantly influence the design and operation of future power grids, paving the way for a cleaner, more efficient, and more reliable energy system.

1.3. RESEARCH APPROACH

The output of renewable energy sources such as wind and PVs is inherently variable and depends on the weather conditions and the time of day. Power grids with a high penetration of DRES are subject to various sources of uncertainty, such as fluctuations in renewable energy generation, varying load profiles, and equipment failures. To address the research question Q1 and efficiently handle the uncertainties, variability, and complexities associated with DRES integration in DNs, the stochastic simulation-based approach is used by simulating multiple scenarios with different renewable generation profiles, allowing for a more comprehensive assessment of the performance of the system. Moreover, exploring a wide range of scenarios can lead to a better understanding of the limitations and challenges associated with DRES integration in DNs. The central Battery

Energy Storage System (BESS) is commonly employed to mitigate power fluctuations in upstream DNs [26]. I also use a stochastic simulation-based approach to determine the required installed capacity for BESS. A large number of scenarios with varying load and generation profiles are created to identify the most suitable BESS installed capacity for power smoothing. By analyzing these scenarios, this thesis evaluates the performance of different central BESS capacities. It selects the optimal size to ensure reliable and efficient DN operation, particularly in the presence of high penetration of DRES. These insights can be used to inform decision-making processes regarding the planning, design, and operation of future DNs, ensuring that they can accommodate increasing levels of renewable energy while maintaining system stability and reliability. To use the stochastic simulation-based method for solving research question Q1, the following steps can be followed:

Modeling the DN: Develop a detailed model of the DN under study, including components such as transformers, lines, loads, and DRES units. This model serves as the basis for simulation and analysis.

Stochastic generation of scenarios: Use random sampling techniques to generate multiple scenarios based on the probability distributions defined for the input parameters. Each scenario represents a possible realization of the system's behavior under different conditions.

Conducting simulations: For each generated scenario, perform a simulation using the DN model to analyze the system performance with different DRES penetration levels.

Simulation data analysis: Analyze the simulation results from various scenarios to identify trends, patterns, and relationships between DRES penetration levels and system performance, which solves sub-question 2. This analysis determines the optimal DRES penetration level for the given DN and the required central BESS capacity for power smoothing, solving sub-questions 1 and 3.

The development of monitoring and communication infrastructure has played a crucial role in the evolution of voltage regulation strategies. With the growth of DRES and flexible demand, there is an increasing need for efficient methods to coordinate various devices and manage voltage levels across the network. While centralized control approaches offer the advantage of providing optimal control instructions to different agents by having access to all information within the network [27, 28], they are not feasible to implement in complex DNs due to the challenges of data acquisition from all agents, information exchange between the central operator and controlled devices, and ensuring complete supervisory control to all agents. Additionally, the issue of time delays can arise as the central operator is responsible for receiving messages, conducting computations, and sending messages at each control time step [29]. If the central controller experiences any issues, the entire system is at risk of breakdown.

In contrast, distributed control methods are able to adapt to changes in network conditions and function without a centralized control unit. Thus, it can enable effective management of voltage levels in complex networks with multiple assets. In a distributed control system (DCS), each controllable node operates autonomously and is responsible for a subset of the overall control tasks, which can provide more efficient and robust control of complex systems [30]. The agents exchange the information with their neighborhood agents to achieve global voltage regulation. This bottom-up approach based on

multi-agent systems offers a novel perspective for resolving the voltage problem through self-organizing mechanisms.

Applying the distributed control method for voltage regulation to address the research question Q2 involves the following steps:

Designing a distributed control architecture: Develop a control architecture that allows each control node or agent to operate autonomously and to be responsible for a subset of the overall control tasks. This architecture should facilitate information exchange between neighboring agents to achieve global voltage regulation.

Algorithm for coordinating individual control actions: Ensure that individual agent control actions are coordinated to achieve the desired global voltage regulation. This coordination can be achieved through communication and information sharing between neighboring agents, allowing them to adjust their control actions based on the overall system state.

Monitoring and adapting the control strategy: Continuously monitor the performance of the distributed voltage regulation system and adapt the control strategy as needed. This may involve updating local control algorithms, communication protocols, or control node configurations to address changes in network conditions, such as load growth or increased renewable generation.

To achieve smart grid transition, intelligent control of the energy community is also essential, related to research question Q3. Numerous algorithms have been proposed for energy management, each possessing unique strengths and weaknesses. Techniques such as Linear Programming (LP) and Mixed-Integer Linear Programming (MILP) are widely employed but often grapple with uncertainties and non-linearities [31]. Dynamic Programming (DP) can effectively address complex dynamics, yet its efficiency is hampered by the "curse of dimensionality" in large-scale applications [32]. Evolutionary optimization algorithms (EOA), including Genetic Algorithms (GA) and Particle Swarm Optimization (PSO), excel at exploring solution spaces but encounter difficulties with constraints and uncertainties [33, 34]. Machine learning and AI-based techniques, such as Fuzzy Logic Control, Artificial Neural Networks, and Reinforcement Learning, can manage uncertainties and complex dynamics. However, they require significant computational resources and data that may not be readily available [35, 36].

Model Predictive Control (MPC) is suitable for local EMS applications for several reasons. First, MPC can handle constraints and uncertainties, making it highly applicable to local energy systems with fluctuating generation and demand profiles [37]. Second, MPC employs an adaptive and responsive control strategy using real-time measurements and mathematical models, which is crucial for local EMS where energy profiles can change rapidly [38]. Finally, the successful application of MPC in various aspects of EMS, such as demand response, integration of renewable energy, and energy storage management, demonstrates its versatility and effectiveness in managing complex energy systems. Consequently, this thesis employs MPC and seeks to enhance its capabilities. The following steps outline the process for implementing MPC in an EMS and testing the self-organizing voltage regulation performance:

Define the optimization function: Establish the objectives of the EMS, typically involving cost minimization, efficiency maximization, or maintaining a certain level of system performance. Formulate an optimization function that incorporates these ob-

jectives while considering the constraints the system must adhere to, such as generation limits, storage capacities, and grid constraints.

Determine prediction and control horizons: The prediction horizon is the time window over which the future behavior of the system is predicted and optimized, while the control horizon is the time window over which control actions can be applied. A longer prediction horizon allows for better planning and decision-making but increases computational complexity. The control horizon should be chosen based on the desired responsiveness and flexibility of the EMS.

Propose advanced improvements: Suggest enhancements to the MPC approach, making it suitable for various time-scale assets, and adapt it to diverse conditions within the energy system.

Evaluate the reliability of the self-organizing voltage regulation method: Analyze the performance of the EMS algorithm used by each agent in the simulation to assess the reliability of the self-organizing voltage regulation method.

By following the steps described for research questions Q2 and Q3, the distributed control method can be successfully applied to voltage regulation tasks in future power systems in the layer of energy community and DSO. In order to prepare well for the algorithm on site and answer the research question Q4, the kit needs to achieve the following design requirements:

Ensure extendability: A custom kit can be designed to be easily extendable, allowing for the integration of new components, systems, or control algorithms as needed.

Maintain applicability: By designing the kit with applicability in mind, it can be easily adapted to various use cases, such as testing, demonstration, and education.

Offer flexibility and scalability: A custom kit can be designed to accommodate changes in network size, structure, and operation conditions, providing a scalable and flexible solution for voltage regulation testing.

Facilitate HIL Testing: By ensuring that the custom kit is compatible with HIL testing environments, it can support real-time simulation and testing scenarios.

To develop the real-time digital environment, the open-source Mosaik co-simulation platform is used [39]. Mosaik is a powerful and flexible tool that integrates various energy technologies and systems into a coherent environment, which can increase the extendability and ease of use of the kit. Using Mosaik, the kit can be designed to meet the aforementioned design requirements, ensuring its suitability for testing the voltage regulation algorithm and taking care of time synchronization and interactions across the integrated models.

Raspberry Pi serves as an ideal hardware platform for the kit due to its low cost, high versatility, and ease of use. Its compatibility with various industries, including energy, automation, and IoT, simplifies integration and collaboration efforts. Furthermore, Raspberry Pi can be configured to support real-time applications, making it suitable for testing and validating time-critical algorithms and control strategies.

1.4. RESEARCH CONTRIBUTIONS

The primary contribution of this research study is the method to identify the main barrier to increasing the integration of DRES in DNs and present the method to achieve self-organizing voltage in DNs to achieve a high DRES penetration level. In order to ful-

fill the main research objectives and answer the research questions, the contributions of this research are as follows:

- A stochastic simulation-based approach for sizing DRES penetration level and central BESS capacity in DNs, addressing research question Q1. This approach enables users to determine the highest level of penetration of DRES while maintaining network stability and acceptable voltage profiles in power grids, which is essential for planning and designing DRES integration, considering the constraints of existing grid infrastructure. Power grid planners and operators can use the presented tool and approach to evaluate the potential for integration of DRES into the grid. A method is proposed to analyze the performance of different local voltage control methods and assess the impact of varying DRES installations on the maximum acceptable DRES capacity. This method helps identify the most effective local voltage control method for specific large-scale DNs with high DRES penetration, optimizes the voltage regulation process in DNs, and promotes efficient use of DRES, thus reducing reliance on traditional generators and decreasing greenhouse gas emissions. In addition, a method for sizing a central BESS to achieve smoother active power profiles injected to the upstream voltage level and enhance stability is proposed. The proposed method considers different/the most popular state-of-the-art power smoothing techniques.

- A novel algorithm is proposed that achieves optimal voltage regulation through the self-organizing actions of agents, addressing research question Q2. The proposed method leverages a distributed cooperation approach, enabling power grids to maintain voltage stability under varying conditions. In this system, distributed agents autonomously adjust their real-time behavior based on local data and collaborate by exchanging information with neighboring agents. This cooperative strategy allows each agent to operate independently yet synergistically, optimizing the overall system performance efficiently. The core innovation of this algorithm lies in its use of bottom-up coordination and self-organization, enabling the power grid to sustain stable and consistent voltage regulation even amidst rapidly evolving energy scenarios. By allowing distributed agents to coordinate and collaborate effectively in real time, the algorithm addresses the challenges of voltage regulation in DNs with high DRES penetration. Utilizing the strengths of self-organization and distributed computing, the algorithm responds dynamically to fluctuations in load and generation, swiftly adapting to new operational conditions. Its potential to significantly boost the reliability and efficiency of voltage regulation makes it highly applicable across various contexts, including smart grids, microgrids, and the integration of DRES. This adaptability and robustness highlight the algorithm's potential as a transformative tool for modern energy management systems.

- A comprehensive four-stage energy management approach is proposed that leverages receding-horizon optimization to regulate power fluctuations in a PV-BESS-electrolyzer-fuel cell residential energy community system, addressing research question Q3. This innovative approach uniquely integrates four optimization stages:

yearly, monthly, day-ahead, and intra-day. By merging long-term and short-term optimization strategies in EMS development, it capitalizes on hydrogen produced through the electrolyzer for seasonal storage. The introduced algorithm incorporates three modes with distinct objective functions for improved user adaptability. The approach is tested through simulations and operational analysis of an on-site field lab (PV–BESS–electrolyzer–fuel cell energy system). It is also used to test the reliability of the self-organizing voltage algorithm for the identification of potential failures or shortcomings in the voltage regulation algorithm, enabling necessary improvements to ensure its reliability and robustness.

- A kit for validating intelligent grid control algorithms, addressing research question Q4, named The Illuminator is proposed. This platform highlights the challenges emergent from the energy transition, serving as both a visual aid and a sandbox for the real-time and asynchronous testing of intelligent grid control algorithms. The Illuminator technology is primarily a modular software platform developed to run on a Raspberry Pi (RasPi) cluster. It is open-source, available on GitHub and developed in Python. This environment offers a digital platform for testing and showcasing intelligent algorithms that work in the local energy community or the power grid. This could lead to the development of more efficient and effective control algorithms, refined through insights drawn from real-time simulations and hardware-in-loop evaluations.

In summary, the research contributions of this study will provide a method to identify the main barrier to increasing the integration of DRES in DNs, enhance the understanding of voltage regulation in DNs with high DRES penetration, provide innovative solutions for the realization of self-organizing voltage regulation in DNs and present a kit for validating the intelligent algorithms.

1.5. OUTLINE OF THE THESIS

This thesis is divided into six chapters. Chapter 1 is a foundational introduction that clarifies the background, research question, methodology, and contributions. The following Chapters 2,3,4 and 5 address research questions Q1 to Q4, respectively. These chapters clarify the methodology employed and illustrate the key findings. Chapter 6 provides a concise summary and synthesizes the discussion by drawing insightful conclusions from the key findings.

Chapter 1: Introduction. This opening chapter offers a comprehensive introduction to the research topic, questions, and methodologies. To aid readers, it also outlines the structure of the thesis content.

Chapter 2: A Stochastic Simulation-Based Approach to Integrate DRES. This chapter presents a stochastic simulation-based approach to evaluate DRES penetration levels and BESS capacity within DNs, considering the network's specific characteristics. Additionally, data analysis methods are used to compare the performance of various local voltage and central BESS control methods, providing information for network planners through simulation experiments.

Chapter 3: Distributed Cooperative Voltage Regulation. This chapter proposes a distributed cooperative voltage regulation algorithm, as local voltage control methods

are insufficient to support the desired DRES capacity. The algorithm facilitates self-organizing voltage regulation in DNs with substantial DRES penetration. Furthermore, the performance of the proposed method is compared with that of centralized and ADMM methods using simulation experiments.

Chapter 4: Enhanced MPC Algorithm for Energy Communities. This chapter introduces a novel four-stage energy management strategy, harnessing receding-horizon optimization to manage energy consumption within a PV-BESS-electrolyzer-fuel cell residential energy community setup. The performance of the strategy is discussed through multiple simulations.

Chapter 5: An Open Source Validation Kit for DRES Integration. This chapter describes the development of a testing and analysis kit for intelligent grid control algorithms. The performance of the kit is shown in a local energy community study and a DN study.

Chapter 6: Conclusions and Discussion. The final chapter summarizes the research contributions, discusses the study's limitations, and examines the potential practical implications of the findings. It also explores future research directions in intelligent grid control algorithms.

2

A Stochastic Simulation-based Approach to Integrate DRES

This chapter introduces a stochastic simulation-based method designed to precisely estimate the maximum feasible penetration of DRES and the optimal sizing of central BESS within DNs. The necessity for this approach arises from the challenge of maintaining grid stability amidst the variability and intermittency inherent to DRES. By generating many scenarios reflecting diverse grid conditions, this methodology not only calculates feasible DRES penetration levels and BESS capacities but also evaluates different control strategies under varying operational conditions. The primary innovation of this approach lies in its ability to offer DSOs a comparative analysis of various voltage control and power smoothing techniques, thereby facilitating informed decisions on grid enhancements to accommodate higher levels of renewable integration. Case studies employing four voltage control algorithms and three power smoothing methods validate the versatility and efficacy of the proposed approach.

Parts of this chapter have been submitted to the International Journal of Electrical Power & Energy Systems with the title: *A stochastic simulation-based approach for sizing DRES penetration level and BESS capacity in distribution grids.*

2.1. INTRODUCTION

The integration of high levels of DRES poses significant challenges to grid stability, primarily due to the unpredictability and variability of renewable energy sources. Addressing these challenges requires robust and flexible grid management strategies. The increased intermittency of DRES and the variability of loads not only cause voltage fluctuations and violations but also compel TSO to serve more energy and commit more fuel-driven reserves for the intraday market. Conventional voltage control methods include constant Q and $Q(V)$ droop control strategies, as presented in [19]. However, a systematic method to determine the maximum allowable DRES penetration under diverse conditions using different voltage control strategies remains undeveloped [40, 41]. Moreover, many grid codes impose specific limits on DRES power fluctuations [42]. As the penetration level of DRES increases in DNs, the power fluctuation problem arises. The central BESS is commonly employed to mitigate fluctuating power at the upstream distribution grids [26]. A Ramp-rate limitation algorithm is proposed in [43] and [44] for smoothing DRES power. A novel controller utilizing a neural network model is suggested for smoothing solar power fluctuations with BESS in [45]. Various smoothing methods and algorithms, as presented in [43, 44, 46, 45], and [47], offer methods to obtain more accurate representative days for optimizing BESS size within the optimization horizon. However, there is still a lack of a systematic simulation-based approach to compare different power smoothing methods and size the central BESS for power smoothing to achieve high DRES penetration levels.

Given these complexities, a stochastic simulation-based approach is suited for this research because it models the dynamic interactions within power systems where analytical solutions are impractical or insufficient. This approach allows for the examination of a wide range of scenarios reflecting the stochastic nature of renewable energy sources and load demands. It provides a robust framework for assessing the impacts of various control strategies and system configurations on grid stability, which is critical for developing resilient power systems.

This chapter proposes a stochastic simulation-based framework to fill these gaps by providing a comprehensive analysis tool for DSOs to assess and optimize DRES integration and BESS utilization. First, various stochastic scenarios are generated based on existing grid conditions. Then, through the analysis of various simulation results based on each generated scenario, the maximum allowable penetration level of DRES for the DN is determined. Finally, an incremental approach to size the central BESS capacity is implemented with different power smoothing logic to mitigate the influence of power fluctuations on the upstream voltage levels.

The main contributions of this chapter are threefold. Firstly, by providing a variety of conditions and control logic, numerous stochastic scenarios can be automatically generated. A comparative analysis of voltage control and BESS power smoothing methods is performed. Second, the risk of technical violation and power smoothing target failure can be analyzed by examining a long period of simulation results. Thirdly, the primary advantage of this tool is that it allows the DSOs to assess their preferred voltage regulation and power smoothing methods and decide which one to use based on their network and needs.

The remainder of this chapter is structured as follows: Section 2.2 details the pro-

posed stochastic simulation-based approach. Case studies illustrating the method's application and effectiveness are presented in Section 2.3, followed by a discussion of the results and concluding remarks in Section 2.4.

2.2. APPROACH FOR SIZING DRES AND CENTRAL BESS

The approach for sizing the maximum DRES penetration level in DNs is summarized in four steps. First, a large number of scenarios are generated with various conditions. Second, scenario-based results are analyzed using different control logic to determine a reasonable upper limit for the DRES penetration level. Third, various power smoothing methods are employed to reduce the influence of power fluctuations caused by high DRES penetration levels to the upstream voltage level. Fourthly, the simulation results are analyzed to determine the suitable central BESS capacity. A single simulation platform cannot achieve the desired goals and verify my proposed sizing methodology. Therefore, Python and PowerFactory [48] are combined to create a simulation platform capable of manipulating data, changing model parameters, and performing simulations.

2.2.1. EVALUATION ITEMS AND METHODS

MAXIMUM DRES PENETRATION LEVEL DETERMINATION

The maximum DRES penetration level is defined as the total installed DRES capacity that can be achieved without violating the grid's technical constraints: the nodes' voltage and the lines' thermal limits. Various combinations of the number of DRES and the number of DRES capacity allocations are assessed, as they can all affect the maximum DRES penetration level. An iterative procedure is used for each combination to calculate the maximum DRES penetration level. In each scenario, the DRES location and power are allocated randomly, and the penetration level of DRES is incrementally increased until the technical constraints are reached. With a given voltage control method and the number of installed DRES, the flow chart of the maximum DRES penetration simulation method is shown in Figure 2.1.

The process for calculating the maximum DRES penetration level is as follows:

- Define technical constraints: Establish the grid's technical constraints, such as the nodes' voltage limits and the lines' thermal limits, which must not be violated during the analysis.
- Assess various combinations: Evaluate different combinations of the number of DRES installations and their capacity allocations, as these can impact the maximum DRES penetration level.
- Iterative procedure: For each combination, employ an iterative procedure to calculate the maximum penetration level of DRES. In each scenario, allocate DRES location and power randomly.
- Incrementally increases DRES penetration level: Gradually increase the DRES penetration level until the technical constraints are reached. The last value before the violation(s) occur is chosen as the maximum DRES penetration level for the specific scenario.

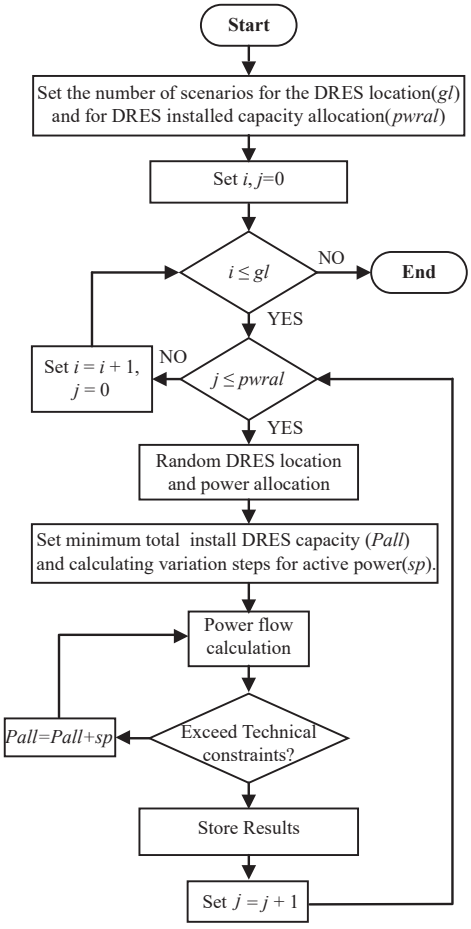

Figure 2.1: The flowchart of maximum DRES penetration sizing method

Within the platform, any voltage control methods can be utilized as inputs. However, only the most popular localized approaches are focused on and included in the development. These methods are specified in current grid codes and standards [49] [50], increasing the practical nature and broad applicability of the proposed stochastic simulation-based approach. The specific methods integrated are Constant Q, $PF(P)$ droop control, $Q(P)$ droop control, and $Q(V)$ droop control. Each method has been selected for its relevance and compliance with contemporary regulatory frameworks, demonstrating the platform's capability to address real-world challenges effectively. In Constant Q mode, the reactive power from DRES is set as a constant value, and in this section the reactive power is set as 10% of DRES rated power. In $PF(P)$ droop control mode, the power factor (the ratio of active power to apparent power) of the DRES generator is adjusted based on the generated active power, as shown in Figure 2.2. When the DRES output active power is lower than 50% of the rated active power, the power factor is set to one. Conversely, when the DRES output power is higher than 50% of the rated active power, the power factor is set to 0.89. In the $Q(P)$ control droop mode, the reactive power changes based on the generated active power, as illustrated in Figure 2.3. In the $Q(V)$ droop mode, the reactive power varies according to the voltage value, with the settings for the $Q(V)$ droop mode displayed in Figure 2.4. In this mode, the reactive power from DRES follows the voltage values, enabling effective voltage regulation. After the initial setup, a loop is created in which the active power of DRES is increased incrementally by 2 kW for Low Voltage (LV) grids and 100 kW for Medium Voltage (MV) grids until voltage or loading violations occur. The last value before the violation(s) is chosen as the maximum DRES power penetration level for the specific scenario. Subsequently, the DSO can compare the results and decide on the most suitable method for their Distribution System.

To determine the maximum penetration level of DRES in power grids, a probability distribution analysis of a large number of results based on different scenarios is performed. However, despite the comprehensive analysis to establish the maximum DRES penetration level, there remains a possibility that technical constraints may be exceeded. Therefore, it is essential to investigate the voltage violation risk for a given network, considering the desired installed DRES power, DRES locations, and specified voltage control method. To analyze the risk of technical violations, a long-period dynamic simulation needs to be performed (in this chapter, a one-year simulation is conducted).

REQUIRED MINIMUM CENTRAL BESS CAPACITY SIZING

The BESS is utilized to smooth out the fluctuation power at the connection point between the transmission grid and the distribution grids to decrease the fluctuation power. Because centralized BESS in the distribution feeder is more effective in managing system-wide issues and easier to control and manage for reliable operation comparing with distributed BESS, the central BESS installed upstream of the feeder is used to do the power smoothing. The central BESS capacity is determined as the minimum capacity required to meet the ramp rate limit (RRL) after smoothing the power. The platform can determine the central BESS capacity using any power smoothing method. In this chapter, simulations are conducted using three well-known power smoothing methods: the Moving Average method, the Low-pass Filter method [51], and the Step Ramp-rate Control method [52]. The outcomes of each are analyzed and compared to evaluate their effectiveness.

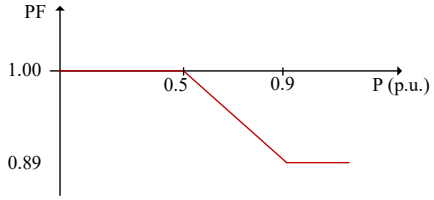

Figure 2.2: $PF(P)$ droop control curve [19].

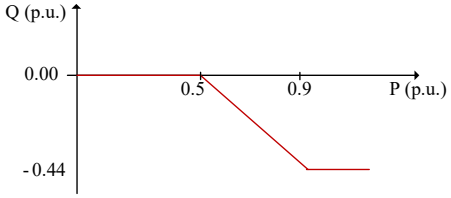

Figure 2.3: $Q(P)$ droop control curve [19]. The negative sign indicates operation in the under-excitation mode, i.e., DRES absorbs the reactive power.

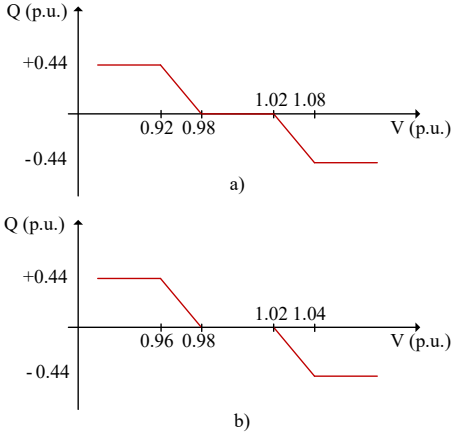

Figure 2.4: $Q(V)$ droop control curves [19]: (a) LV grids, and (b) MV grids. The negative sign indicates operation in the under-excitation mode, i.e., DRES absorbs the reactive power.

The Moving Average is a time series smoothing method that calculates the average of several sequential values of another time series. It is given by:

$$z_t = \frac{1}{k}\sum_{j=0}^{k-1} y_{t-j}, \quad t \in k, k+1, \ldots, n, \tag{2.1}$$

where z_t is the DRES output series power after smoothing, based on the average of the original DRES output series power y_{t-j}. When utilizing the Moving Average method, the window size for the Moving Average method, TW_{mvps} (i.e., the k in Equation 2.1), needs to be set up.

The Low-pass Filter method is a typical smoothing method that removes short-term fluctuations and retains the longer-term trend. It is widely used in DRES power smoothing [51]. The normalized cutoff frequency CF_{lfps} (a number between 0 and 1, representing the cutoff frequency ratio to twice the sampling frequency) must be set for the Low-pass Filter method.

The Step Ramp-rate Control method directly controls the ramp-rate of power within a set limitation [52], which is given by:

$$z_t = \min\left(\max\left(y_t, y_{t-1} - RR \cdot \Delta t\right), y_{t-1} + RRL \cdot \Delta t\right), \tag{2.2}$$

where RRL is the ramp-rate limitation, and Δt is the sampling time. The ramp-rate limitation (RRL) must be set to use the Step Ramp-rate Control method.

An iterative procedure will be adopted for different power smoothing methods to calculate the minimum central BESS capacity requirement during the simulation time period. The central BESS capacity determination flow chart is shown in Figure 2.5.

The initial set of power smoothing parameters, TW_{mvps} for the Moving Average method and CF_{lfps} for the Low-pass Filter method, should be set as a small value and then iteratively increased with steps δ_{CF} and δ_{TW} to find the smallest value of TW_{mvps} and CF_{lfps} that meets the ramp-rate limit after power smoothing. It is noted that in the Low-pass Filter method and the Moving Average methods, the finally achieved RRL cannot be precalculated but only evaluated by progressively improving the setup like the approach followed in this thesis. The initial central BESS capacity, denoted as C_{ba}, should be set at a small value or zero, and the central BESS increasing step capacity is represented as C_{ra}. The settings of the central BESS parameters include the name of central BESS, the rated charging and discharging power (max_p, min_p), the charge and discharge efficiency ($charge_{eff}$, $discharge_{eff}$), the initial state of charge (SOC) (SoC_{init}), and SOC limitation ([SoC_{min}, SoC_{max}]). The remaining parameters are the simulation time step (t) and simulation period(T).

The processes of central BESS capacity determination are as follows:

- Determine the power smoothing method: Choose the power smoothing method to be used for the simulation.
- Set the power smoothing method and required value: Configure the selected power smoothing method and its corresponding target value.
- Set up all central BESS parameters: Establish the initial parameters for the central BESS, such as state of charge, maximum and minimum SOC limits, charge and discharge power limits, and ramp rates.

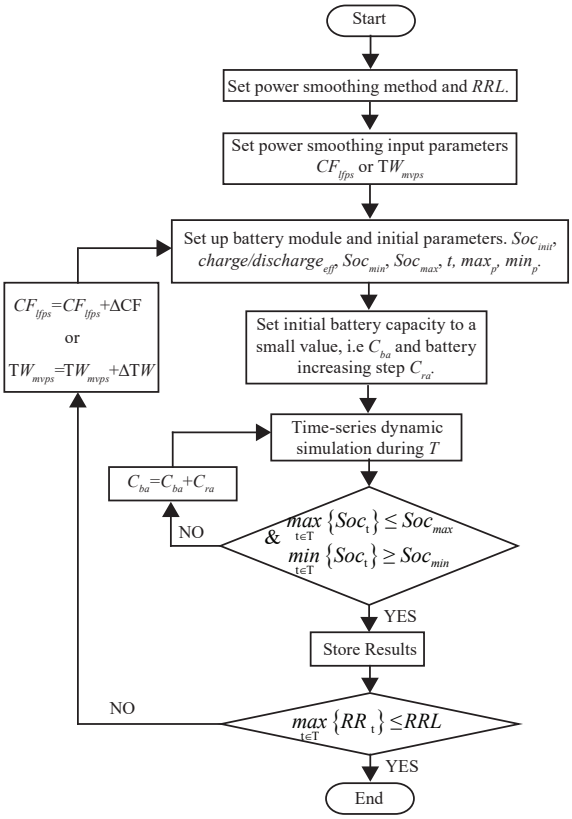

Figure 2.5: The flowchart of central BESS capacity determination.

- Perform time-series dynamic simulation: Conduct a time-series dynamic simulation during the time period T, considering the power fluctuations from DRES and load consumption.
- Check SOC limitations: After the simulation, ensure that the SoC_t values are within the specified limitations during the time period T. If all values are within limits, proceed to the next step; otherwise, increase the central BESS capacity and repeat the simulation until the SoC_t values are within limits.
- Check ramp-rate limit compliance: Verify if the power after smoothing meets the ramp-rate limit standards. If it does, the simulation is complete and the BESS capacity is chosen as the minimum central BESS capacity requirement; otherwise, update the power smoothing parameters and repeat the simulation.

Since the generated power of DRES and load consumption exhibit similar patterns each day, simulations are performed iteratively to determine the central BESS capacity requirements for each day. To size the central BESS, a large number of minimum central BESS required capacities need to be calculated using different load and DRES profiles. Consequently, various scenarios based on diverse load and DRES generation profiles in different weather conditions and seasons must be simulated. The central BESS capacity is then sized as a min-max problem over the entire set of scenarios.

2.2.2. SIMULATION PLATFORM BUILD UP

The framework for studying the high DRES penetration level networks is summarized in four steps. The relevant scenarios are first generated to calculate the maximum DRES penetration level within the technical constraints. Secondly, a large amount of scenario-based results are analyzed to determine the best voltage control method, the reasonable top DRES penetration level and the best DRES location number. Thirdly, central BESS capacity is estimated for power smoothing to decrease the volatility of high DRES penetration for the grid. Finally, a large amount of data-based results are analyzed to determine the reasonable central BESS capacity. One simulation platform is insufficient to achieve the desired goals, which can generate and analyze the scenarios automatically and build detailed assets and power grid models. In the platform, Python and PowerFactory [48] are combined to construct the functional DRES penetration calculation framework. Python is used to control PowerFactory [48], which can manipulate data, change the parameters of models and perform simulations.

The platform is compatible with any power grid built in PowerFactory. In this chapter, the CIGRE MV network [53] and IEEE European LV Test Feeder [54] are employed as benchmarks for simulation and case studies. PVs are installed at each power grid node to represent the DRES for simulation, while BESS are installed upstream of each feeder. The CIGRE MV grid is depicted in Figure 2.6, with the central BESS named *battery_1* and *battery_2* in the topology. The IEEE European LV Test Feeder grid is illustrated in Figure 2.7. The power grid model can be imported and applied to the simulation study using Python scripts.

For accessing PowerFactory models, simulating results and achieving the framework functions to study the high DRES penetration level power grid, a class *PowerFactorySim*

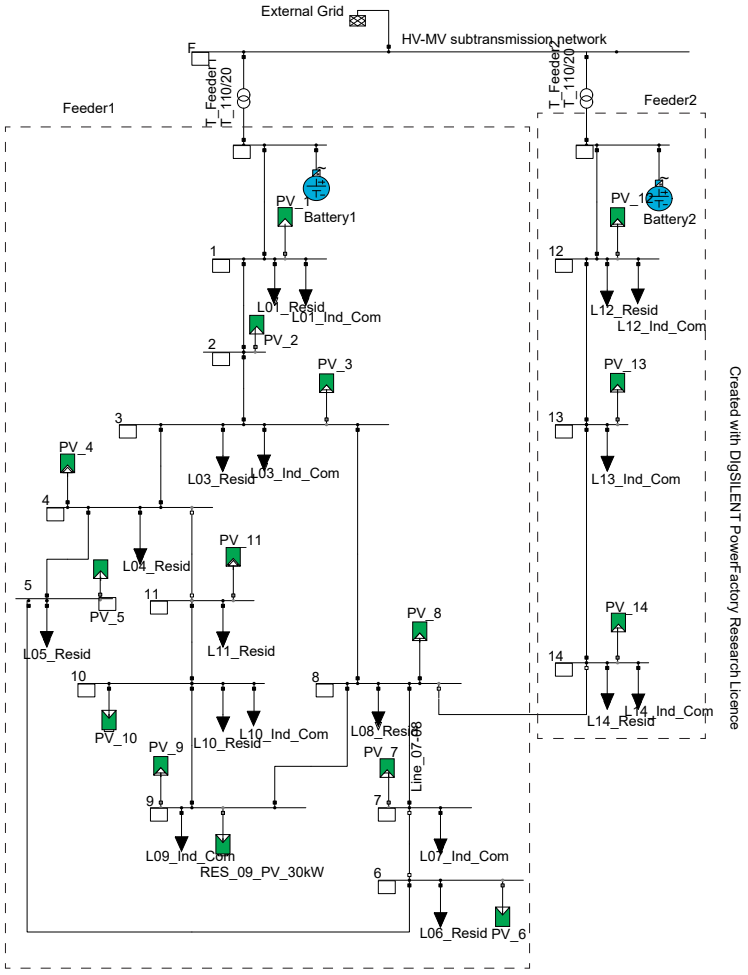

Figure 2.6: Cigre MV grid with installed PVs and batteries.

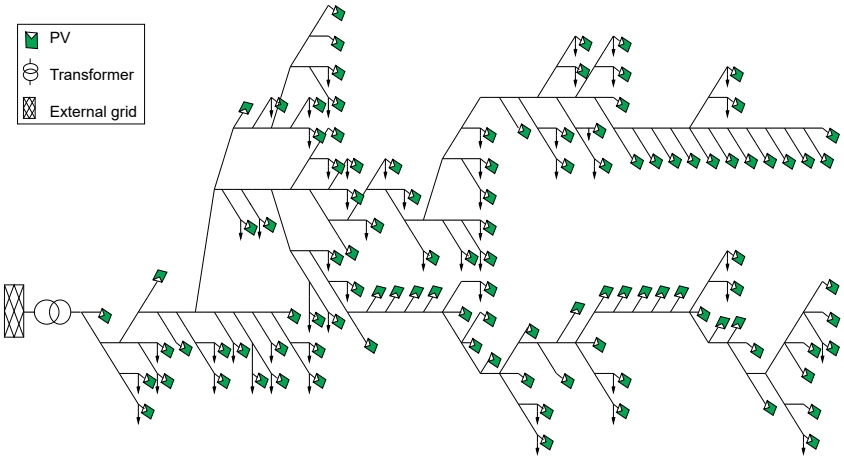

Figure 2.7: IEEE LV Test Feeder grid.

is developed in Python. The class has functions for power flow and dynamic simulations, creating load and faults events, checking grid technical constraints, and manipulating DRES parameters and central BESS parameters, which are explained below.

- Functions for power flow simulation: These functions prepare for power flow simulations, enabling the power flow simulation to run and read the results. The result of the running function is `true` if there is no convergence, i.e., if there is no power flow simulation.

- Functions for dynamic simulations (RMS and EMT): It is possible to run RMS or EMT simulation by selecting `sim_type` inside the function call as `rms` or `emt`, respectively. In addition, the start time, end time and simulation time step can be defined. In the `monitored_variables` a list of PowerFactory variables is provided that will be monitored and whose data will be saved.

- Functions for events (load events and faults): These functions have been used for creating short circuit events (faults) and any other events (e.g., load percentage change in active/reactive power w.t.r. to nominal value). The location of the fault/event and its duration can be specified inside the function.

- Functions for reading data: These functions are used for reading bus voltages after performing load flow calculations, active and reactive PV power, delivered upstream power, etc.

- Functions for checking violations: These functions return `true` if the violation occurs in any transmission line, transformer, capacitor, inductor, etc. (Thermal limit is checked by comparing current flowing through lines, transformers and serial components with the maximum allowed current for each component.) or in the

case of the bus voltages is outside of the permissible operating conditions (i.e. if any bus voltage appears to be outside the set $[V_{min}, V_{max}]$).

- Functions for DRES: These functions are used for manipulating PV data. There are functions for setting of the active/reactive powers, or apparent power and an angle, to all DRES or a certain DRES. Besides, the DRES control method can be chosen between standard ones or specifically defined voltage control methods.

- Functions for central BESS: These functions are used for manipulating data of central BESS. There are functions for getting all data of central BESS from PowerFactory, activating/inactivating the central BESS and setting the charging/discharging power of central BESS.

2.3. CASE IMPLEMENTATIONS AND RESULTS ANALYSIS

The sizing approach proposed in Section 2.2 provides methods for assessing the maximum DRES penetration level and central BESS capacity. This section evaluates the proposed sizing approach using multiple simulations with different voltage control and power smoothing methods. The CIGRE MV benchmark network load information and IEEE LV Test Feeder grid follow their official documents [53] [54]. A typical daily PV and load profiles for residential and commercial or industrial loads are shown in Figure 2.8. The one-year load and PV profiles for the simulation are obtained from Liander open data [55].

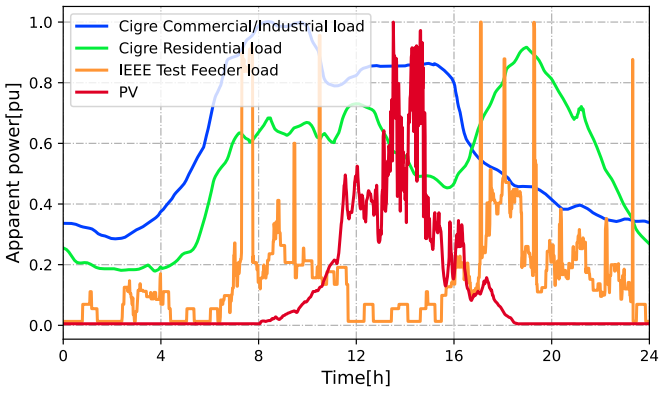

Figure 2.8: Daily load and PV profiles of the network [53]

.

Table 2.1 gives the values of the rated apparent power and power factors of all loads in the CIGRE MV network. The power factor of all loads in the IEEE European LV Test Feeder network is 0.95.

Table 2.1: Load parameters of the MV CIGRE network [53]

Node	Apparent Power, S [kVA]		Power Factor, pf	
	Residential	Commercial/ Industrial	Residential	Commercial/ Industrial
1	15300	5100	0.98	0.95
2	—	—	—	—
3	285	265	0.97	0.85
4	445	—	0.97	—
5	750	—	0.97	—
6	565	—	0.97	—
7	—	90	—	0.85
8	605	—	0.97	—
9	—	675	—	0.85
10	490	80	0.97	0.85
11	340	—	0.97	—
12	15300	5280	0.98	0.95
13	—	40	—	0.85
14	215	390	0.97	0.85

2.3.1. CASE STUDY FOR MAXIMUM DRES PENETRATION LEVEL DETERMINATION

In order to estimate the limit of DRES penetration levels, a significant number of scenarios are generated using my approach. The voltage limit of the network is set to 0.95-1.05 p.u according to EN 50160 standards [56]. To simulate 100 scenarios for each control method (Constant Q, $PF(Q)$, $Q(P)$, and $Q(V)$), the number of different DRES geographic location allocations (gl) is set to 10, and the power allocation scenarios of DRES ($pwral$) is also set to 10.

Using the CIGRE MV grid, the installed DRES numbers is simulated as 3, 6, 9, and 12, resulting in a total of 1600 scenarios. For the IEEE European Test Feeder grid, the installed DRES numbers are simulated as 10, 20, 30, 40, 50, 60, 70, 80, 90, and 100, yielding a total of 4000 scenarios. This comprehensive set of scenarios allows us to evaluate the maximum DRES penetration level under various conditions, providing valuable insights into the potential of integrating DRES into different network configurations.

CASE STUDY WITH CIGRE MV BENCHMARK GRID

In my analysis, a scenario with node voltages exceeding the standard limitation is considered to have a voltage violation problem. Conversely, if all node voltages are within the limit, there is no voltage violation problem. Among the 1600 generated scenarios, only one exhibited a maximum DRES penetration level limited by thermal violation instead of voltage violation. Consequently, my analysis primarily focuses on voltage violation constraints related to the maximum DRES penetration level.

The distribution of maximum accepted DRES capacity in the CIGRE MV grid for all 1600 generated scenarios is depicted in Figure 2.9. The figure displays the minimum value, maximum value, lower quartile ($qut1$), mean value (μ), and upper quartile ($qut3$)

for specific voltage control methods and DRES numbers. The figure shows that as the number of DRES connections increases, the interquartile range narrows, leading to a tighter clustering of median values. This trend indicates that the network becomes more consistent in terms of its DRES capacity acceptance as the number of DRES installations rises.

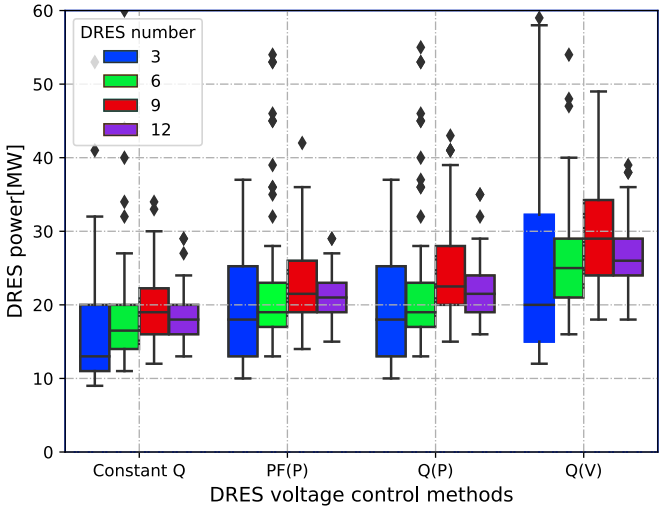

Figure 2.9: Maximum DRES penetration level at CIGRE MV network with different voltage control methods and installed DRES number.

The distribution analysis of the maximum DRES penetration level at the CIGRE MV network with different voltage control methods is illustrated in Figure 2.10 and Table 2.2. This analysis aims to evaluate the impact of voltage control methods on the maximum acceptable penetration level. Simulation results indicate that when using the constant Q control method, to ensure voltage violations remain within the acceptable limits, a conservative choice for DRES power penetration level would be 9 MW. However, as seen in Figure 2.10, only a small fraction of all scenarios (0.75%) have a penetration level below 10 MW with the constant Q control method. Therefore, while selecting the minimum value from all scenarios as the limit for DRES penetration level may be the safest option, it is not the most sustainable choice.

In distinct scenarios characterized by specific capacity allocations and installation locations, the grid can accommodate up to 48 MW of DRES utilizing the Constant Q control method, which extends to 65 MW under the $Q(V)$ control method shown in Table 2.2. Given that the DRES installed capacity allocation and installation locations are randomly selected, the decision by the DSO regarding the DRES installation and penetration level hinges on striking a balance between the extent of DRES penetration and the associated risk of voltage violations. For instance, if we opt for the $qut1$ value, although it may result in a voltage violation probability of 75%, it permits an increase in DRES capacity up to 14 MW. This effectively underscores the flexible and strategic trade-off between maximizing renewable energy integration and ensuring network reliability

and stability.

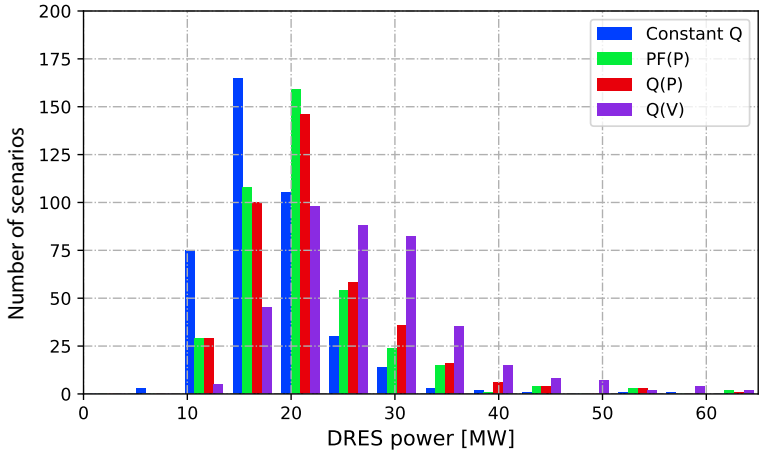

Figure 2.10: The histogram of the maximum DRES penetration level for different voltage control methods.

Table 2.2: Influence of Control Methods on DRES Penetration in MW

Control method	min	$qut1$	μ	$qut3$	max
Constant Q	9	14	18	21	48
$PF(P)$	10	17	22	24	61
$Q(P)$	10	17	22	25	62
$Q(V)$	12	21	28	31	65

To investigate the impact of the number of installed DRES on their acceptable capacity, a distribution analysis of all 1600 scenarios are conducted with different numbers of installed DRES. The histogram for various DRES installation numbers is displayed in Figure 2.11, while the analysis data is presented in Table 2.3. The table and figure show that as the number of installed DRES increases, the distribution of maximum installed capacity becomes tighter. With more DRES integrated into the network, the total DRES power increases; however, the increment rate appears to diminish. Due to the limited number of nodes in the CIGRE MV grid, we cannot increase the number of DRES beyond 14 to verify if this trend persists. To further explore this trend, the IEEE LV feeder grid, which has a greater number of nodes, can be utilized for analysis.

CASE STUDY WITH IEEE EUROPEAN TEST FEEDER GRID

This section analyzes 4,000 scenarios with different DRES installation numbers and control methods in the IEEE European Test Feeder grid. The distribution of maximum accepted DRES capacity in the IEEE European Test Feeder grid, considering different control methods, is depicted in Figure 2.12. Compared to the $PF(Q)$, $Q(P)$, and $Q(V)$ control methods, the constant Q control method appears to be less effective.

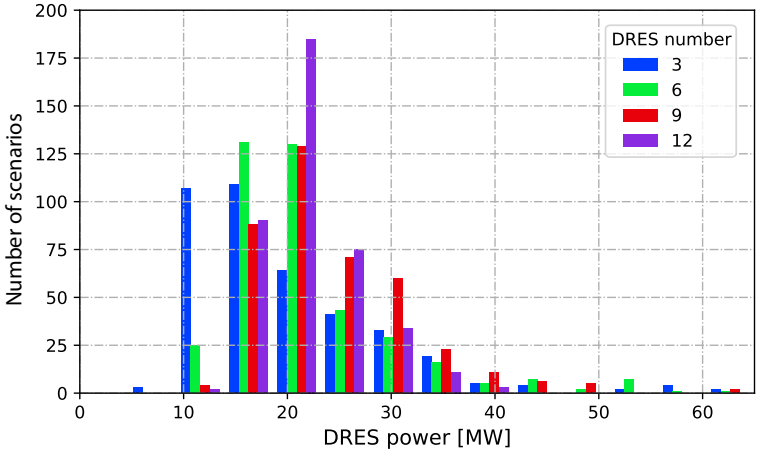

Figure 2.11: The histogram of the maximum DRES penetration level for different DRES installed numbers.

Table 2.3: Influence of DRES number on DRES penetration in MW

DRES number	min	$qut1$	μ	$qut3$	max
3	9	13	21	25	61
6	11	17	22	25	62
9	12	19	24	28	65
12	13	19	22	25	39

The distribution of maximum accepted DRES capacity in the IEEE European Test Feeder grid with varying installed DRES numbers is illustrated in Figure 2.13. This exhibits a similar pattern to the simulation results in the CIGRE MV network: as more DRES are integrated into the network, the overall DRES power increases, but the increment rate diminishes.

RELIABILITY ANALYSIS WITH ONE-YEAR SIMULATION

Following the conclusions drawn above, the acceptable DRES installed capacity in the network can be determined with a given control method and DRES number. Although a large number of simulated scenarios are analyzed, voltage violations still occur due to dynamic changes in the load profile and DRES-generated power. To assess the risk of voltage violations in the MV CIGRE network, a one-year simulation with a 15-minute time step is performed. The DRES installed capacity in the Cigre MV network is set to 28 MW (mean value of $Q(V)$ control method with 9 DRES in Figure 2.9) located at buses 1, 4, 5, 7, 8, 10, 11, 12, and 14. In the one-year simulation, the risk of voltage violations is only 5.68%, which occurs only at node 11 (with a voltage rise problem). Following EN 50160 standard [56], Under normal operating conditions, 95% of the time over one week should keep within the voltage limit. Thus, a voltage violation rate of 5.68% over a one-year simulation is within acceptable bounds according to the EN 50160 standard.

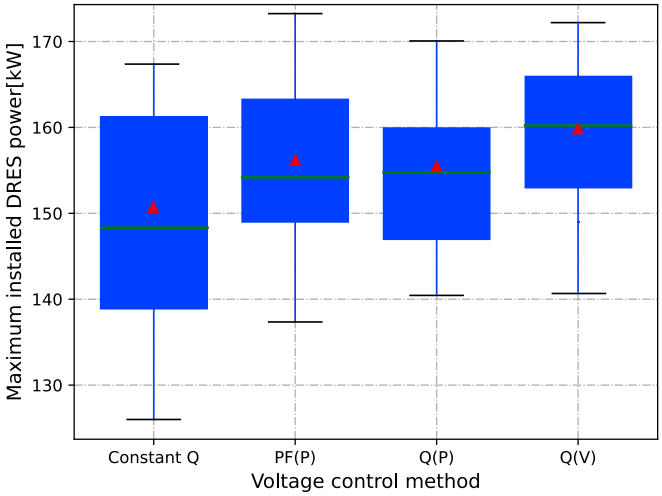

Figure 2.12: The maximum DRES penetration level in IEEE European Test Feeder grid with different DRES control methods.

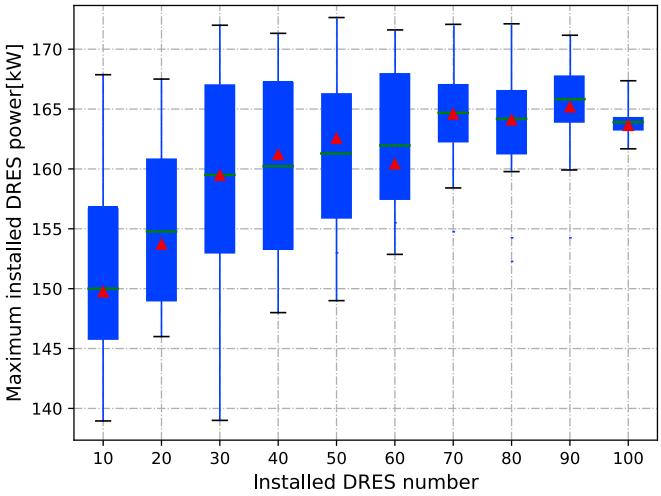

Figure 2.13: The maximum DRES penetration level in IEEE European Test Feeder grid with different DRES penetration numbers.

The risk of over-voltage is at its peak in August, specifically at 12:30 PM. There are 9 days in August has the over-voltage problem (with the probability 28.22%) at 12:30 PM. The over-voltage probability of Node 11 in August is shown in Figure 2.14, and the most severe instance of this issue observed was a voltage surge to 1.0504 pu.

The simulation results show that my stochastic simulation-based method can successfully determine the maximum DRES penetration level based on the different DRES

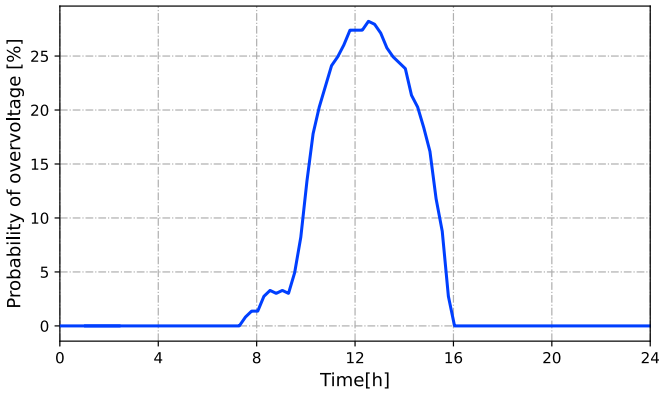

Figure 2.14: The over-voltage probability of Node 11 in August.

numbers and control methods. the statistical analysis is performed for many simulated scenarios for a given voltage control method to guarantee the DRES penetration within the maximum allowed limits. the DRES penetration level can be determined based on the probability distribution analysis. Moreover, the proposed stochastic simulation-based method can explore the voltage violation risk for a given network with the desired installed DRES power, DRES locations, and specified voltage control method. By performing a simulation over a long period (in this section, a one-year simulation is performed), the risk of voltage violations and the time in which the risk of violations is concentrated for each node can be obtained.

2.3.2. CASE STUDY FOR CENTRAL BESS CAPACITY DETERMINATION

In this section, a case study is conducted to determine the required central BESS capacity for power smoothing. The same scenario described in subsection 2.3.1 is utilized, which involves the installation of 28 MW DRES using the $Q(V)$ control method to carry out the power smoothing case study. The Moving Average method, Low-pass Filter [51], and a specific Step Ramp-rate Control Strategy [52] are employed to achieve power smoothing. The ramp-rate limit is defined as $\Delta P/min \leq 10\%$ of the total DRES rated power [57, 58], which amounts to 2.8 MW per minute.

The simulation results show the required power smoothing central BESS capacity for each method in Table 2.4, where P_{ch}^{max} represents the maximum charging power requirement, and P_{dch}^{max} denotes the maximum discharging power requirement. To achieve the ramp-rate limit of 10% per minute, a window size of 4 minutes is calculated as the moving window for the Moving Average method, while a normalized cutoff frequency of 0.21 is employed for the Low-pass Filter method. From the results, these three power smoothing methods do not show significant differences in the maximum requirements of charge and discharge rated power of the central BESS converter. However, the Step Ramp-rate Control Strategy requires much less central BESS capacity compared to the Low-pass Filter and Moving Average methods.

Since the PV-generated power and load consumption exhibit a similar pattern each

Table 2.4: Calculated MV CIGRE network central BESS sizing

Control method	Central BESS capacity [MWh]	$P_{ch}^{max}[MW]$	$P_{dch}^{max}[MW]$
Low-pass filter	2.00	4.57	6.89
Moving average	2.10	4.70	7.24
Step ramp-rate	0.60	3.82	6.79

day, Simulations are performed iteratively to determine the central BESS capacity requirements for each day. For one day with the profile shown in Figure 2.8. The central BESS charging/discharging power is displayed in Figure 2.15 during the simulation to limit the ramp-rate within limitation after power smoothing.

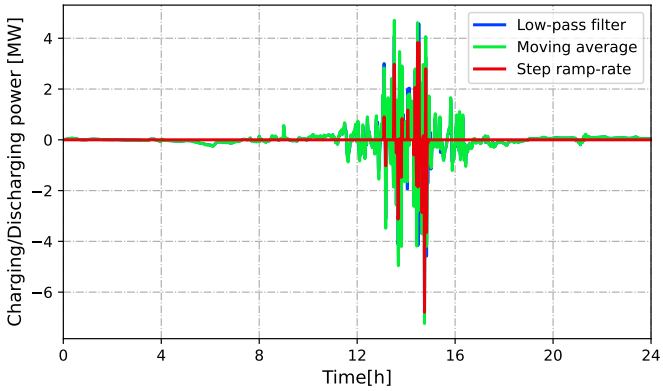

Figure 2.15: Charging/Discharging power of the *battery1* (positive value for charging; negative value for discharging).

The central BESS is primarily active during daytime hours when the DRES generates significant power because most power fluctuations occur during that period. The corresponding central BESS SOC from 8:00 AM to 8:00 PM on that day is depicted in Figure 2.16. We can observe that the SOC of the central BESS maintains an acceptable value throughout the day, demonstrating the effectiveness of my model. The power before and after power smoothing for different methods is shown in Figure 2.17. The black line represents the power through line *Line Feeder 1*, which is the power without power smoothing. The blue line indicates the power through transformer *T Feeder 1* when the Low-pass Filter method is applied to smooth the power in *Feeder 1*.

To accurately determine central BESS capacity, it is critical to conduct a simulation spanning a minimum of one year, considering the variation in seasons and weather conditions. The research presented in this section encompasses such a one-year simulation. As depicted in Figure 2.18, the daily central BESS capacity requirements vary throughout the year. Specifically, the requirements in January, February, November, and December are lower due to decreased DRES-generated power. Furthermore, there is a marked increase in central BESS capacity needs on days with significant intermittency in DRES-generated power.

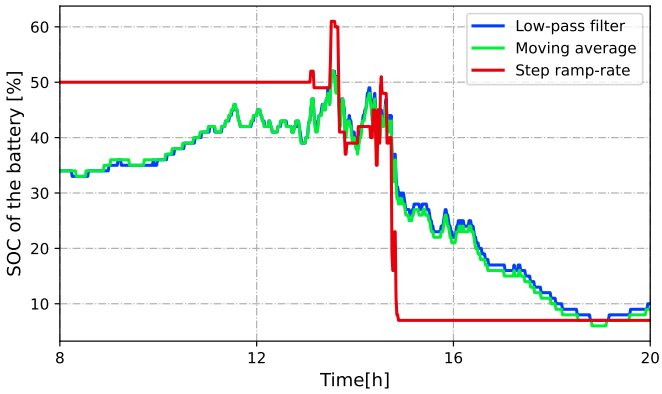

Figure 2.16: Soc of *battery1* during one day.

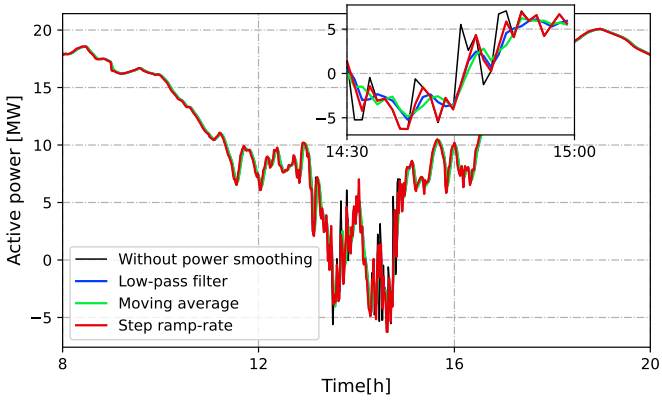

Figure 2.17: Power smoothing performance during one day at *Feeder 1*.

A comparative analysis of the Low-pass Filter, Moving Average, and Step Ramp-rate methods reveals that the latter necessitates substantially less central BESS capacity. In order to meet the power smoothing goal all year round, the Low-pass Filter, Moving Average, and Step Ramp-rate methods necessitate central BESS capacities of 4.18 MWh, 3.70 MWh, and 1.01 MWh, respectively. However, tolerating brief periods of non-adherence to the power smoothing target can significantly reduce the requisite central BESS capacity. For instance, if a 10% deviation from the power smoothing target is permissible, the necessary central BESS capacities diminish to 3.89 MWh, 3.44 MWh, and 0.45 MWh, respectively.

The sensitivity analysis, as shown in Table 2.5, elucidates the impact of varying allowable deviations from the power smoothing target on the central BESS capacity requirements for the three power smoothing methods. Notably, the Step Ramp-rate method consistently requires the least central BESS capacity, attesting to its efficiency in power smoothing. As the acceptable deviation shrinks, signifying stricter power quality stan-

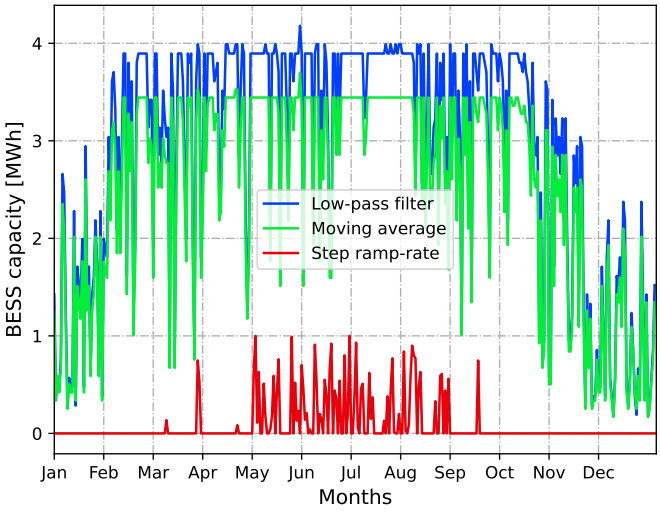

Figure 2.18: Central BESS capacity requirements at each day during one year.

dards, all methods demand increased central BESS capacity, thereby underscoring the trade-off between power quality and central BESS capacity requirements. Moreover, the Step Ramp-rate method exhibits more significant reductions in central BESS capacity requirements than the Low-pass Filter and Moving Average methods.

Table 2.5: Central BESS capacity sensitivity analysis considering the deviation allowable

Deviation possibility	Lower-pass fliter	Moving average	Step ramp-rate
10%	3.89	3.44	0.45
5%	3.95	3.45	0.63
2%	3.99	3.47	0.82
1%	4.01	3.50	0.92
0%	4.18	3.69	1.01

The simulation results demonstrate that my stochastic simulation-based approach effectively compares the performance of various power smoothing methods and performs central BESS sizing using probability density analysis of at least one year of simulation results. By considering different power smoothing methods, the optimal central BESS capacity can be determined through striking a balance between economic considerations and power smoothing performance. This approach ensures a more informed decision-making process for selecting and implementing suitable power smoothing techniques and central BESS capacity in renewable energy systems.

2.4. CONCLUSION

In this chapter, the effects of increased DRES penetration on voltage violations and evaluated the necessary central BESS capacity for power smoothing in distribution networks are examined. The analysis demonstrated that the $Q(V)$ control method yielded superior results compared to other control methods, and an increased number of DRES installations resulted in a tighter distribution of DRES maximum installed capacity. A one-year simulation indicated that the risk of voltage violations could be minimized to 5.68% with an appropriately designed DRES installation and control strategy. The case study for determining central BESS capacity for power smoothing revealed that the Step Ramp-rate Control Strategy necessitated significantly lower central BESS capacity than other methods while preserving power quality. These findings can assist network operators and planners in efficiently integrating renewable energy sources and storage systems for a reliable and sustainable power grid.

3

DISTRIBUTED COOPERATIVE VOLTAGE REGULATION

This chapter proposes a novel distributed cooperation voltage regulation method for future DNs. The proposed method can minimize the number of agents involved in the voltage regulation and minimize the change of required power for voltage regulation, which together minimizes the need for re-dispatching, i.e. the impact of voltage regulation on the exchange of energy. Moreover, the proposed method performs on-line optimization, i.e. the value of the decision variable is physically implemented as a controller set-point at each iteration, reducing the response time. The algorithm presented is benchmarked against the alternate direction method of multipliers (ADMM) and centralized optimization methods. The results show the voltage regulation effectiveness. The proposed method performs almost the same voltage regulation efficiency as the centralized method, which involves fewer agents. Compared to the ADMM method, the proposed method dramatically reduces the action time and does not require re-tuning if the network topology or agent participation changes.

Parts of this chapter have been published in IEEE Transactions on Smart Grid with the title: *Distributed cooperation for voltage regulation in future distribution networks*, vol. 13, no. 6, pp. 4483-4493, Nov. 2022, doi: 10.1109/TSG.2022.3191389 [41].

3.1. INTRODUCTION

The results in Chapter 2 show that voltage violations rather than thermal violations primarily constrain DRES penetration levels. Although the proposed local voltage control method enhances the maximum DRES penetration level of the power grid, it does not fully meet the anticipated levels for future DNs. For example, using the Q(V) method, even with a penetration level of 60.6% (28 MW in MV CIGRE network), there is a voltage violation risk of about 5.68% during a simulation of a year. Hence, relying solely on the local voltage control method is not adequate to address the voltage violation issue and achieve higher DRES penetration levels in future DNs. The integration of ICT into power grids has led to significant advances in grid management and operation. One such advance is ANM, which has emerged as a new opportunity to control and accommodate DRES to increase renewable energy capacity [23]. ANM aims to optimize grid performance by intelligently managing various grid components and resources.

ANM is suitable for power grid operation and control. It controls and coordinates active units to realize voltage regulation can be divided into three categories: centralized, decentralized, and distributed methods [59]. In all of these approaches, agents must be willing to install smart meters to monitor their information and share resources.

Centralized method: In this approach, a central coordinator has access to all the network information and solves the optimal voltage regulation problem [60, 61]. It collects and processes all the necessary information and issues control commands to maintain the desired voltage levels. The main drawbacks of centralized control are the computational cost of handling large amounts of data and the investments in communication channels. Furthermore, data privacy, cyber-attacks, and communication failure must be considered when implementing centralized methods.

Decentralized method: This approach divides the network into several zones, allowing the application of optimal methods on a smaller scale within each zone [62, 63]. Each has its local controller responsible for managing voltage within its respective zone. However, this method faces challenges, such as determining the optimal partitioning of the network and potential operational conflicts due to simultaneous responses from different zones [64, 65].

Distributed method: This method is based on a network of interconnected agents that collectively exchange information and make local decisions to optimize voltage levels across the network. Distributed convex optimization algorithms, such as the ADMM, are widely used for voltage regulation [66, 67].

Each of these voltage regulation methods has its own advantages and challenges. Centralized methods face computational and communication challenges, decentralized methods grapple with network partitioning and operational conflicts, and distributed cooperation approaches tackle convergence speed and result in accuracy while addressing fairness in power-sharing.

As DRES integration increases, the complexity and variability of the grid will increase, making centralized methods less efficient and scalable. Additionally, the rapid development of ICT will enable more effective peer-to-peer communication and information exchange, enhancing the feasibility of distributed cooperation approaches. Furthermore, distributed methods can accommodate data privacy concerns, as they do not require sharing sensitive information with a central coordinator. Moreover, distributed meth-

ods are more resilient to cyber-attacks and communication failures, as they do not rely on a single central control. Finally, the distributed method can adapt more effectively to local voltage violations, as it allows agents with higher potential for voltage regulation to contribute more, resulting in a more optimized and efficient voltage regulation process. This adaptability ensures that the grid can respond dynamically to changing conditions, maintaining stability even as the power system evolves.

The ADMM, an algorithm that blends the benefits of the Dual Decomposition algorithm (DD) and augmented Lagrangian methods, is widely used to solve distributed convex optimization problems, including voltage regulation [66, 67]. This and many other distributed optimization methods decompose the global optimization problem into small local subproblems. The convergence speed and results accuracy are the most important challenges addressed in the literature [68, 69]. References [70, 71, 72] extend the ADMM method to unbalanced three-phase networks, demonstrating successful convergence even for larger networks. In order to realize fairness among agents, consensus-based algorithms are used in references [73, 74, 75] to maintain equal power sharing among resources. However, voltage violation is a local problem; hence, some agents have a higher potential for voltage regulation than others. In this light, fairness in power-sharing is sub-optimal from the purely technical point of view.

Although the ADMM algorithm is one of the most known distributed approaches, it still requires significant computational time to reach convergence for solving the power flow problem [71]. Furthermore, the choice of Lagrange multipliers and penalty parameters plays a vital role in obtaining realistic convergence times [70]. For applications like voltage regulation that require a quick response (spanning seconds to minutes), fewer convergence iterations and a fast response are essential. Therefore, reference [76] based on dual ascent algorithm proposes an online optimization for distributed voltage control, in which set-points are implemented after each iteration.

A novel distributed cooperation method is proposed to get the benefits of distributed control and overcome the above shortcomings. The main contribution of this chapter is twofold. First, the proposed method uses the minimal number of agents and the minimal amount of contributed power to regulate voltage. By reducing the number of agents and their power contribution, the need for re-dispatching is minimized, i.e., the deviations from the nominal power exchange are minimized. The nominal power exchange is associated with comfort levels and financial transactions; hence, it is essential to minimize deviations from it. The proposed algorithm relies on voltage sensitivity to engage only the agents with the highest potential to regulate voltage. Second, the proposed method implements the set points in each iteration in the spirit of online optimization. Hence, the response time of the algorithm is minimal, and the voltage violations are acted upon quickly, much faster than with ADMM and similar algorithms.

The voltage problem formulation is introduced in Section 3.2. In Section 3.3, the distributed cooperation voltage regulation method is proposed. The voltage sensitivity characteristics and the process of applying the method in an online fashion are also presented in this section. In Section 3.4 cases studies are shown. Finally, the concluding remarks are presented in Section 3.5.

3.2. VOLTAGE PROBLEM FORMULATION

The control scheme of the distributed cooperation approach is shown in Figure 3.1 in which communication channels are aligned with cables to realize peer-to-peer information exchange. In the scheme, each node is monitored and controlled by an Intelligent Electronic Device (IED) which is defined as one agent in the proposed distributed cooperation method. The agent can measure the data at its own location, exchange its information with neighbors, do simple calculations, provide its flexibility information (i.e. its available capacity for regulation) and control its own controllable assets to change their absorbed or injected power.

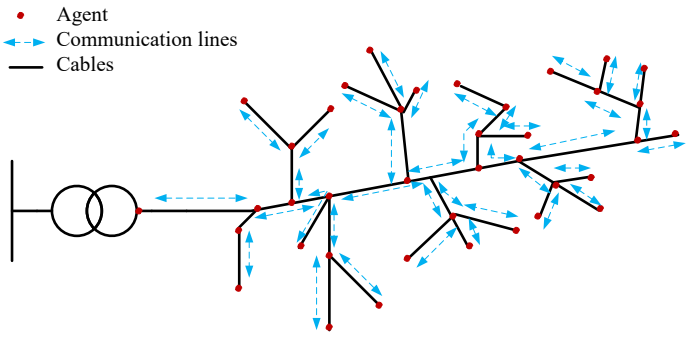

Figure 3.1: Scheme of distributed cooperation control based on the peer-to-peer communication network which is aligned with the network topology

This section outlines the specific network settings and the configuration of DRES and other assets considered for the distributed voltage regulation study. The aim here is to detail the operational environment and constraints that influence the deployment and effectiveness of the proposed methods. Each part of the system's configuration is described to ensure clarity on how the proposed voltage regulation method interacts with the network's dynamic characteristics.

In this chapter, the controllable assets are denoted as DRES and involve plug-in EVs, which can charge or discharge; PV converters which can change the provided active and reactive power; and capacitor banks which can provide reactive power. Because the time-series characteristics of those elements vary significantly, and the energy capacity, SOC and even EV user behavior can be considered internal to the assets and privacy protected, the voltage problem would become too complex to analyze and solve if I included their models in the voltage regulation algorithm. Therefore, I do not include their models in the voltage regulation algorithm in this chapter. Instead, available power limits are assumed to be given and deterministic. The next chapter will discuss how to manage energy to provide the power to regulate the voltage for each agent. The centralized voltage regulation model is presented after the introduction of basic terminology in this chapter. And this model is used as a benchmark for the distributed approach.

3.2.1. POWER FLOW FORMULATION

The radial network structure enables efficient computation and improved convergence properties in power flow problems. Here, I delve into the power flow formulation and present a schematic representation of a distribution feeder, as shown in Figure 3.2. This illustration highlights the key variables and parameters relevant to the derivation of voltage regulation. The parameters are consistent with the following equations, which will be discussed in detail. This graphical representation assists in understanding the underlying relationships between the variables, providing insights into how voltage regulation can be effectively modeled and controlled in radial DNs.

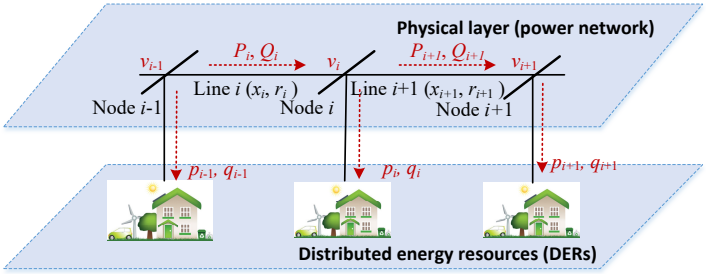

Figure 3.2: Distribution feeder with variables of relevance for derivation of voltage regulation

For radial DNs with a discrete set of loads, the branch flow model is well established based on the DistFlow equations [77] as:

$$P_{i-1} = P_i + r_i \frac{P_i^2 + Q_i^2}{v_i^2} + p_{i-1}, \tag{3.1}$$

$$Q_{i-1} = Q_i + x_i \frac{P_i^2 + Q_i^2}{v_i^2} + q_{i-1}, \tag{3.2}$$

$$v_{i+1}^2 - v_i^2 = -2\left(r_i P_i + x_i Q_i\right) + \left(r_i^2 + x_i^2\right) \frac{P_i^2 + Q_i^2}{v_i^2}, \tag{3.3}$$

where $i = 1, 2, ..., n-1$ enumerates DERs agents of the feeder sequentially connected in a line, P_i and Q_i are the active power and reactive power from agent $i-1$ to agent i. The positive value of P_i and Q_i represents that the power is transferred from agent $i-1$ to agent i, while if the power is transferred from agent i to agent $i-1$, the value of P_i and Q_i are negative. v_i represents the voltage at agent i, and r_i and x_i are separately the resistance and reactants of the line i. p_i and q_i describe the net demand of agent i which are composed of local consumption (p_i^c and q_i^c) minus local generation (p_i^g and q_i^g) and power adjustment (p_i^a and q_i^a) controlled by agent, i.e.,

$$p_i = p_i^c - p_i^g - p_i^a, q_i = q_i^c - q_i^g - q_i^a. \tag{3.4}$$

The positive value of p_i^a and q_i^a is the increased injection power from assets of agent i into node i. On the contrary, the negative value of p_i^a and q_i^a means the power is transferred from the node to the assets of the agent.

The finite feeder line with the tap changing transformer located upstream can be modeled by the boundary conditions in the rescaled p.u. variables:

$$v_0 = 1, p_n = q_n = 0. \tag{3.5}$$

3.2.2. VOLTAGE DEVIATION MODEL

The voltage deviation between node i and node $i+1$ can be expressed as:

$$\begin{aligned} \Delta v_i &= v_i - v_{i-1} \\ &= I_i \left(r_i + j x_i\right) \\ &= \frac{P_i - jQ_i}{v_i} \left(r_i + j x_i\right) \\ &= \frac{P_i r_i + x_i Q_i}{v_i} + j \frac{P_i x_i - r_i Q_{ti}}{v_i}. \end{aligned} \tag{3.6}$$

As the voltage difference angle between two nodes is small in DNs, the voltage deviation across the feeders is approximately equal to the real part of the voltage drop. Therefore, the voltage deviation (Δv_i) can be approximated as:

$$\Delta v_i \approx \frac{P_i r_i + x_i Q_i}{v_i}. \tag{3.7}$$

Then the voltage at node i can be expressed as:

$$\begin{aligned} v_i &= v_0 - \sum_{k=1}^{i} \left(v_{k-1} - v_k\right) \\ &= v_0 - \sum_{k=1}^{i} \frac{P_k r_k + x_k Q_k}{v_k}. \end{aligned} \tag{3.8}$$

It is obvious that the voltage at node i depends on the injected and absorbed power of all the nodes in the network. As the resistances and the reactance of the lines are constant values and the voltage at node i (v_i) depends on the power injected or absorbed in the networks, Equation 3.8 can be expressed as:

$$v_i = f\left(p_1, p_2, ..., p_n, q_1, q_2, ...q_n\right). \tag{3.9}$$

From the above analysis, the increment of generated power from the agent will automatically lead to the voltage rise problem, and the decrements of generated power from DERs will lead to the voltage drop problem. Thus the voltage deviation problem will become much heavier with increasing installation of DERs. Moreover, due to the intermittent characteristic of DERs, future DNs will face the voltage deviation problem more often. Fortunately, if the negative reactive power is applied or the load is sufficiently flexible to be increased, the voltage rise problem can be reduced. Vice versa, the voltage

drop problem can be solved by applying positive reactive power or reducing consumption. That means if I can make good use of DERs, their high penetration would not have a bad influence on the voltage stability, but can instead be utilized to solve the voltage problem.

3.2.3. VOLTAGE REGULATION MODEL

In the centralized voltage regulation approach, the main objective is to lower the use of power to regulate the voltage, while staying within desired limits.

$$\min_{p_i^a, q_i^a} \sum_{i=1}^{n-1} \left(\| p_i^a \| + \varphi \| q_i^a \| \right), \tag{3.10}$$

In Equation 3.10, $\varphi > 0$ represents the price ratio of reactive power and active power for voltage regulation, i.e. if the price to provide reactive power for voltage regulation is lower than active power, then the value of φ will be lower than 1. The term φ shows preference for using active or reactive power, which means curtial active power or use reactive power. To ease notation and without loss of generality, I drop this term from further derivations by setting its value to one. The agent operation set-point should be constrained by the room of controllable power as:

$$\underline{p_i^a} \leq p_i^a \leq \overline{p_i^a}, \forall i, \tag{3.11}$$

$$\underline{q_i^a} \leq q_i^a \leq \overline{q_i^a}, \forall i, \tag{3.12}$$

where $\underline{p_i^a}$ and $\underline{q_i^a}$ are negative and represent the highest controllable active and reactive power that can be absorbed by agent i to regulate the voltage, while $\overline{p_i^a}$ and $\overline{q_i^a}$ are positive values that represent the highest controllable active and reactive power that can be generated by agent i.

The power flow equations are represented by the DistFlow model as from Equation 3.1 to Equation 3.5 in Section 3.2.1.

The bus voltage magnitudes should be maintained within the acceptable range as:

$$\underline{v} \leq v_i \leq \overline{v}, \forall i, \tag{3.13}$$

where $\underline{v}$ is the voltage lower limitation, and $\overline{v}$ is the voltage upper limitation, according to voltage violation standard of the DN.

3.2.4. LINEARIZED VOLTAGE PROBLEM

The formulation of the voltage regulation problem as a linear program is presented with a detailed description of the constraints and objectives. The optimal voltage regulation model given by Equation 3.1-Equation 3.5, and Equation 3.10-Equation 3.13 is non convex because of the flow related constraints Equation 3.1-Equation 3.3. Therefore, the voltage regulation model must be linearized in order to solve the regulation problem. In this chapter, Equation 3.3 is linearized as:

$$v_i = v_i^b + v_i^a, \tag{3.14}$$

$$v_i^a = \sum_{j=1}^{n-1} \left(\frac{\partial v_i}{\partial p_j} p_j^a + \frac{\partial v_i}{\partial q_j} q_j^a \right), \tag{3.15}$$

where v_i^b is the voltage at agent i before voltage regulation, v_i^a is the difference in the voltage value caused by voltage regulation. The voltage sensitivities $\frac{\partial v_i}{\partial P_j}$ and $\frac{\partial v_i}{\partial Q_j}$ show the voltage regulation potential of agents. The higher voltage sensitivity of an agent, the higher its voltage regulation potential and lower is the power needed to perform regulation.

In this chapter, Perturb and Observe Power Flow Based method [78] is applied to get the voltage sensitivity. The voltage sensitivity to active power s_{ij}^p is defined as the deflection per unit voltage at node i across the active power at node j ($\partial v_i / \partial p_j$), and s_{ij}^q is defined as $\partial v_i / \partial q_j$. If the voltage sensitivity $s_{ij}^p$is needed, the calculation steps of the Perturb and Observe Power Flow Based method are as follows,

1. Record the voltage v_i.
2. Add a small active power injection Δp_j at node j.
3. Record the new voltage $v_i^{'}$, and get the difference Δv_i through subtracting the voltage $v_i^{'}$ ($\Delta v_i = v_i^{'} - v_i$).
4. Δv_i is divided by Δp_j to obtain voltage sensitivity s_{ij}^p ($\partial v_i / \partial p_j$).

Finally, the linear formulation of the voltage regulation model is given as:

$$\min_{p_i^a, q_i^a} \sum_{i=1}^{n-1} \left(\| p_i^a \| + \| q_i^a \| \right), \tag{3.16}$$

$$s.t. \quad \underline{p_i^a} \le p_i^a \le \overline{p_i^a}, \forall i, \tag{3.17}$$

$$\underline{q_i^a} \le q_i^a \le \overline{q_i^a}, \forall i, \tag{3.18}$$

$$\underline{v} \le v_i \le \overline{v}, \forall i, \tag{3.19}$$

$$v_i = v_i^b + \sum_{j=1}^{n-1} \left(s_{ij}^p p_j^a + s_{ij}^q q_j^a \right). \tag{3.20}$$

According to the Perturb and Observe Power Flow Based method, the values of voltage sensitivities s_{ij}^p and s_{ij}^q can be seen as known time-varying constants, and the only unknown variables are p_i^a and q_i^a. Therefore, the voltage regulation problem becomes linear and convex.

The linearized and centralized voltage regulation from Equation 3.16-Equation 3.20 is used as a benchmark for the distributed approach, which is described in the following section.

3.3. DISTRIBUTED COOPERATION FOR OPTIMAL VOLTAGE REGULATION

In the distributed approach, beside the effort to minimize the contribution of active and reactive power to regulate the voltage, I also try to minimize the number of engaged agents. To do this properly, I dispatch the agents according to their capacity to regulate, which is derived based on voltage sensitivity.

3.3.1. VOLTAGE SENSITIVITY CHARACTERISTIC

The voltage sensitivity of node i to node $i+1$ ($\frac{\partial v_i}{\partial p_{i+1}}$) can be shown as:

$$\frac{\partial v_i}{\partial p_{i+1}} = \left(\frac{\partial v_i}{\partial p_i} / \frac{\partial P_i}{\partial p_i}\right) \cdot \frac{\partial P_i}{\partial P_{i+1}} \cdot \frac{\partial P_{i+1}}{\partial p_{i+1}}. \tag{3.21}$$

For an arbitrary agent (node i) in radial DNs, if only p_i changes, the increment of P_i is approximately equal to the increment of p_i, namely $\frac{\partial P_i}{\partial p_i} \approx 1$, then $\frac{\partial v_i}{\partial p_{i+1}}$ can be derived as:

$$\frac{\partial v_i}{\partial p_{i+1}} = \frac{\partial v_i}{\partial p_i} \cdot \frac{\partial P_i}{\partial P_{i+1}}. \tag{3.22}$$

Based on Equation 3.1, the $\frac{\partial P_{i-1}}{\partial P_i}$ can be derived as follows:

$$\begin{aligned} \frac{\partial P_{i-1}}{\partial P_i} &= 1 + 0 - 2r_i \frac{{P_i}^2 + {Q_i}^2}{{v_i}^3} \cdot \frac{\partial v_i}{\partial P_i} + 2r_i \frac{P_i}{{v_i}^2} \\ &= \frac{{v_i}^3 - 2r_i({P_i}^2 + {Q_i}^2)\frac{\partial v_i}{\partial P_i} + 2r_i P_i v_i}{{v_i}^3}. \end{aligned} \tag{3.23}$$

If nodes $i-1$, i and $i+1$ extract power, then p_{i-1}, p_i, and p_{i+1} in Figure 3.2 are positive. The transferred power over lines $i-1$, i and $i+1$ (P_{i-1}, P_i , P_{i+1}) is positive, and the relationship of voltage from node $i-1$ to node $i+1$ is $v_{i-1} \geq v_i \geq v_{i+1}$. Since the value of $\frac{\partial v_i}{\partial P_i}$ is negative and the value of P_i is positive, the value of $\frac{\partial P_{i-1}}{\partial P_i}$ is larger than 1.

$$\frac{\partial P_{i-1}}{\partial P_i} > 1. \tag{3.24}$$

Based on Equation 3.24, the value of $\frac{\partial P_i}{\partial P_{i+1}}$ is also bigger than 1, and $\left|\frac{\partial v_i}{\partial p_{i+1}}\right| > \left|\frac{\partial v_i}{\partial p_i}\right|$ in Equation 3.22. Evidently, in the case of a voltage drop, voltage regulation can be achieved with less resources (i.e. power) if I perform regulation on the neighboring node with lower voltage.

The characteristic of voltage sensitivity $\frac{\partial v_i}{\partial p_{i-1}}$ can be derived similarly as for $\frac{\partial v_i}{\partial p_{i+1}}$, and it is shown as:

$$\begin{aligned} \frac{\partial v_i}{\partial p_{i-1}} &= \left(\frac{\partial v_i}{\partial p_i} / \frac{\partial P_i}{\partial p_i}\right) \cdot \frac{\partial P_i}{\partial P_{i-1}} \cdot \frac{\partial P_{i-1}}{\partial p_{i-1}} \\ &= \frac{\partial v_i}{\partial p_i} \cdot \frac{\partial p_i}{\partial P_{i-1}}. \end{aligned} \tag{3.25}$$

Based on Equation 3.24, the value of $\frac{\partial p_i}{\partial P_{i-1}}$ is smaller than 1, and $\left|\frac{\partial v_i}{\partial p_{i-1}}\right| < \left|\frac{\partial v_i}{\partial p_i}\right|$. It is easy to show that $\left|\frac{\partial v_i}{\partial p_i}\right| < \left|\frac{\partial v_i}{\partial p_{i+1}}\right|$. If I consider reactive power, following the same steps I arrive at a similar result for voltage sensitivity to reactive power. Therefore, Proposition 1 is presented.

Proposition 1. In the case of a voltage drop, the characteristic of voltage sensitivity is as follows:

$$\begin{cases} \left|\frac{\partial V_i}{\partial P_{i-1}}\right| < \left|\frac{\partial V_i}{\partial P_i}\right| < \left|\frac{\partial V_i}{\partial P_{i+1}}\right|, \\ \left|\frac{\partial V_i}{\partial Q_{i-1}}\right| < \left|\frac{\partial V_i}{\partial Q_i}\right| < \left|\frac{\partial V_i}{\partial Q_{i+1}}\right|. \end{cases} \tag{3.26}$$

In words, if the voltage drop happens at node i, it is more beneficial to adjust the power of the neighboring node with lower voltage.

Now I consider the case in which the nodes $i-1$, i and $i+1$ inject power, and p_{i-1}, p_i, and p_{i+1} are negative. The power in lines P_{i-1}, P_i , P_{i+1} is negative, and the respective voltages are $v_{i+1} \geq v_i \geq v_{i-1}$. Since the value of $\frac{\partial v_i}{\partial P_i}$ is positive and the value of P_i is negative, estimating the range of values for $\frac{\partial P_{i-1}}{\partial P_i}$ from Equation 3.23 is not as straightforward. However, if the increment in line losses is negligible, the value of $\frac{\partial P_{i-1}}{\partial P_i}$ is equal to 1, and $\frac{\partial v_i}{\partial p_{i+1}} \approx \frac{\partial v_i}{\partial p_i}$. The higher the voltage, the lower are the line losses, and the value of $\frac{\partial P_{i-1}}{\partial P_i}$ is closer to 1 and the value of $\frac{\partial v_i}{\partial p_{i+1}}$ is closer to $\frac{\partial v_i}{\partial p_i}$. In the case of reactive power, following the same steps I reach at the same conclusions for sensitivity. Therefore, Proposition 2 is presented.

Proposition 2. In the case of voltage rise, the characteristic of voltage sensitivity is:

$$\begin{cases} \left|\frac{\partial v_i}{\partial p_i}\right| \approx \left|\frac{\partial v_i}{\partial p_{i+1}}\right|, \\ \left|\frac{\partial v_i}{\partial q_i}\right| \approx \left|\frac{\partial v_i}{\partial q_{i+1}}\right|. \end{cases} \tag{3.27}$$

In words, if the voltage rise problem happens at node i, there is a relatively small difference in either adjusting the power by node i itself or by its neighboring nodes with higher voltage.

3.3.2. THE PROCESS OF ONLINE DISTRIBUTED COOPERATION FOR VOLTAGE REGULATION

In Section 3.3.1, I arrived at the conclusion that to mitigate voltage rise, it is almost equally optimal if I regulate the voltage on the node that faces voltage rise or on one of its neighbors. And in the case of the voltage drop, it is much more sensible to regulate it on one of the neighbors. Moreover, in order to guarantee that the DN operates well, the agent who faces severe voltage problem should be regulated first. Therefore the agent i with the most severe voltage problem is chosen and given the priority for regulation. In this chapter, I define the set NC_i as the union of agent i and its nearest neighbors with voltage regulation ability. If the voltage cannot be regulated only by agents NC_i, all the

available power of these agents will be used up. On the other hand, if the voltage problem can be regulated only by agents NC_i, the power requirement for each of them will be determined.

The evaluation of agents NC_i voltage regulation ability is based on Equation 3.28. If the voltage of agent i was lower than the voltage limit $\underline{v}$ and at the same time the maximum voltage regulation capability by agents NC_i ($|\sum_{j\in NC_i}\left(\frac{\partial v_i}{\partial p_j}\underline{p_j^a}+\frac{\partial v_i}{\partial q_j}\underline{q_j^a}\right)|$) is higher than the voltage deviation from the limit ($|\underline{v}-v_i|$), agents NC_i can regulate the voltage drop problem by themselves. Similarly, if the voltage of agent i was higher than the voltage limit $\overline{v}$ and at the same time the maximum voltage regulation capability by agents NC_i ($|\sum_{j\in NC_i}\left(\frac{\partial v_i}{\partial p_j}\overline{p_j^a}+\frac{\partial v_i}{\partial q_j}\overline{q_j^a}\right)|$) is higher than the voltage deviation from the limit ($|\overline{v}-v_i|$), the voltage rise problem can also be regulated only by agents NC_i.

$$\begin{aligned}&|\underline{v}-v_i|\le\left|\sum_{j\in NC_i}\left(\frac{\partial v_i}{\partial p_j}\underline{p_j^a}+\frac{\partial v_i}{\partial q_j}\underline{q_j^a}\right)\right| \text{ and } v_i\le\underline{v},\\ &\qquad\qquad\text{or}\\ &|\overline{v}-v_i|\le\left|\sum_{j\in NC_i}\left(\frac{\partial v_i}{\partial p_j}\overline{p_j^a}+\frac{\partial v_i}{\partial q_j}\overline{q_j^a}\right)\right| \text{ and } v_i\ge\overline{v}.\end{aligned}\tag{3.28}$$

In order to use the minimal power to regulate the voltage when voltage regulation ability of agent NC_i is sufficient, the optimal voltage regulation model in Section 3.2.4 is applied in distributed and online fashion among the neighbors to determine the regulation setpoint of each node. The online distributed optimal model can be formulated based on Equation 3.16-Equation 3.20 as:

$$\min_{p_{j,t}^a,q_{j,t}^a}\sum_{j\in NC_{i,t}}\left(\|p_{j,t}^a\|+\|q_{j,t}^a\|\right),\tag{3.29}$$

$$s.t.\quad \underline{p_{j,t}^a}\le p_{j,t}^a\le\overline{p_{j,t}^a},\ j\in NC_{i,t},\tag{3.30}$$

$$\underline{q_{j,t}^a}\le q_{j,t}^a\le\overline{q_{i,t}^a},\ i\in NC_{i,t},\tag{3.31}$$

$$\underline{v}\le v_{i,t+1}\le\overline{v},\ i\in NC_{i,t},\tag{3.32}$$

$$v_{i,t+1}=v_{i,t}^b+\sum_{j\in N_{i,t}}\left(s_{ij,t}^p p_{j,t}^a+s_{ij,t}^q q_{j,t}^a\right),\tag{3.33}$$

where $p_{j,t}^a$, $q_{j,t}^a$, $\underline{p_{j,t}^a}$, $\overline{p_{j,t}^a}$, $s_{ij,t}^p$, $s_{ij,t}^q$ are the p_j^a, q_j^a, $\underline{p_j^a}$, $\overline{p_j^a}$, s_{ij}^p, s_{ij}^q,of agent j at time t separately, and $\overline{NC_{i,t}}$ is the NC_i of agent i at time t, and $v_{i,t+1}$ is the regulated voltage at time $t+1$.

An event-triggered communication approach is used to relax the requirement for continuous real-time information exchange among agents. If the agent does not face any voltage problem and does not get any requests from others, then there is no need to transfer its information to its neighbor and do any actions. The process of distributed cooperation for optimal voltage regulation is as follows:

1. All agents check if they face the voltage problem or get information exchange requests from others or voltage regulation requirements from neighbors. If the agent faces a voltage problem, go to the next step. If the agent gets an information exchange request from others, it will exchange the information. If the agent gets a voltage regulation order from neighbors, do the voltage regulation action as orders. Otherwise, the agent does not act.
2. Exchange the information (v_t) with its neighbors and find the agents who face the most severe problem, i.e agents i. Agents i with the most severe problem can be more than one in the network because there may be several feeders in a network.
3. Agent i finds the agent set $NC_{i,t}$ to regulate the voltage.
4. If $NC_{i,t}$ is empty, the voltage problem cannot be regulated, and the process stops. If $NC_{i,t}$ is not empty, go to the next step.
5. Calculate the voltage sensitivity ($\partial v_i/\partial p_j, j \in NC_{i,t}$ and $\partial v_i/\partial q_j, j \in NC_{i,t}$) using the Perturb and Observe Power Flow Based method in Section 3.2.4.
6. Judge the agents $NC_{i,t}$ voltage regulation ability based on Equation 3.28. If the condition Equation 3.28 is satisfied then nodes $NC_{i,t}$ can regulate the voltage at agent i within the limits and I can proceed to step 7; otherwise, go to step 8.
7. Calculate the power agents $NC_{i,t}$ need to provide ($p^a_{j,t}, q^a_{j,t}$) based on Equation 3.29.
8. Agents $NC_{i,t}$ provide all the power they can provide to regulate the voltage.

The flow chart of distributed cooperation for voltage regulation is shown in Figure 3.3. The voltage is regulated firstly from the agents which face the worst voltage problem, and then through peer-to-peer communication, the DN gradually realizes self-organized voltage regulation actions. The voltage regulation support searching and information spreading will not stop until the voltage is regulated within the permitted limits or there are no resources available for voltage regulation. If there are sufficient resources, through continuous support from neighbors, the voltage will finally be regulated to an acceptable value. In order to handle singular situations, if one agent receives different voltage regulation instructions, then it will provide the average requested power.

The information exchange scheme based on agent i of the proposed method is shown in Figure 3.4. The algorithm assumes that the connectivity of agents follows the topology of the DN. If one of the agents falls out of the network, or if one of the nodes does not contain an agent, it is assumed that the existing agents are capable of reconnecting and bypassing the troubling node. Therefore, for the DNs, the proposed method can tolerate the failure of a single agent.

3.3.3. CONVERGENCE ANALYSIS

The voltage problem shown in Equation 3.29 is a convex problem with linear inequality constraints and can be written more compactly as

$$\begin{aligned} &\min_X C^T M, \\ s.t. \quad &AM \leq B, \end{aligned} \tag{3.34}$$

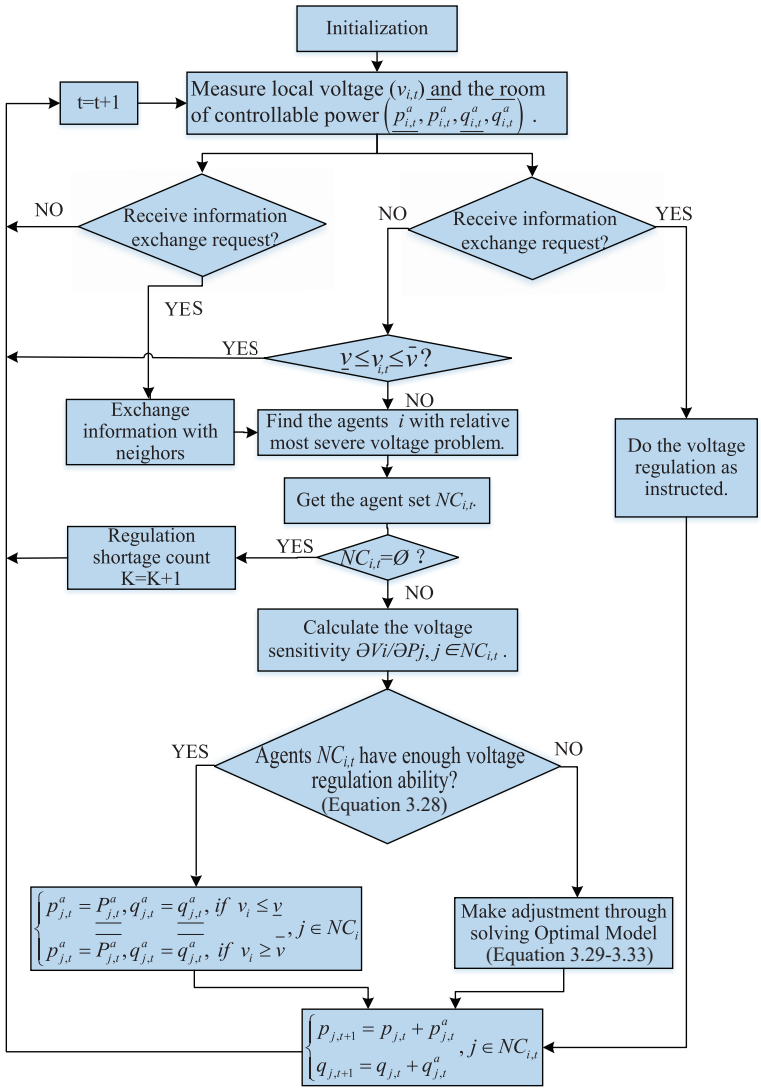

Figure 3.3: Flow chart of the distributed cooperation for voltage regulation approach

where M is the vector of decision variables collecting p_i^a and q_i^a, A is a coefficient matrix, C and B are coefficient vectors.

Despite the problem of linear formulation, a Lagrangian approach is still needed to facilitate the decomposition and analysis of the convergence. The Lagrangian equation of this voltage problem is

$$L(X,\lambda) = C^T X + \lambda(AM - B). \tag{3.35}$$

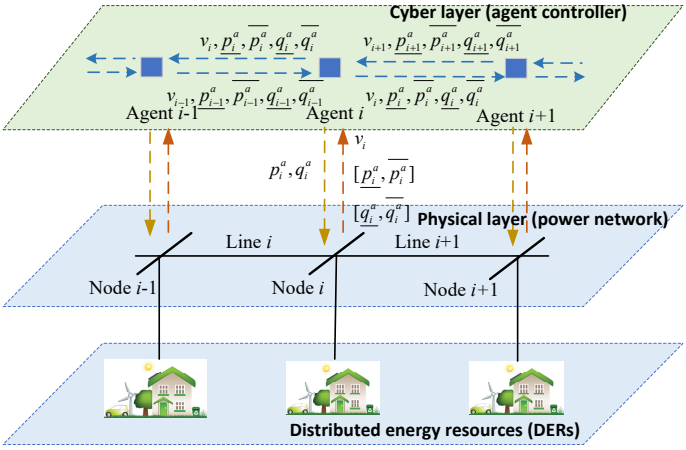

Figure 3.4: Information exchange scheme of proposed distributed cooperation optimal voltage regulation method

The voltage sensitivity S, which is equal to $\partial V/\partial X$, is in the gradient of the Lagrangian function. The update rules of M are from the higher gradient to the lower gradient, proving that the voltage can be asymptotically regulated within the limits. Details on how the Lagrangian method is implemented in a distributed manner, including the communication and computation steps involved, are provided to illustrate the practical application of this theoretical approach.

3.4. SIMULATION

3.4.1. TEST GRID

To demonstrate the effectiveness of the proposed method, case studies are carried out at the CIGRE LV distribution residential sub-network, and the topology is shown in Figure 3.5 [53]. There are 18 load nodes which host controllable elements to regulate the voltage, and they all can be controlled by the node agents. The base voltage in this test grid is 0.4kV. Each node's agent power comprises PVs, plug-in EVs and typical residential load. The PVs model is NA-V135h1 in DIgSILENT, while the load power and plug-in EVs follow reference [79]. According to this reference, the energy consumption of all plug-in EVs and energy generation of all PVs is 5.52% and 20.81% of the total load in the CIGRE LV network. These total values are equally distributed across the nodes. The EVs, PVs, pure residential load and net active power demand at each node in a typical day is shown in Figure 3.6.

3.4.2. CASES AND RESULTS

The simulation is performed in three parts. Firstly, in case 1, several single snapshot simulations are performed to evaluate the performance of minimizing the power usage

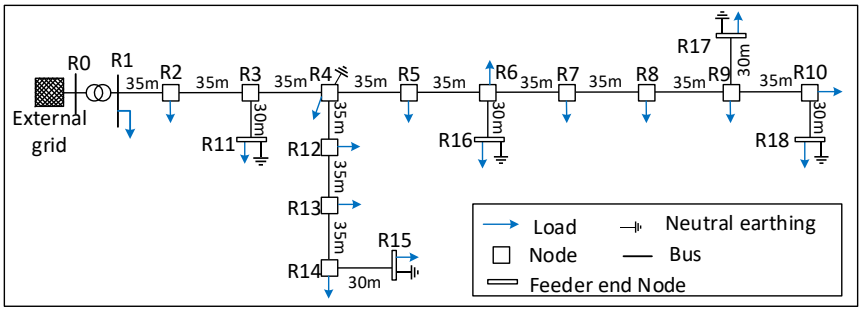

Figure 3.5: CIGRE LV distribution residential sub network [53]

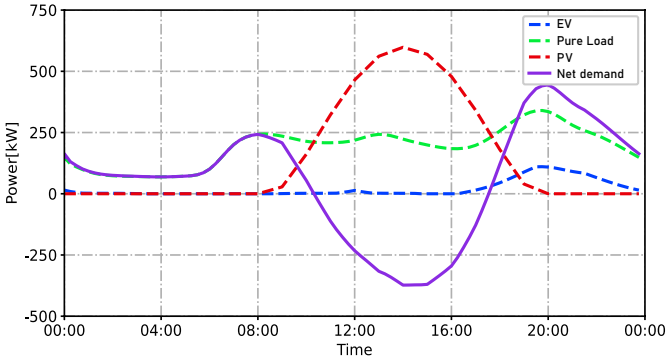

Figure 3.6: Active power demand in a typical day

for voltage regulation and to analyze the effect of the proposed method at one time step. Then, in case 2, a time-series simulation on a typical day is performed.

SINGLE SNAPSHOT SIMULATION

The power consumption data at one time step in the test grid is set to 20kW and 0.19kVar of all nodes, and the voltage limit is $0.95pu - 1.05pu$ [17]. In the first simulation, the available power for voltage regulation at each agent is within [-10kW, 10kW] and [-10kVar, 10kVar]. I make a comparison between three different objectives. They are minimizing contributing power for voltage regulation as shown in (Equation 3.16), minimizing the power flow losses, and minimizing voltage deviation. The mathematical formulation of the last two objectives is given in [80]. The total power usage for voltage regulation and power flow losses among these objectives are shown in Table 3.1. We can easily see that the power flow losses in the network do not show a considerable difference among the three objectives, with the maximum power loss difference being 8.71 kW for the minimum contribution power objective. Notably, its power usage for voltage regulation with the minimum contribution power objective is less than half compared to the other two objectives (82.39 VS 180). Hence, when compared to power losses, the power utilized for voltage regulation is substantially greater. Additionally, the power allocated for voltage

regulation displays a significant variation between different objectives. The voltage profiles among those three objectives are shown in Figure 3.7. We can see that all of these three objectives regulate the voltage within the limitation. Therefore, when minimizing contributing power to regulate the voltage, I not only keep the voltage within limits but also achieve this at minimal power expense.

Table 3.1: Comparison results between different objectives

Objectives	Power losses[kW]	Power usage for voltage regulation[kW]
Min contribution power	8.71	82.39
Min voltage deviation	7.80	180.00
Min power flow losses	7.79	180.02

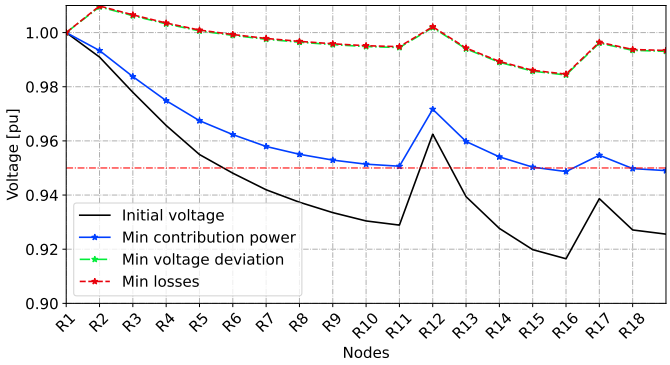

Figure 3.7: Voltage profiles before and after voltage regulation with different objectives

In the second single snapshot simulation, the proposed method, centralized optimization, ADMM and centralized optimization with fairness are simulated with Intel(R) Core(TM) i7-7700K CPU. The voltage is regulated within the limits after three iterations using the proposed method with 2.02 seconds. The ADMM can get relatively good results after 100 iterations, which need 45 minutes. The required regulation power from agents is shown in Figure 3.8. The required active power for each agent has a big difference between those three methods. The centralized fairness method engages all agents equally and uses the most power. The centralized method and ADMM result in the minimal required power, however compared to the proposed method, more power is needed to perform regulation (86.3 and 84.8 vs 58.9) and more agents are required (10 agents vs 8 agents). To appreciate the performance of the proposed method, the regulated voltage profiles between those methods are shown in Figure 3.9. I can see that the voltage can be regulated in a better way through the proposed method. It is because the voltage limitation constraint in my method is the precondition to quit an iteration, while in other methods, the voltage limitation constraint is handled as the penalty item in the objective function. The final results for voltage regulation performance depend on the setting of the penalty parameter.

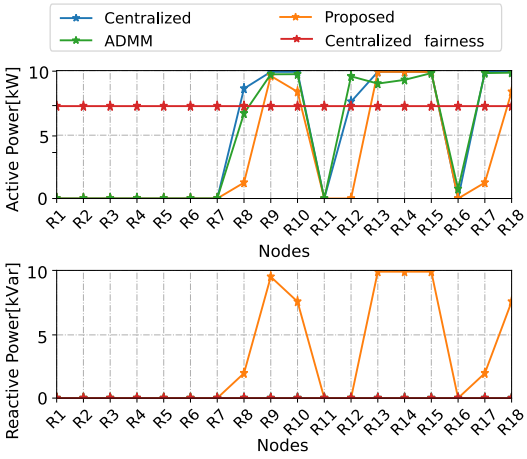

Figure 3.8: Required power to regulate the voltage

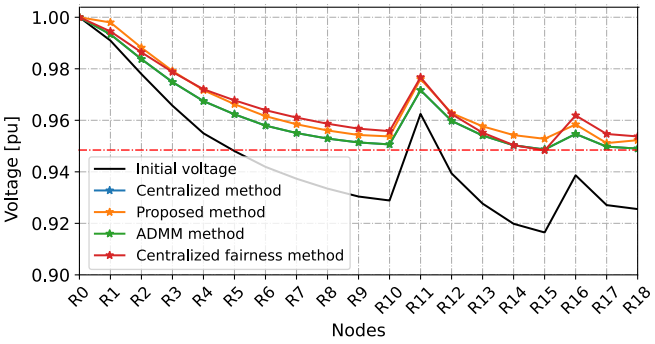

Figure 3.9: Voltage profile in the CIGRE LV residential sub-network

TIME-SERIES SIMULATION

A time-series simulation is performed to better observe the proposed method's voltage regulation efficiency. The net power consumption at each node follows Figure 3.6. The available reactive power and active power for voltage regulation at each agent can vary over the day. However, in the time-series simulation, the available power for voltage regulation at each agent is assumed to be at all times within [-15kW, 15kW]. The voltage limit is $0.95pu - 1.05pu$ and the time resolution is 15 minutes. The voltage profile at several nodes before voltage regulation is shown in Figure 3.10. The red dashed lines are the voltage limits. It is easy to notice that the voltage drop problem happens in the morning and evening (7:00-8:00; 18:0-23:00), and the voltage rise problem happens at noon (12:00-16:00).

When the proposed method is applied to regulate the voltage, the voltage profile after the regulation is shown in Figure 3.11 and the required active power of some agents

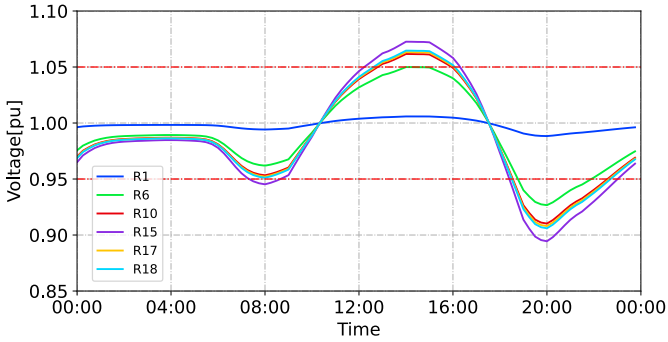

Figure 3.10: Voltage profile before voltage regulation in a typical day

is shown in Figure 3.12. It can be observed that the voltage can be regulated within the limits. In this simulation, once the agent indicates their power flexibility for voltage regulation, they will be treated equally. The preferences and constraints of agents are expressed through their available capacity for regulation. The effective agents are naturally first chosen to regulate the voltage within these limits. It is quite possible that the most effective agents will be chosen to provide voltage regulation often and for longer periods, while the ineffective agents will be utilized sporadically. As an example of higher agent utilization, see R1 in Figure 3.12. Although the agents should take into account their own preferences and capabilities for continuous engagement when they report their flexibility for the next time instance (next 15 minutes in this chapter), I still propose a weighting factor ρ to reduce the possibility that a misjudgment will have a high impact on the overall regulation. On one side, the weight factor can make all agents take on voltage regulation tasks more equally. On the other side, it can avoid asset discomfort caused by the agent taking on the voltage regulation task for a long duration. The weight factor is used to find the agent set NC_i in the Figure 3.3. In this simulation, the $NC_{i,t}$ is not the union of agent i and its nearest neighbors with voltage regulation ability but is defined as the union of agent i and the neighbors with the lowest value of Equation 3.36 who have voltage regulation ability. The formula for selecting agents using the weighting factor is:

$$\rho \frac{d_{j,t}}{\sum_{j=1}^{j=n-1} d_{j,t}} + (1-\rho) \frac{u_{j,t}}{\sum_{j=1}^{j=n-1} u_{j,t}}, \tag{3.36}$$

where $d_{j,t}$ is the distance of agent j and the agent with severe voltage problem i at time t, and $u_{j,t}$ is the total utilization time of agent j before time t.

The value of the weight factor is between zero and one, and it is used to indicate the operator's willingness to place greater value on effectiveness or fairness when choosing agents to regulate the voltage. The higher the weight factor, the more effectiveness is valued. In Figure 3.11 and Figure 3.12, the weight factor value is 1. Keeping everything else the same, the simulation results with weight factor 0 are shown in Figure 3.13. By comparing these Figures, it can be seen that the agents are more equally chosen when the weight factor is 0. The power providing time period during one day of each agent

is shown in Table 3.2. This table shows that the bigger the weight, the more fairness in total regulation hours. The required power at agent R17 with different weight factors is shown in Figure 3.14. I see that a lower weight factor prevents the use of one agent for a long continuous period of time. As a downside, the most effective agent is not always engaged in voltage regulation, leading to a higher contributing power for the regulation.

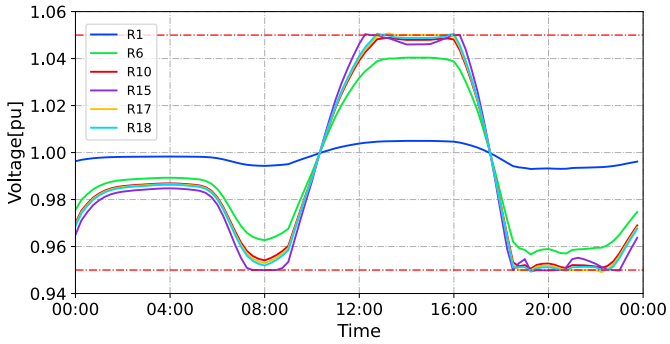

Figure 3.11: Voltage profile after voltage regulation by proposed method

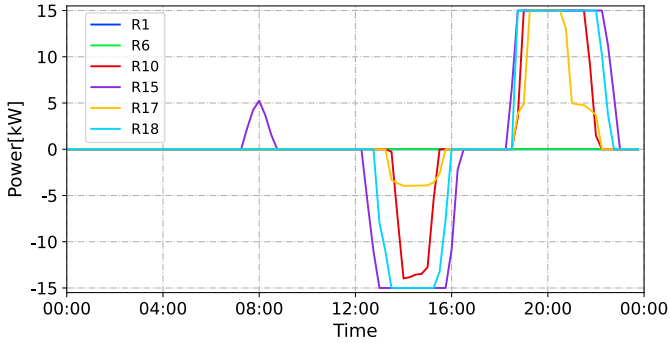

Figure 3.12: Required power to regulate the voltage by applying proposed method

3.5. CONCLUSION

This chapter proposes a novel distributed cooperation method for voltage regulation. Compared to the centralized control, the proposed method does not have a central controller which is limited by a single point of failure, high communication requirement, and computation burden. A study was performed in which one agent suddenly stopped providing voltage regulation without previous notice, and the robustness of the proposed method is observed in Section 4.4.5. The proposed distributed cooperation method is naturally reliable and suitable for complex DNs. Secondly, it uses fewer agents to regulate the voltage within the limits. The proposed method has a faster response time to the

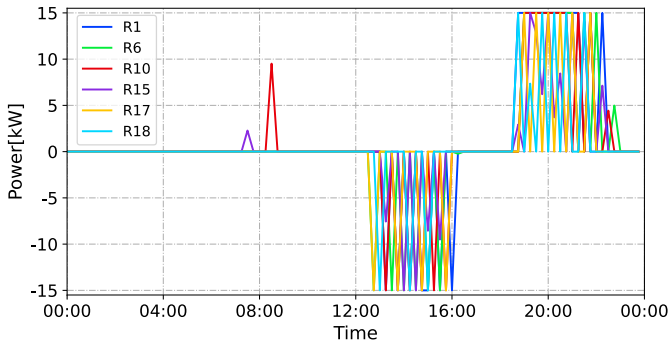

Figure 3.13: Required power with weight factor 0

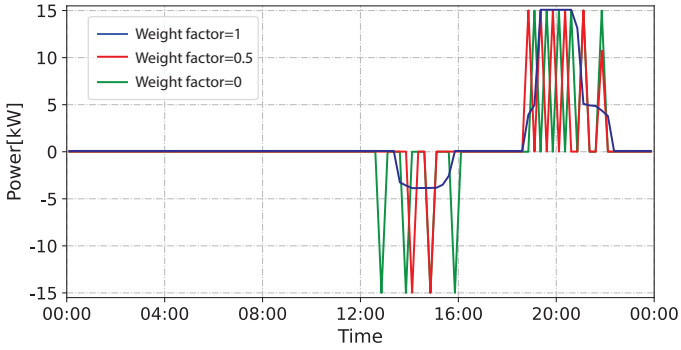

Figure 3.14: Required power of agent R17 with three different weight factors

Table 3.2: Hours to provide voltage regulation support at different agent with different weight factor

Weight factor	R1	R2	R3	R4	R5	R6	R7	R8	R9
0	5	4.5	4.5	4.75	4.75	4.5	4.75	4.5	4.5
0.5	2.25	3.75	4.5	5	4.5	4.25	2	2.25	3.5
1	0	0	0	0.5	0	0	1	1.5	2.75
Weight factor	R10	R11	R12	R13	R14	R15	R16	R17	R18
0	4.5	4.5	3.75	4	3.75	4	2.75	2.5	2.25
0.5	3.5	3	4.75	4.5	4.75	4.25	2	2	2.25
1	5.25	0	1.25	4	6.75	9.75	0	5.75	7

voltage problem than other distributed methods. It directly applies the calculated injections in each iteration rather than waiting for convergence before implementation. Considering unexpected errors, the proposed method can automatically regulate the voltage within the limits while relying on cooperation among neighbors. However, this study

does not investigate a special case in which one agent needs to regulate the voltage rise and the voltage drop problem at the same time. Agents simply average different voltage regulation instructions.

In this chapter, the voltage regulation from the perspective of the DSO has been approached. To accomplish effective voltage regulation, the internal energy management of the agent, ensuring adequate flexibility, is crucial. As a result, in the subsequent chapter, the energy management system from an agent's perspective will be delved deeply. This will enable the agent to offer flexibility to the DSO, achieve self-sufficiency, and more.

4

ENHANCED MPC ALGORITHM FOR ENERGY COMMUNITIES

This chapter introduces a novel four-stage energy management strategy, harnessing receding-horizon optimization to manage energy consumption within a PV-BESS-electrolyzer-fuel cell residential energy community setup. My approach uniquely sequences four optimization stages: yearly, monthly, day-ahead, and intra-day. This integration blends both long-term and short-term strategies in EMS development, positioning hydrogen produced by an electrolyzer as seasonal storage and a BESS for daily utilization. The algorithm presents three modes, each defined by a distinct objective function, catering to different user preferences: self-sufficiency, profit maximization in the energy market, and provision of balancing services to grid operators and external entities. The method's efficacy is demonstrated through simulations and a detailed analysis of an on-site PV-BESS-electrolyzer-fuel cell lab setup, encompassing algorithm efficiency assessment and a comparative performance review across the different operational modes. Furthermore, the reliability of the proposed distributed control algorithm in the event of the failure of a single agent is investigated, demonstrating its superiority over the centralized control algorithm. In general, the proposed algorithms can help energy communities achieve self-sufficiency, flexibility, and reliability, making a significant contribution to the sustainable development of the energy system.

Parts of this chapter have been submitted to IEEE PES ISGT EUROPE 2024 with the title: *A Multi-Stage Energy Management Approach Incorporating Seasonal Hydrogen Storage in a PV-BESS-Electrolyzer-Fuel Cell System* and 52nd IEEE Photovoltaic Specialists Conference with the title: *Design and Implementation a Local Energy Hub for Urban Environment.*

4.1. INTRODUCTION

Advanced technologies, such as ICT and AMI, are crucial for promoting effective communication between various agents—from industrial and commercial to residential end-users. This enhanced communication allows these agents to actively participate in the ancillary market to support the efficient operation of power grids. The EnergieKoplopers project in Heerhugowaard implemented a USEF flexibility market that allows end users to participate in energy trading. In its paradigm, each household can trade slightly more than 1 kWh per day [81].

The previous chapter proposes a distributed cooperation method for voltage regulation from the DSO perspective. However, it does not address the agent's internal energy management within the agent, which is needed to ensure voltage regulation flexibility. Developing an EMS is a foundational step to realizing the potential of distributed cooperative methods in the future power grid. An EMS ensures optimal usage of DRES, reducing waste and ensuring efficient operation. Providing the necessary controls and optimization strategies can help the DSO solve the power grid problem by smartly managing distributed energy.

Previous research, such as [82], delved into a stochastic EMS tailored for plug-in electric vehicles within parking lot aggregators. Studies [83] and [84] enhanced home EMS algorithms, emphasizing the importance of load flexibility and demand responsiveness to aggregator or system operator instructions. Given the increasing commitment to green energy, aligning supply with demand is paramount. In line with this, [85] introduced an EMS model based on mixed integer linear programming (MILP) for intelligent scheduling of smart devices and charging cycles of EVs to minimize energy costs. Similarly, references [86] and [87] utilized Demand-Side Management (DSM) techniques to balance energy consumption with supply, curb consumption peaks, and ensure closer alignment with power supply trajectories. More advanced algorithms, including deep reinforcement learning, have been incorporated into EMS to harmonize DRES with smart homes [88, 89].

In the quest for efficient, commercially viable energy storage, hydrogen fuel cells have emerged as front runners [90]. Combined with Lithium-ion batteries, it presents an ideal energy storage solution, supporting energy autonomy and trade [91]. The EMS model detailed in [92] aimed to reduce hydrogen production costs by optimizing the net costs associated with industrial hydrogen operations while ensuring system reliability. [93] employed fuzzy logic to guarantee that the hybrid system met the requisite load demands. In addition, [94] introduced an operational methodology for integrated energy systems comprising electrolyzers, fuel cells, BESS, hydrogen storage (HS), and PV. This approach sought to enhance the economic efficiency of the system by tapping into intraseasonal complementary energy through HS, while respecting the reliability constraints of photovoltaic energy.

However, the task of crafting an EMS that is adaptable to a diverse range of user needs and capable of handling the intricacies common to real-world hydrogen systems remains largely unaddressed. Additionally, the integration of long-term and short-term optimization strategies within the EMS, tailored to unique energy storage system attributes, requires deeper exploration.

In response to these challenges, a comprehensive four-stage energy management

strategy is proposed, using receding horizon optimization to regulate power fluctuations in a residential energy community system (ECS) of PV-BESS-electrolyzer-fuel cell. This strategy seamlessly melds four optimization stages: yearly, monthly, day-ahead and intraday, integrating long-term and short-term optimization strategies in the development of EMS, thus facilitating the use of hydrogen generated through electrolysis for seasonal storage. The algorithm presents three distinct modes designed to cater to different user preferences. Using a digital representation of the 24/7 Energy Lab, a real-world system located in The Green Village of TU Delft [95, 96], the performance of the proposed EMS algorithm is evaluated. Subsequent case studies investigate the robustness and versatility of the algorithm against traditional rule-based models. Additionally, comparative evaluations across different operational modes and insights for potential scalability are provided.

The subsequent sections of this chapter are as follows: Section 4.2 offers an overview of the energy system. Section 4.3 delineates the core challenge, explores the proposed algorithmic modes, and elaborates on the four-stage receding horizon optimization technique. Section 4.4 conducts a rigorous assessment of the EMS algorithm's efficiency. Finally, Section 4.5 summarizes the primary insights derived throughout this chapter.

4.2. SCHEMATIC OF THE ENERGY SYSTEM

The ECS under study integrates several key components: PV panels with a peak capacity of 6 kW, a household with the assumption of annual electricity consumption 4,200 kWh, a 14 kWh lithium-ion BESS, and an extensive hydrogen system. Power generated by the PV panels primarily satisfies household demand, with any surplus energy being diverted to storage solutions. The layout of this energy system is depicted in Figure 4.1. All elements of the ECS are connected on the alternating current (AC) side, each with its dedicated inverter, which enhances the system's adaptability. Within this setup, the lithium-ion BESS acts to even out daily fluctuations in energy generation and consumption, whereas the hydrogen system is designed to address longer-term seasonal imbalances. This sophisticated hydrogen setup comprises a 2.3 kW fuel cell, a 2.4 kW electrolyzer, a compressor, and an HS tank capable of holding up to 60 kilograms of hydrogen at 300 bar pressure (approx. half the annual electricity consumption). The electrolyzer, powered by the PV panels, splits water into hydrogen and oxygen. The stored hydrogen then serves as an energy reserve, with the fuel cell converting it back into electricity during periods of low PV output or when the BESS is fully utilized. The compressor maintains optimal hydrogen storage and facilitates hydrogen efficient transport. The ECS explored in this paper is not merely a theoretical or digital construct; it has been physically constructed and is operational within the Green Village at TU Delft, serving as a concrete example of sustainable energy integration in an urban setting [95, 96].

The Lithium-ion BESS addresses day-to-day energy fluctuations within this configuration, whereas the hydrogen system mitigates long-term or seasonal energy variances. This complementary interplay guarantees a consistent and reliable energy source, catering to various demand and supply conditions.

Regarding ancillary service for the DSO, the ECS can provide its available flexibility for trading within the ancillary service market as a flexibility service provider [97]. This prompts the ECS to recalibrate and align with the requirements laid out by the grid op-

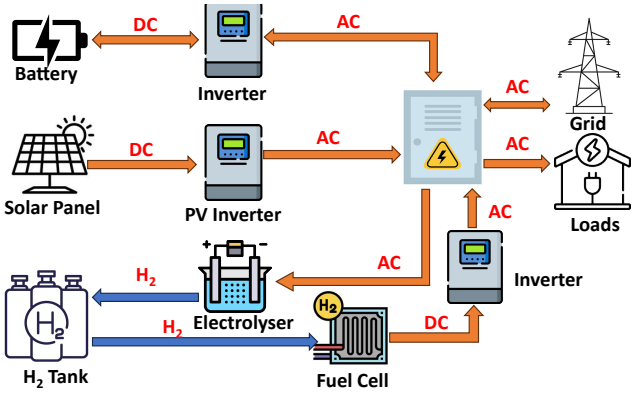

Figure 4.1: Schematic representation of the energy system

erator. Such a collaborative strategy enhances the efficiency, robustness, and dependability of the larger power grid.

4.3. ENERGY MANAGEMENT SYSTEM

The EMS holds a key position in the efficient and reliable operation of the ECS. It governs energy flow between different components, optimizes consumption and generation, and ensures the stability and reliability of the system. To keep the system balanced and facilitate ancillary services, it is essential that the EMS has the ability to make intelligent decisions regarding the actions of different components. Therefore, the process begins with the formulation of the ECS models (Section 4.3.1) and the operation modes (Section 4.3.2), followed by the application of a four-stage receding horizon optimization algorithm (Section 4.3.3) to address the optimization problem. The ECS models include Lithium-ion BESS model, the Power-to-Hydrogen-to-Power (P2H2P) system model and the slack bus model, and the operation modes represent different operating objectives of the EMS.

4.3.1. ECS MODEL

LITHIUM-ION BESS MODEL

The BESS in this setup utilizes lithium-ion batteries with a maximum charge/discharge power of 4 kW. The system assumes no degradation of BESS capacity. The dynamic BESS SOC at the end of each time slot, given in percentage, can be calculated using the following equations.

$$SoC_{BT,t} = SoC_{BT,t-1} + \frac{\eta_{char} P^{char}_{BT,t} \Delta t}{C^N_{BT}} - \frac{P^{disc}_{BT,t} \Delta t}{\eta_{disc} C^N_{BT}} \tag{4.1}$$

where the $P^{char}_{BT,t}$ and $P^{disc}_{BT,t}$ are the BESS charge and discharge power, respectively; $SoC_{BT,t}$ and $SoC_{BT,t-1}$ are the dynamic SOC of the BESS at the time slot t and $t-1$; η_{char} and η_{disc} are the charging and discharging efficiency of the BESS and the C^N_{BT} is the BESS

capacity. The dynamic SOC at the end of each time slot is calculated using Equation 4.1, which considers the charging and discharging of the BESS and the efficiency of the charging and discharging processes.

The charge and discharge power are all positive, and the BESS cannot charge and discharge simultaneously with the mathematical formula:

$$P_{BT,t}^{disc} \cdot P_{BT,t}^{char} = 0 \tag{4.2}$$

$$P_{BT,t}^{disc} >= 0 \tag{4.3}$$

$$P_{BT,t}^{char} >= 0 \tag{4.4}$$

The rated power and available energy of BESS should limit the BESS charge and discharge power with the mathematical formulate:

$$\begin{cases} P_{BT,t}^{disc} \leq \min\{P_{BT}^{discN}, \frac{C_{BT}^{N}(SoC_{BT,t-1} - SoC_{BT,min}) \times \eta_{disc}}{\Delta t}\} \\ P_{BT,t}^{char} \leq \min\{P_{BT}^{charN}, \frac{C_{BT}^{N}(SoC_{BT,max} - SoC_{BT,t-1})}{\eta_{char}\Delta t}\} \end{cases} \tag{4.5}$$

where P_{BT}^{discN} and P_{BT}^{charN} are the maximum discharge and charge power of the BESS, respectively. $SoC_{BT,max}$ and $SoC_{BT,min}$ are the maximum and minimum limited value of BESS SOC. and $C_{BT}^{N}\left(SoC_{BT,t-1} - SoC_{BT,min}\right)$ and $C_{BT}^{N}\left(SoC_{BT,max} - SoC_{BT,t-1}\right)$ are the available BESS energy capacity for discharging and charging at time t considering the maximum and minimum BESS SOC values.

P2H2P SYSTEM MODEL

The P2H2P system is a closed-loop energy storage system that uses hydrogen as an energy carrier to store the electricity generated by PV. It enables excess energy generated during peak periods to be stored as hydrogen and utilized during periods of low energy production. It involves several steps, including Power-to-Hydrogen (P2H), Hydrogen-to-Power (H2P) and Hydrogen Recycling (H2H).

P2H: In this step, excess electricity generated by renewable sources produces hydrogen through an electrolyzer. The amount of hydrogen produced is limited by the capacity of the hydrogen storage tank and the efficiency and rated power of the electrolyzer. The mathematical equation for the P2H step can be represented as:

$$\max(0, P_{EL,t-1} - R_{EL}\Delta t) \leq P_{EL,t} \leq \min(P_{EL}^{N}, \frac{E_{HT,t}^{vaca}}{\eta_{EL}\Delta t}, P_{EL,t-1} + R_{EL}\Delta t) \tag{4.6}$$

$$H_{prod,t} = \frac{\eta_{EL} P_{EL,t} \Delta t}{Q_{H2P}} \tag{4.7}$$

where $P_{EL,t}$ and $P_{EL,t-1}$ are the power supplied by the electrolyzer at time t and $t-1$; P_{EL}^{N} is the rated power of the electrolyzer; $E_{HT,t}^{vaca}$ is the available energy of the hydrogen tank at time t in kWh; Δt is the time resolution; R_{EL} is the ramp rate limit of the electrolyzer; $H_{prod,t}$ is the amount of hydrogen produced by the electrolyzer at time t in kg; η_{EL} is the efficiency of the electrolyzer. And Q_{H2P} is the hydrogen energy transfer

efficiency of 33.33 kWh/kg. Equation 4.6 sets limits on the power supplied by the electrolyzer. The lower limit is determined by the power provided at the previous time step minus the ramp rate limit R_{EL} to ensure that the power change between time steps is within a certain range. The upper limit is the minimum of the electrolyzer's rated power, the hydrogen tank's available energy divided by the time step, and the power supplied at the previous time step plus the ramp rate limit. Equation 4.7 calculates the amount of hydrogen produced by the electrolyzer at time t in kg, assuming that all the hydrogen produced is stored in the hydrogen tank for later use. The P2H step is an important component of the P2H2P system, allowing the storage and utilization of excess renewable energy, which can improve the reliability and efficiency of the system.

H2P: In this step, the stored hydrogen is used to generate electricity through a fuel cell. The amount of electricity generated is limited by the rated power of the fuel cell and the efficiency of the fuel cell system. The equation for this step can be expressed as follows:

$$\max(0, P_{FC,t-1} - R_{FC}\Delta t) \leq P_{FC,t} \leq \min(P_{FC}^{N}, \frac{E_{HT,t}^{avai}\eta_{FC}}{\Delta t}t, P_{FC,t-1} + R_{FC}\Delta t) \tag{4.8}$$

$$H_{cons,t} = \frac{P_{FC,t}\Delta t}{Q_{H2P}\eta_{FC}} \tag{4.9}$$

where $P_{FC,t-1}$ and $P_{FC,t}$ are the fuel cell generated electrical power at time $t-1$ and t; P_{FC}^{N} is the rated power of the fuel cell, and R_{FC} is the ramp rate of the fuel cell; η_{FC} is the fuel cell efficiency. Equation 4.8 defines the allowable range of power output for the fuel cell at time t, based on the previous time step's power output, the rated power of the fuel cell, and the available hydrogen energy at time t ($E_{HT,t}^{avai}$). The ramp rate of the fuel cell is also considered, limiting the change in power output over a single time step. The equation ensures that the power output of the fuel cell stays within the allowable range. Equation 4.9 calculates the hydrogen consumption rate of the fuel cell at time t based on its power output and efficiency in the unit of kg.

H2H: In this step, we calculate the stored hydrogen denoted as $SoC_{HS,t}$ (Level of Hydrogen in the percentage of the storage) after P2H and H2P process and is given by:

$$SoC_{HS,t} = SoC_{HS,t-1} - \frac{H_{prod,t}}{C_{HT}^{N}} + \frac{H_{cons,t}}{C_{HT}^{N}} \tag{4.10}$$

where C_{HT}^{N} is the nominal capacity of the hydrogen tank in kg. The available hydrogen stored in the hydrogen tank is denoted as $E_{HT,t}^{avai}$ in kWh, and is given by:

$$E_{HT,t}^{avai} = (SoC_{HS,t-1} - SoC_{HS,min})C_{HT}^{N}Q_{H2P} \tag{4.11}$$

where $SoC_{HS,min}$ is the minimum level of hydrogen allowed in the tank. The vacant hydrogen capacity of the hydrogen tank to store hydrogen is denoted $E_{HT,t}^{vaca}$ in kWh, and is given by:

$$E_{HT,t}^{vaca} = \frac{(SoC_{HS,max} - SoC_{HS,t-1})C_{HT}^{N}}{Q_{H2P}} \tag{4.12}$$

where $SoC_{HS,max}$ is the maximum level of hydrogen allowed in the tank.

Generally, the P2H2P system works by balancing the power limits of the electrolyzer and fuel cell and ensuring that the hydrogen produced and consumed is within the limits of the hydrogen tank's capacity.

SLACK BUS MODEL

The ECS must be connected to the grid to ensure a reliable and stable energy supply. Any imbalance in power flow can result in instability and disruptions in energy supply, which can have severe consequences for the entire energy system. Therefore, it is crucial to maintain balance in the power flow at the interface to ensure a stable and reliable energy supply. The power balance refers to the equilibrium between the power consumed and produced at the point of common coupling (PCC) of the grid, and it can be expressed as

$$P_{grid,t} + P_{generation,t} + P^{dis}_{storage,t} = P_{load,t} + P^{cha}_{storage,t} \tag{4.13}$$

where $P_{grid,t}$, $P_{renew,t}$, and $P^{dis}_{storage,t}$ are the net power from the grid, renewable energy sources, and energy storage systems (during discharge) respectively, at time t. $P_{load,t}$, and $P^{cha}_{storage,t}$ are the power inputs of the load and energy storage systems (during charge) at time t. In the specific system, the power balance constraints are expressed as follows:

$$P_{FG,t} + P_{PV,t} + P^{disc}_{BT,t} + P_{FC,t} = P_{EL,t} + P_{LD,t} + P^{char}_{BT,t} + P_{TG,t} \tag{4.14}$$

$$0 \le P_{FG,t} \le P^{N}_{FG}, \tag{4.15}$$

$$0 \le P_{TG,t} \le P^{N}_{TG} \tag{4.16}$$

They indicate that the total power produced or consumed by the different components of the system must be equal. The terms on the left-hand side of the equation represent the consumed power. Specifically, $P_{FG,t}$, $P_{PV,t}$, $P^{disc}_{BT,t}$, and $P_{FC,t}$ denote the power from the grid, PV generated power, BESS discharging power, and the power from fuel cell systems at time t. While the terms on the right-hand side represent the consumed power. $P_{EL,t}$, $P_{LD,t}$, $P^{char}_{BT,t}$, and $P_{TG,t}$ represent the power to the grid, the consumed power of the electrolyzer, the load consumption and the charging power to the BESS, respectively, at time t. This equation is crucial in ensuring the system's energy balance and is essential for achieving efficient and effective energy management.

4.3.2. OBJECTIVES

It is recognized that energy users have individualized preferences and priorities regarding energy consumption and management. For instance, a residential building owner may prioritize minimizing their energy bill, while a commercial building owner may seek to maximize profit by selling energy back to the grid during peak hours. In contrast, a utility company may utilize the building's energy storage system to provide balancing services to the grid. Thus, to address the varying needs and objectives of different owners or users, three modes are offered in the EMS to optimize the system's benefits.

Mode 1: Zero Power Exchange with the Grid

This mode aims to minimize the power exchanged between the energy system and the grid at each time step. This mode is helpful for users who want to become more self-sufficient and reduce their reliance on the grid. The optimization problem for this mode is formulated with an objective function that minimizes the absolute values of the power exchanged with the grid at each time step. The objective function is as follows:

$$\min_{P_{FG,t},P_{TG,t}} \sum_{t=1}^{T} P_{FG,t} + P_{TG,t} \tag{4.17}$$

The variables $P_{FG,t}$ and $P_{TG,t}$ represent the power from the grid and to the grid, respectively.

Mode 2: Maximizing Profit in the Energy Market

In this mode, the goal is to maximize the profit from selling energy back to the grid while minimizing the energy consumption costs of the grid. To achieve this, the system optimizes the energy production and consumption schedule to sell energy to the grid during peak hours when the price is high and to minimize the energy consumption from the grid during the same period. This mode requires access to real-time electricity prices, which can be obtained from energy markets or demand-response programs. The optimization problem for this mode is formulated with an objective function that maximizes the revenue generated from selling energy and minimizes the cost of energy consumed from the grid. The objective function is expressed as follows:

$$\max_{P_{FG,t},P_{TG,t}} \sum_{t=1}^{T} \left(P_{TG,t} \cdot Price_{sell,t} - P_{FG,t} \cdot Price_{buy,t}\right) \tag{4.18}$$

where $Price_{sell,t}$ and $Price_{buy,t}$ are the electricity sell and buy prices, respectively, at time t.

Mode 3: Balancing Services to Grid Operators and External Actors

Regarding ancillary service for the DSO, the ECS can provide its available flexibility for trading within the ancillary service market as a flexibility service provider [97]. In this mode, the goal is to provide balancing services to DSO and external actors by minimizing the difference between the flexibility supply by ECS and flexibility requirements. In the setup, the system can get the signal from DSO or aggregator on the power they need, and the system needs to minimize the difference between the signal and the actual import or export of electricity from the grid. The optimization problem for this mode is formulated with an objective function that minimizes the difference between the actual power supply and the required flexibility at each time step. The objective function is as follows:

$$\min_{P_{FG,t},P_{TG,t}} \sum_{t=1}^{T} \left|P_{TG,t} - P_{TG,s,t}\right| + \left|P_{FG,t} - P_{FG,s,t}\right| \tag{4.19}$$

where $P_{TG,s,t}$ and $P_{FG,s,t}$ are the flexibility requirements from the grid operators and external actors, respectively. They represent the power that the ECS should provide to the grid and the power that the ECS should consume, respectively. The objective is to minimize the difference between the actual power supply and the required flexibility at each time step.

For all modes, certain constraints must be satisfied to ensure the safe and efficient operation of the energy system. The mathematical model equations represent the physical laws and operational requirements that the energy management system must satisfy to ensure safe and efficient operation. The optimization objectives for each mode are subject to these constraints to ensure that the resulting operation plan is feasible and meets the desired performance criteria. These constraints include power balance equations, power output limits, and ramp rate limits for energy sources and storage systems, which are equations from Equation 4.1 to Equation 4.15. By satisfying these constraints, the energy management system can optimize its operation while ensuring the safety and reliability of the energy system.

4.3.3. RECEDING HORIZON OPTIMIZATION APPROACH

I present a four-stage energy management approach that uses receding horizon optimization to address power fluctuations within a PV–BESS–electrolyzer–fuel cell Energy Community system. This specific energy system, characterized by limited start-up capabilities and high storage capacity, is designed for hydrogen production and consumption. Conversely, the Lithium-ion BESS system within this energy community boasts fast start-up capabilities, albeit with limited storage capacity.

The proposed approach effectively merges long- and short-term optimization strategies. The aim is to leverage hydrogen production to balance seasonal power fluctuations and utilize the BESS to manage daily power surges. To do this, my approach encompasses four optimization stages: one year, one month, one day ahead, and intra-day. The annual optimization addresses the significant seasonal variations observed in renewable generation power, residential consumption, and energy pricing. The monthly optimization leverages the findings from the annual optimization to achieve finer temporal resolution and enhanced outcomes, setting the stage for more accurate day-ahead planning. The day-ahead optimization is crucial as it capitalizes on the predictability of electricity prices and improved weather and energy consumption forecasts, allowing for detailed 15-minute interval scheduling for forthcoming operations. Lastly, the intra-day optimization provides a mechanism for adjustments in response to unforeseen events or forecasting inaccuracies. Each stage contributes to an adaptive, flexible control strategy for complex energy systems.

This four-stage energy management approach, as shown in Figure 4.2, is specially designed to ensure that the energy system adapts in real time and maintains operations within its constraints.

At the beginning of each new month, the one-year optimization stage occurs. This optimization process identifies approximate monthly hydrogen consumption or production values using forecast power demand and the potential of available renewable energy sources.

Next, the one-month optimization stage is carried out at the beginning of each day to ascertain the daily hydrogen consumption or production, informed by the one-year optimization results. At the same time, a day-ahead optimization is executed to designate the operating hours of the electrolyzer or fuel cell to satisfy the hydrogen demand.

The fourth and final stage, intraday optimization, is undertaken every 15 minutes to manage BESS charge and discharge power. If the BESS SOC is within the acceptable

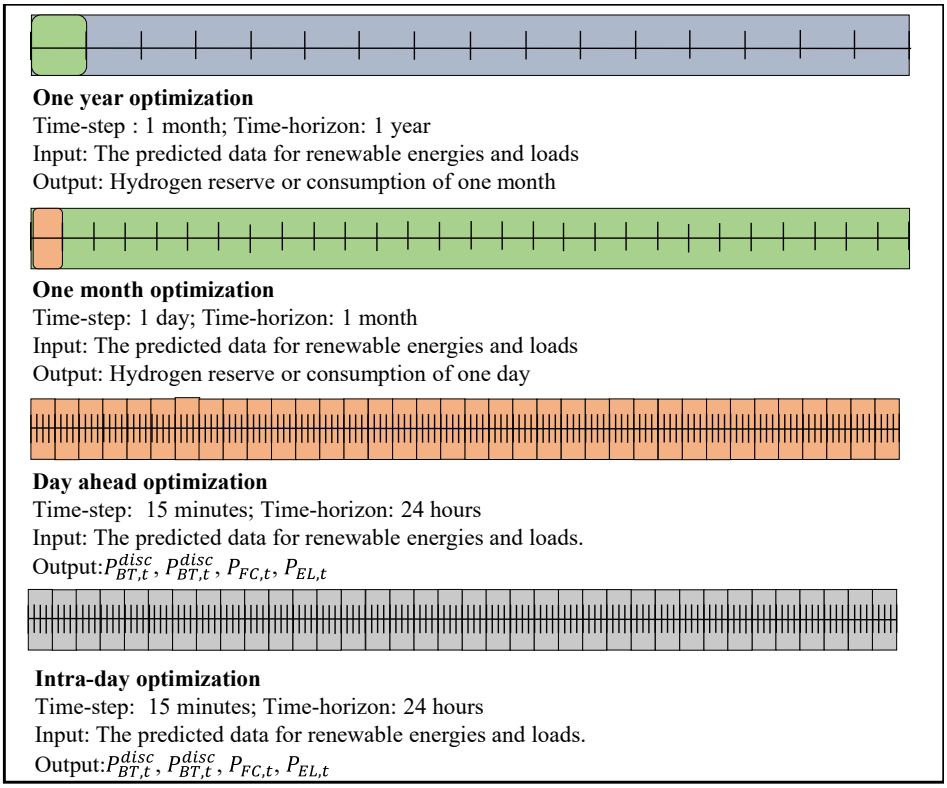

Figure 4.2: The scheme of the four-stage receding horizon optimization algorithm

range, the intra-day optimization proceeds based on the current BESS schedule. However, if the battery SOC deviates from the acceptable range, the hydrogen system is triggered to adjust the SOC to an acceptable level. Upon SOC adjustment by the hydrogen system, intra-day optimization resumes based on the revised BESS schedule.

As shown in Figure 4.3, the one-year and one-month long-term optimization stages primarily consider strategic energy decisions, accounting for larger, slower-varying energy components in the PV–BESS–electrolyzer–fuel cell Energy Community system. On the contrary, due to its rapid response and dynamic SoC, the lithium-ion BESS is suited for the short-term stages, wherein it can adeptly manage daily fluctuations and mismatches between generation and demand. This justifies the exclusion of the BESS model in the long-term optimization stages, as it would only add computational complexity without substantially improving the decision-making process. Consequently, the constraints that must be satisfied include only the PV model, P2H2P system model, and slack bus model. Specifically, the slack bus model needs to be adjusted as follows:

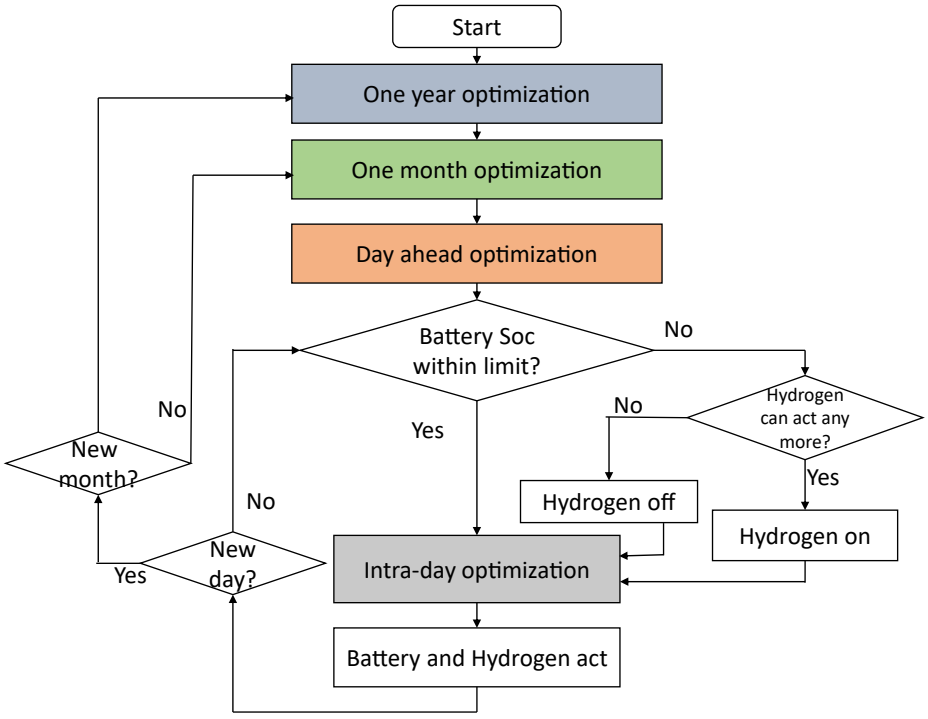

Figure 4.3: The flow chart of the EMS algorithm

$$\begin{aligned} P_{FG,t} + P_{PV,t} + P_{FC,t} &= P_{EL,t} + P_{LD,t} + P_{TG,t} \\ 0 \leq P_{FG,t} &\leq P_{FG}^{N}, \\ 0 \leq P_{TG,t} &\leq P_{TG}^{N} \end{aligned} \tag{4.20}$$

The day-ahead optimization stage integrates all constraints of the PV model, Lithium-ion BESS model, P2H2P system model, and slack bus model to inform the actions of the BESS, fuel cell, and electrolyzer every 15 minutes. Intraday optimization determines BESS action and, if necessary, modifies the P2H2P system action with updated information. Modifying the P2H2P system involves reviewing the BESS SOC and deciding whether the predefined schedule requires modification. Based on the action of the P2H2P system, the optimization problem in the intra-day optimization stage should consider the constraints of the PV, slack bus, and BESS models. Specifically, the slack bus model needs to be adjusted as follows:

$$\begin{aligned} P_{FG,t} + P_{PV,t} + P_{BT,t}^{disc} &= P_{BT,t}^{char} + P_{LD,t} + P_{TG,t} \\ 0 \leq P_{FG,t} &\leq P_{FG}^{N}, \\ 0 \leq P_{TG,t} &\leq P_{TG}^{N} \end{aligned} \tag{4.21}$$

In summary, the proposed energy management approach employs a combination of long-term and short-term optimizations to balance seasonal power fluctuations with hydrogen and daily power fluctuations with the battery. This approach ensures that the energy system operates within its constraints, promoting efficient and resilient energy management in the PV-BESS-electrolyzer-fuel cell energy community system.

4.4. CASE STUDY

4.4.1. DATA ACQUISITION AND REFINEMENT

The study studies draw its primary data set from the Open Power System Data (OPSD) platform [98]. Specific to this investigation, the focus has been on the PV-generated power and the residential load data emanating from the Netherlands. To better align with typical residential parameters:

- PV-generated data was adjusted to simulate a peak power capacity of 6 kW, and the total generated energy is 7122 kWh.
- The residential load was tailored to reflect an annual electricity consumption of approximately 4200 kWh.

The beginning of my simulation saw both BESS and hydrogen storage systems initialized at a SOC of 50%. This was done to ensure a neutral starting point, thereby allowing the simulation to be influenced primarily by the input data and the EMS's operational strategy. To provide comprehensive insight into the EMS's adaptability and performance, its behavior across two distinct days is spotlighted: a quintessential winter day and a summer day. These intentional selections demonstrate the system's resilience under contrasting energy conditions.

The PV power generation trends, the domestic consumption trajectories, and the Mode 3 flexibility supply during these days are illustrated in Figure 4.4. A salient observation from the winter dataset underscores the PV system's limitations, as it struggles to satiate residential energy appetites. In stark contrast, summer showcases an energy bounty, with the PV system's generation far outstripping domestic consumption.

In the context of energy trading and profitability, the electricity price dynamics, pivotal for Mode 2's operation, for these illustrative days can be discerned in Figure 4.5.

4.4.2. SNAPSHOT SIMULATION

First, the snapshot simulation results of time 00:00 on 1st January are presented in Figure 4.6. At 00:00 on the first day of a month, one-year optimization, one-month optimization, one-day optimization, and intra-day optimization are all acts. Figure 4.6 a) illustrates the one-year optimization results. It shows that the SOC of the hydrogen storage in one-year optimization is higher during the summer months when renewable energy generation is abundant, while during the winter months, the stored hydrogen is utilized to generate power to supply the shortage. This demonstrates the effectiveness of the proposed algorithm in balancing seasonal power fluctuations and ensuring that the energy system operates efficiently throughout the year. Figure 4.6 b) presents the one-month optimization results, indicating that the hydrogen is gradually utilized to generate power for consumption, further demonstrating the ability of the algorithm

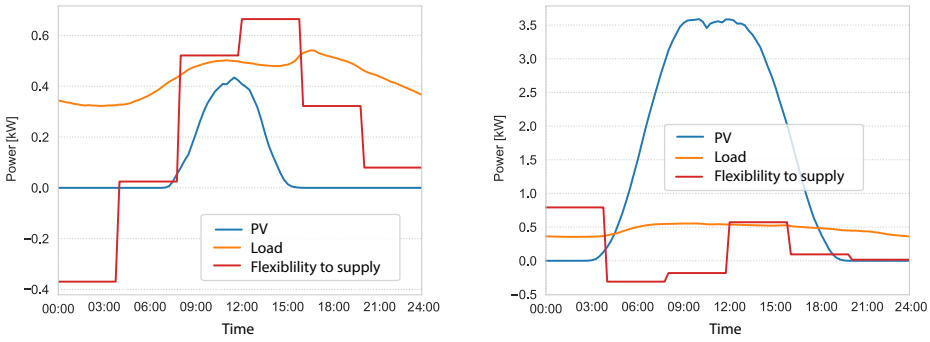

Figure 4.4: PV generated power, domestic consumption, and Mode 3 flexibility supply during typical winter and summer days.

to adapt to short-term power fluctuations. Furthermore, Figure 4.6 c) display the day-ahead optimization results for the charge and discharge power of both the battery and hydrogen, along with the SOC for these storage solutions. These visuals demonstrate the algorithm's capability to determine daily hydrogen and BESS charge and discharge power, drawing upon yearly and monthly optimization outcomes. Notably, After 18:00 PM on the simulation day, when the battery SOC becomes lower, the fuel cell works to generate electricity both for battery recharge and residential use.

4.4.3. ALGORITHM ANALYSIS ON TYPICAL DAYS

In this section, simulations on typical days are conducted and analyzed. One-day simulations on typical winter and summer days are performed to demonstrate the algorithm's performance in different modes. Figure 4.7 and Figure 4.8 show the change of BESS and hydrogen systems over a typical winter day, while Figure 4.9 and Figure 4.10 show the change of BESS and hydrogen systems on a typical summer day. Where a negative power reading implies the BESS is storing PV-generated energy, a positive one signifies its charging phase.

WINTER ANALYSIS

During winter, the fuel cell meets household energy demands, which is evident by the constant decrease in HS SOC. On the other hand, the BESS portrays considerable SOC variations, highlighting its essential role in regulating daily power fluctuations, while the hydrogen system caters to more extended, seasonal energy requirements.

Mode 1: Fuel cell actives, especially when no PV power is generated during the night, highlighting the crucial role of the hydrogen system in maintaining energy reserves during periods of limited solar output (Figure 4.7 a)). **Mode 2**: Guided by market trends, the BESS synchronizes its charge/discharge cycles with fluctuating electricity prices to maximize economic benefits. This alignment of BESS activities with price patterns is clearly observed (Figure 4.7 b)). **Mode 3**: The BESS adjusts its functions according to the DSO's flexibility requirements. In parallel, the fuel cell ensures that the BESS remains optimal

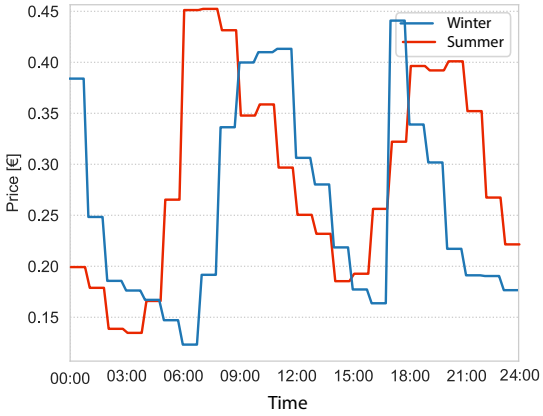

Figure 4.5: Electricity price evolution on representative winter and summer days.

for the coming day (Figure 4.7 c)).

SUMMER ANALYSIS

The summer landscape, as depicted in Figure 4.9 and Figure 4.10, witnesses the electrolyzer in action, transforming surplus electricity into hydrogen.

Mode 1: With abundant sunlight, the electrolyzer actively channels excess PV-generated energy (Figure 4.9 a)). This mode emphasizes strategic capture and conversion of surplus power into hydrogen, prepping for future energy requirements. **Mode 2**: Reflecting its winter behavior, the BESS adeptly modulates its operations according to electricity market prices, ensuring optimal economic gains (Figure 4.9 b)). **Mode 3**: The BESS seamlessly aligns its functions with the DSO's guidelines. Interestingly, its SOC is deliberately maintained at a lower threshold at night, positioning it optimally for the anticipated influx of the next day's PV energy (Figure 4.9 c)).

In summary, the three operational modes of the EMS algorithm demonstrate its multifaceted utility. Mode 1 ensures that the system is always ready to meet energy demands. Mode 2 adeptly responds to market dynamics, optimizing for economic benefits. Lastly, Mode 3 collaboratively supports the grid while strategically anticipating future energy requirements. Together, these modes showcase the EMS's integral role in achieving self-sufficiency, maximizing economic benefits, and providing robust grid support in modern energy infrastructures.

4.4.4. RELIABILITY ANALYSIS THROUGH ONE-YEAR SIMULATION

A year-long simulation was conducted to evaluate the robustness of the EMS algorithm thoroughly. This extended analysis offers a deeper understanding of the algorithm's performance over diverse time frames, underscoring its efficacy.

Mode 1: Figure 4.11 illustrates the power interactions with the grid. A negative value indicates the power flows to the grid. The system remains consistent with self-sufficient

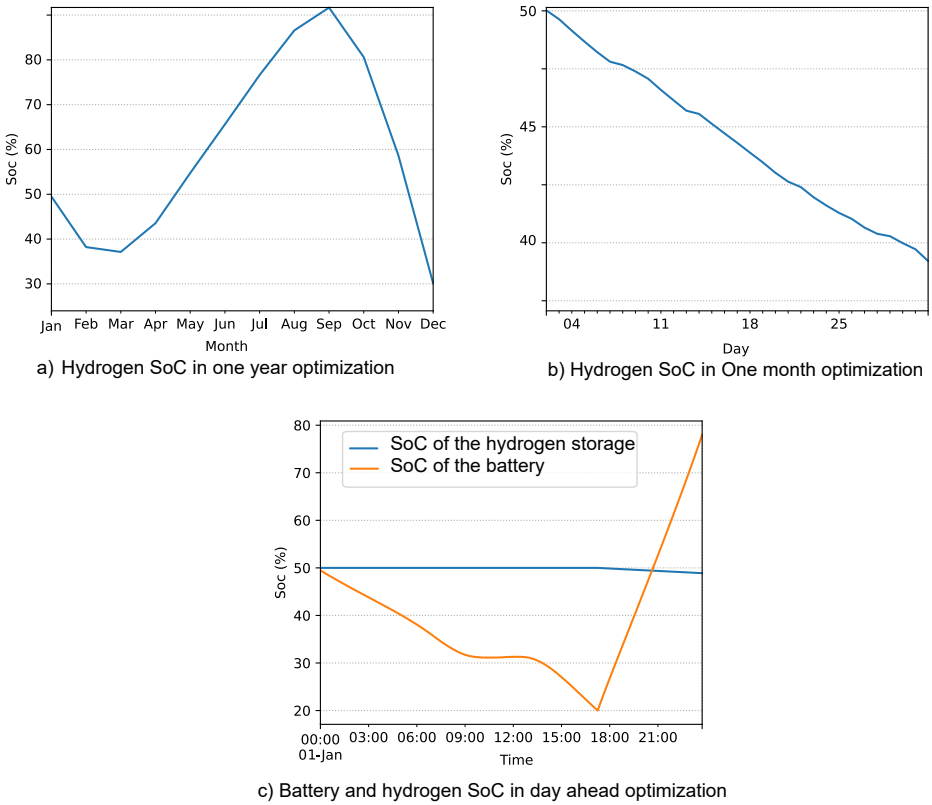

Figure 4.6: Hydrogen storage SOC in the four-stag receding horizon optimization ems algorithm

throughout the year without receiving any power from the external grid. The HS SOC in Mode 1 is depicted by the red line in Figure 4.12. In particular, the system ensures a significant hydrogen reserve, positioning it well for upcoming energy requirements.

Mode 2: The annual net sales power yields a notable profit of 2637.48€, as displayed in Figure 4.13. In comparison, the energy contribution to the grid under Mode 1 offers a gain of only 45.04€. This demonstrates that Mode 2 can achieve a significantly higher profit than Mode 1. Mode 2 has price fluctuations throughout the day, though these variations aren't as pronounced over the year. As a result, the battery primarily purchases electricity when prices are low and sells when they are high. In this mode, the hydrogen system doesn't play a pivotal role in profit maximization. Consequently, the SOC for hydrogen storage remains relatively stable throughout the year.

Mode 3: In Figure 4.12, the blue line depicts the HS SOC for Mode 3. The HS SOC exhausts by year-end as a result of the persistent alignment with DSO's flexibility demands over the year. The total flexibility offered to the grid in this period is significant, amounting to 4622.81 kWh, consuming all initial hydrogen reserves. It is pertinent to mention

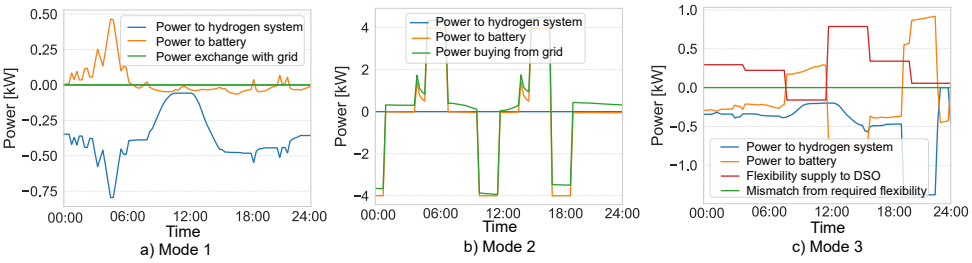

Figure 4.7: The changes in the BESS and hydrogen system during the typical winter day

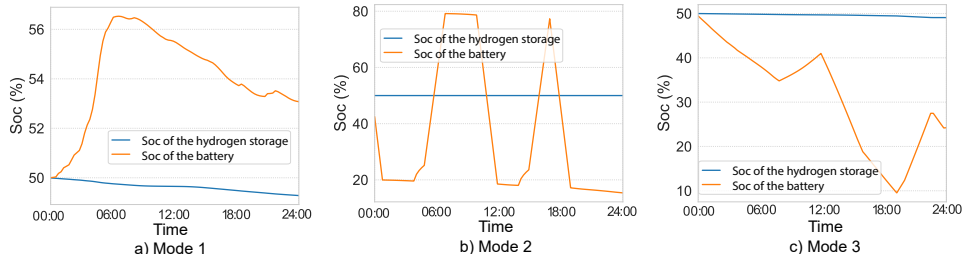

Figure 4.8: The SOC profile of BESS and hydrogen system during the typical winter day

that in Modes 2 and 3, the primary aim is not solely self-sufficiency. Therefore, the complete depletion of the HS SOC by the year's end aligns with the predetermined objectives. Figure 4.14 indicates the inability of the EMS to handle the flexibility requirement. The mismatch, which the system cannot provide, is 161.89 kWh. This implies that the EMS was able to provide 96.50% (161.89 kWh VS 4622.81 kWh) of the flexibility requirements, and this year, 96.80% moment, the flexibility requirement can be met by the EMS. These results suggest that the EMS effectively provides balancing services and contributes to the overall stability and reliability of the grid. Nonetheless, the potential for an EMS mismatch varies based on the DSO's specific flexibility requirements. A stochastic approach should be employed to assess these possibilities for a comprehensive analysis. This paper, however, does not delve into such detailed analysis.

The proposed EMS algorithm shows good performance in all modes. This resilience highlights its ability to adapt to the unique goals set for each mode. In particular, the proposed method allows the ECS to transition smoothly between priorities and modes of operation. For example, when the ECS operates in Mode 1, it can deftly switch to Mode 2 if it finds that hydrogen build-up is getting close to the edge of storage capacity. This strategy allows it to optimize its hydrogen reserves over the following months to exploit the potential for grid switching. Exploring how to integrate different modes for optimal operation provides an exciting avenue for future research.

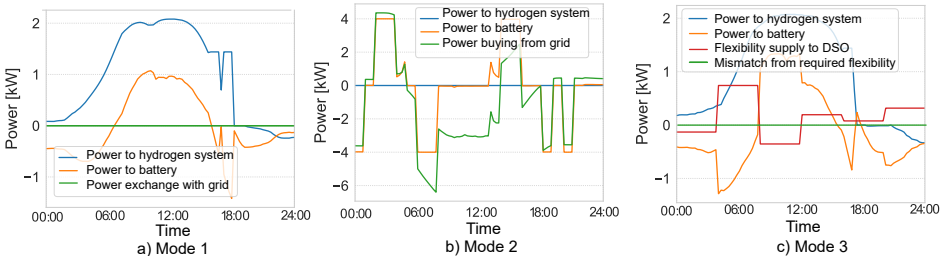

Figure 4.9: The changes in the BESS and hydrogen system during the typical summer day

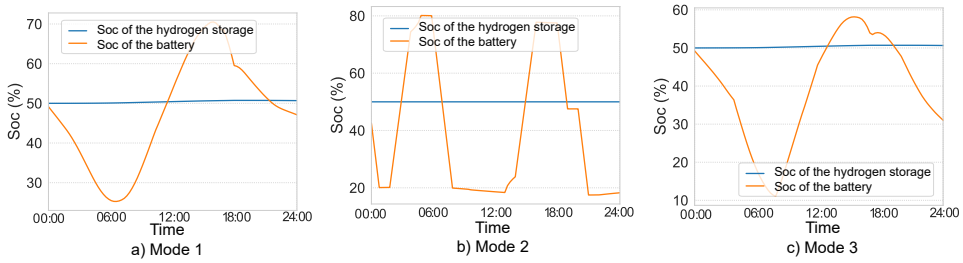

Figure 4.10: The SOC profile of BESS and hydrogen system during the typical summer day

4.4.5. RELIABLITY TEST OF THE SELF-ORGANIZING VOLTAGE REGULATION METHOD

Providing balancing services to grid operators and external actors is a crucial function of an EMS in the modern energy landscape. It enables the system to contribute to the stability and reliability of the grid. To test the effectiveness of the EMS Mode 3 in providing balancing services for self-organizing voltage regulation. From the simulation results, Figure 4.14 demonstrate the effectiveness of the proposed EMS in providing balancing services to grid operators and external actors while operating within technical constraints. The successful implementation of EMS Mode 3 highlights its potential to support the transition to a more sustainable and reliable energy system.

Nevertheless, when an intelligent agent offers flexibility to facilitate self-organizing voltage regulation, there's a risk it might not deliver as guaranteed. As highlighted in Section 4.4.4, accounting for 3.2% of the year when the EMS under Mode 3 fails to provide the pledged flexibility. Furthermore, in modern power systems, multiple controllers are becoming more prevalent. However, as the number of controllers increases, so does the likelihood of a single controller failure. These failures can occur due to data transmission failures or an individual agent refusing to execute orders. In practice, distributed or fully decentralized control methods can help reduce the impact of such failures, making them more resilient than centralized strategies.

An analysis of both centralized and distributed control algorithms was conducted to evaluate the reliability of the proposed control method in Chapter 3 under the failure of a single agent. In both cases, it was assumed that the other controllers expected Agent R15 in the CIGRE LV distribution residential sub network shown in Figure 3.5 in Section

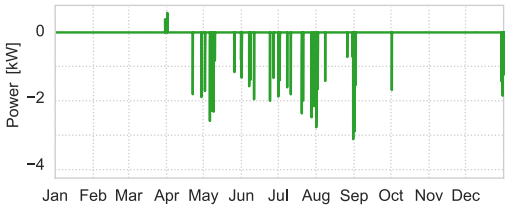

Figure 4.11: Power Exchange with the Grid in Mode 1

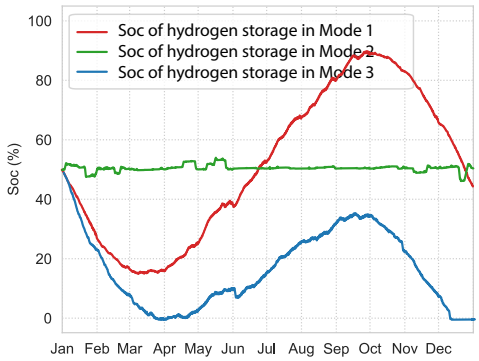

Figure 4.12: The SOC of the HS in different modes

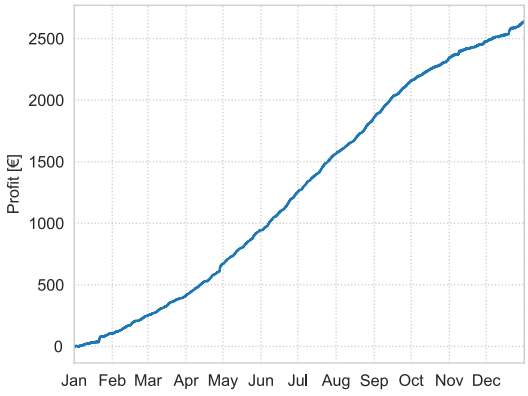

Figure 4.13: Profit in Mode 2

3.4 to provide voltage regulation as promised. The test grid used for the analysis was obtained from [53], and the power consumption data at the one-time step is shown in Table 4.1. The controllable power at each agent was ±20kW/kVar. Agent R15 was randomly selected to refuse to provide voltage regulation service. The maximum number of

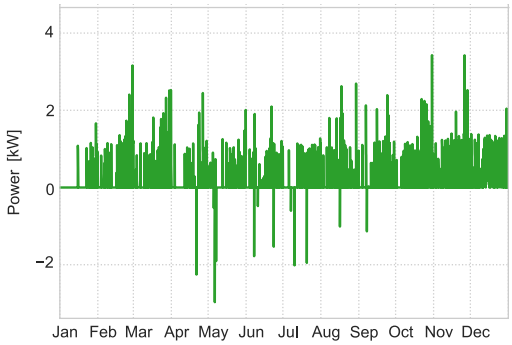

Figure 4.14: The mismatch power of flexibility supply in Mode 3

iterations was set at 20, 50, and 100 to prevent an endless loop and ensure convergence. The results of the proposed method were then compared with those of the centralized method in Section 3.2.

Table 4.1: The load data

Load power	R1	R11	R15	R16	R17	R18
Active [kW]	190.00	14.25	49.40	52.25	33.25	44.65
Reactive [kVar]	62.44	4.68	16.24	17.17	10.93	14.68

The simulation results, presented in Figure 4.15 and Figure 4.16, demonstrate the effectiveness of the proposed distributed voltage regulation algorithm in gradually reducing voltage violations to within acceptable limits. The operational agents are able to provide more power to regulate the voltage, leading to a significant reduction in voltage violations. Although 20 iterations are sufficient to achieve good results, the figures show that increasing the iteration number leads to even better voltage regulation results.

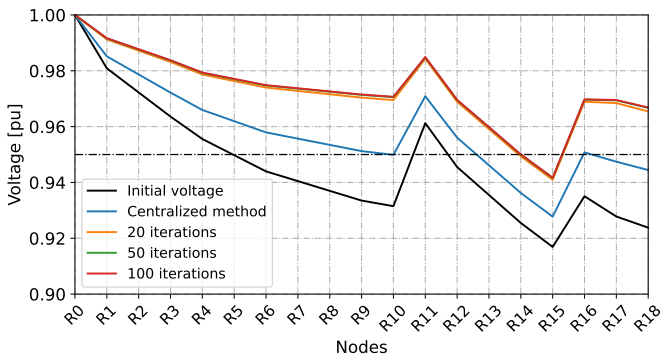

Figure 4.15: Voltage profile after regulation with a single agent failure

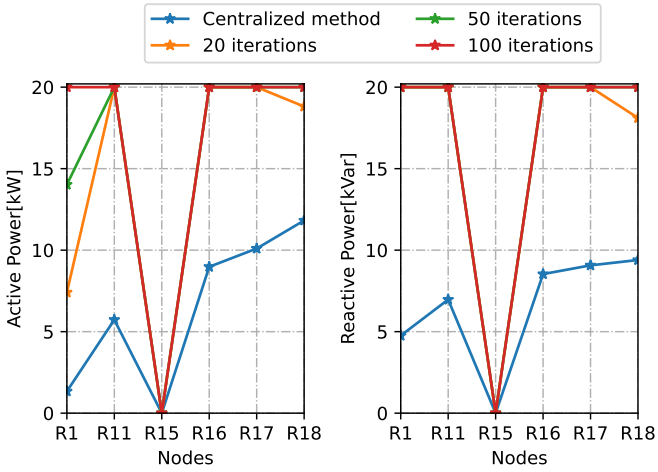

Figure 4.16: Required power to regulate voltage with a single agent failure

Comparing the results of the centralized and proposed methods, the centralized method reduces the voltage violation from 3.31% to 2.23%, while the proposed method reduces it to 0.83%. The proposed method thus achieves a 122% improvement in voltage regulation over 100 iterations compared to the centralized method. These results suggest that the proposed method can gradually reduce the impact of unexpected events, leading to a better overall result compared to the centralized method. In summary, the proposed distributed voltage regulation algorithm demonstrates its effectiveness in gradually reducing voltage violations and improving overall voltage regulation performance. Additionally, the proposed method is more robust than the centralized method, making it better equipped to handle unexpected events and failures of individual agents.

The findings of the study suggest that the proposed distributed control algorithm is more reliable in the event of a single-agent failure and can provide better overall performance than the centralized control algorithm. These results emphasize the significance of taking into account the potential failure of individual agents in distributed control strategies for power grids. Future research could focus on examining the scalability and suitability of the proposed algorithm in larger and more intricate power grids such as considering failures in more agents.

4.5. CONCLUSION

This chapter introduced an ECS and explored the energy management algorithm for future energy communities. A four-stage receding horizon algorithm was developed to optimize the energy management of the ECS. The algorithm effectively balanced the energy system's operation throughout the year, adapted to short-term power fluctuations, and made real-time adjustments based on the latest information. Three modes with different objectives were proposed to achieve individual preferences and priorities. The simulation results demonstrated the effectiveness of the proposed algorithm in achiev-

ing self-sufficiency and providing balance services to grid operators and external actors.

Furthermore, based on the proposed four-stage receding horizon algorithm, the reliability of the distributed cooperation voltage control algorithm discussed in Chapter 3 is investigated, particularly in scenarios involving the failure of a single agent. The results show that the proposed distributed cooperation voltage control algorithm is more reliable and performs better than the centralized control algorithm. The algorithms proposed in this chapter can help energy communities achieve self-sufficiency, flexibility, and reliability, significantly contributing to the sustainable development of the energy system and enhancing the self-organizing voltage regulation algorithm.

Up to this point, the development and evaluation of the self-organizing voltage regulation method from both the grid's and energy community's perspectives in the planning and operation phases have been examined. While our case studies have provided valuable assessments of the proposed algorithms, transitioning to on-site deployment remains a considerable challenge. First, on-site deployment can expose the algorithm to unpredictable and varied real-world conditions. Therefore, it is essential to prepare the algorithm for diverse challenges and reduce surprises during on-site deployment by running real-time and non real-time simulations to mimic a wide range of scenarios. Then, existing on-site systems can be diverse, presenting compatibility issues. Beyond just software, the physical infrastructure might also pose challenges, given potential limitations in processing speed, storage, and other hardware constraints. Therefore, HIL testing is important for mimicking real-world integrations, highlighting compatibility issues early on, and ensuring the algorithm is theoretically sound and optimized for the hardware it will run on. Moreover, certain applications, like our voltage regulation, must react instantly. Therefore, real-time simulation provides a platform to rigorously test the algorithm's responsiveness and speed, ensuring it meets the real-time requirements of on-site operations. To transfer the algorithm to on-site deployment, both real-time assessments and HIL testing must be performed for a large number of scenarios. This will not only ensure seamless integration and operation but also foster confidence among stakeholders.

5

AN OPEN SOURCE VALIDATION KIT FOR DRES INTEGRATION

This chapter introduces a flexible and expandable kit for developing integration systems of renewable energy systems: The Illuminator. The Illuminator illustrates challenges arising from the energy transition and as a sandbox for testing intelligent grid control algorithms in real and non-real time. The Illuminator technology is primarily a modular software platform developed to run on either a RasPi cluster or personal computers. It is open-source, available on GitHub and developed in Python. The Illuminator comprises models of common energy technologies, such as PV panels, wind turbines, batteries, and hydrogen systems. The uniqueness of The Illuminator is in its modularity and flexibility to reconfigure scenarios and cases on the fly, even by non-experts in a plug-and-play fashion. This chapter first introduces The Illuminator and shows its architecture and Libraries. Then the user manual is present. Finally, the performance of The Illuminator is validated in a simple residential case study and a voltage regulation method testing.

Parts of this chapter have been published in 2023 IEEE PowerTech, Belgrade, Serbia with the title: *The Illuminator: An Open Source Energy System Integration Development Kit* pp. 01-05, doi: 10.1109/PowerTech55446.2023.10202816. [99] and in Github https://github.com/Illuminator-team/Illuminator.

5.1. INTRODUCTION

With the binding target of net zero greenhouse gas emissions to achieve a climate neutral Europe by 2050 [100], the energy transition has become a central societal topic. The energy system grows in complexity throughout the transition. Understanding such complex systems calls for a new generation of modeling, analysis, and simulation support tools. Such tools would be able to demystify multi-energy design and operational aspects and improve system integration by enhancing communication amongst domain experts and stakeholders. Moreover, to apply the intelligent control algorithm to on-site deployment, a testing environment is necessary to test the algorithms' speed, robustness, and integration into physical hardware. In this chapter, we introduce a tool called The Illuminator, which is particularly developed for the assessment of intelligent algorithms.

The energy system landscape is full of various tools developed over the years for various purposes that can be deployed to teach energy transition challenges and solutions with various degrees of success. Professional and academic engineering tools, such as Digsilent PowerFactory [48], Matpower [101], PyPSA [102] or PandaPower [103] are developed to teach highly skilled engineers (at the MSc and PhD level) who will one day use the same tools in their work environment. These tools were not designed with education as their primary focus and therefore lack the flexibility and modularity to create educational content outside of specific engineering problems. Similar is the case with energy system optimization models, whose learning curves are quite steep (for example, OSeMOSYS, which focuses on the long-term integrated assessment and energy planning of multi-carrier energy systems [104]). Energy Hub Design Optimization tool is a web tool for designing and optimizing complex multi-energy systems [105]). The web tool is accessible online for free, and the open-source optimization model can be used to support academic teaching. However, its code is not open-source. Hence, it cannot be modified easily to serve specific optimization criteria. The optimization algorithm does not give good access to be changeable.

Other tools are developed with the primary purpose of education. References [106] provides a learning tool in the field of the Internet of Energy through web server applications based on a low-cost single-board computer. Reference [107] and [108] provide educational setup methods for power electronics. Another popular tool is EnergyPLAN [109], which allows macro-scale modeling and optimization of a multi-energy system to evaluate different scenarios. They provide scalability for the simulation, and they can control real devices next to the running simulations, which are suitable for demonstration and education. Even though these tools can easily be used in a classroom, they are not sufficiently modular and flexible to cover a variety of challenges and solutions that energy transition brings. The sheer complexity of the energy transition makes such tools narrowly focused.

Finally, there are tools whose scope and flexibility are better suited for the diverse questions. A Decentralized Energy Management Simulation Toolkit (DEMKit) [110] provides a sandbox to test different optimization algorithms for energy management while allowing HIL experiments. PowerMatcherSuite focuses on real-time market-based coordination of distributed energy resources [111]. The laboratory test beds, such as [112] and [113], can be reconfigured in different connectivity architectures, sometimes emu-

lating entire distribution grids. Such modular and flexible approaches are an inspiration for The Illuminator. PowSyBl project [114] of the Linux Foundation Energy open source initiative LF Energy [115] provides the code building blocks for simulations and power system analysis. They use the modular approach, which allows developers to extend their features. It inspires us to make the kit modular by allowing user customization.

From the review of open source tools, Matpower [101], PyPSA [102], and PandaPower [103] are power flow calculation tools. [106],[107], and [108] focus on education and demonstration and facilitate user participation and involvement. However, they can only demonstrate a simple case unsuitable for complex simulation or research. References [110],[112], and [109] show renewable energy technologies on a physical scale more than just software models. However, the extendability, applicability, and modularity of those tools are not strong. [104], [105], and [114] are pure software tools, and they do well in the modularity to allow user customization. Therefore, the development of a new tool is proposed to combine the advantages of existing tools and improve their shortcomings. This tool aims to address the education and demonstration needs for demystifying energy transition challenges and extend for research purposes to test innovative solutions for energy systems.

In this chapter, a do-it-yourself kit, named *The Illuminator*, is introduced to demonstrate the challenges and solutions associated with energy transition. This kit is flexible and modular, designed to facilitate exploration of a variety of cases. Available on GitHub under the LGPL license [116], The Illuminator includes models, case studies, and scenarios that represent various contexts relevant to the energy transition.

At its core, The Illuminator leverages the capabilities of Mosaik, a dynamic platform that orchestrates seamless data flows and scheduling functionalities. The incorporation of Mosaik ensures that The Illuminator serves as an effective tool to demonstrate the complex processes involved in energy transition to a wide range of audiences. Additionally, The Illuminator serves as a valuable platform for evaluating the efficiency and performance of various intelligent algorithms. Adding another layer to its complexity, The Illuminator seamlessly integrates communication protocols and various techniques with physical hardware components, thereby fostering a hardware-in-the-loop testing environment. By doing so, the quality and realism of the simulations are enhanced, bridging the gap between virtual simulations and real-world conditions.

It is important to recognize the challenges in simulating complicated infrastructures. To address this, The Illuminator combines real hardware with digital tools, creating a hardware-in-loop system. This approach allows researchers to create more realistic simulations by combining the real-world behavior of hardware with the flexibility of digital platforms. Furthermore, before implementing any algorithm in real operational environments, it is crucial to test them extensively. The Illuminator can run real-time simulations, ensuring that the algorithms are suitable for deployment in real-life power grids. The feedback and data gathered from these simulations are invaluable in offering insights into potential improvements to the algorithms and preparing them to address and overcome challenges they might encounter. The Illuminator not only helps in the better application of algorithms, but also supports a smoother move towards renewable energy, aiming for energy systems that are reliable, efficient, and sustainable.

The architecture of The Illuminator is presented in Section 5.2. The libraries of The

Illuminator are introduced in Section 5.3. The Illuminator usage is explained in Section 5.4. Two example case studies showing The Illuminator performance are given in Section 5.5. Finally, the conclusions are presented in Section 5.6.

5.2. ARCHITECTURE OF THE ILLUMINATOR

5.2.1. DESIGN REQUIREMENTS

To address broad education, demonstration and intelligent control algorithm testing for future power grid needs, the most important design requirements of The Illuminator are:

1. represents common energy technologies and systems
2. table-top design
3. extendability
4. plug-and-play capability
5. easy on-the-fly reconfiguration of the examples
6. replicability

To achieve these design requirements, The Illuminator architecture is conceived based on RasPi technology and Mosaik co-simulation framework. Raspberry Pis address design requirements 2, 3 and 4. Mosaik addresses design requirements 3, 4 and 5, while design requirement 6 is ensured by the open source nature of the project. In Section 5.3, it is described how Design Requirement 1 is addressed. To effectively meet Requirements 1, 3, 5, and 6, it should be noted that *The Illuminator* functions primarily as a simulation tool that relies on information exchange, contrasting with power hardware test-beds.

5.2.2. HARDWARE CONSIDERATIONS

The hardware interconnectivity of The Illuminator is shown in Figure 5.1. In the design, RasPis are interconnected using Ethernet cables via a switch. This approach was chosen to facilitate scaling to dozens of RasPis, as it manages both communication and power supply through the same cable. This reduces the cabling required by the system and avoids potential issues with WiFi connectivity. For smaller setups, with only a few RasPis, WiFi and battery supported alternatives can be viable. Two different variants of The Illuminator module are shown in Figure 5.2, one hosting 8 RasPis, another hosting 24 RasPis. These modules can be connected together to scale up the setup capacity.

Each RasPi has its own SD card, enabling simultaneous booting of the entire setup. Although it is possible to configure RasPis to use a shared memory space, i.e., one SD card for multiple units, this approach has been abandoned. This is because shared memory requires sequential access, leading to excessively long boot times in setups involving dozens of RasPis.

In this architecture, one RasPi is defined as the leader RasPi while the rest are the follower RasPis. The leader-follower architecture has been chosen for several reasons. First, the co-simulation framework Mosaik follows the same architecture in order to keep

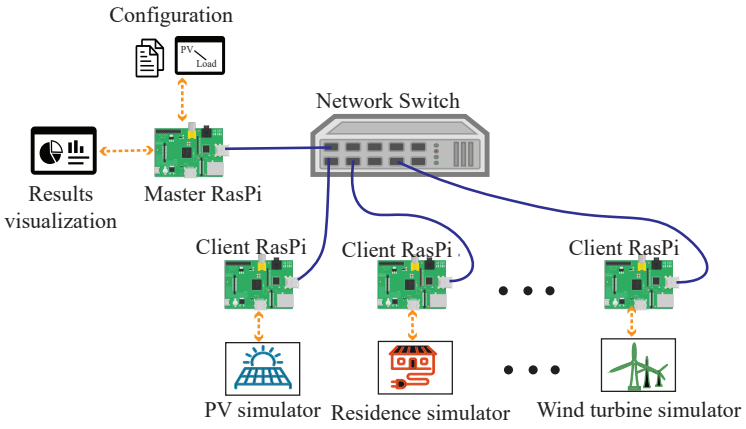

Figure 5.1: The structure of The Illuminator

track of the global time propagation of the entire simulation channeling all the messages between RasPis through one single central point. Second, the auxiliary functionalities, such as configuration, initialization, visualization, logging, etc. can be more easily streamlined from and by the leader.

Beside their table-top qualities, RasPis provide another benefit, namely, an abundance of peripherals that can be used to provide a more tangible feel to education and demonstration activities. They also have a vivid community with strong support.

Although RasPis have been taken as the target deployment platform, the simulation platform described next is Python based and therefore can run on any operating system that supports Python (of course, without exotic peripherals).

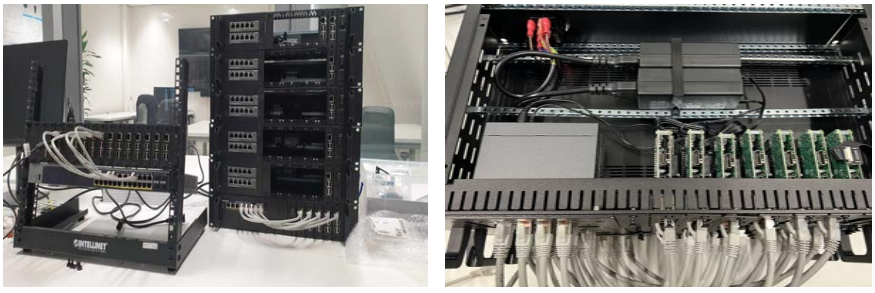

a) Iluminator hardware box b) Devices inside the box

Figure 5.2: Two variants of The Illuminator module

5.2.3. SIMULATION PLATFORM

The Illuminator software platform is largely based on Mosaik. Mosaik [117] is a simulation tool to link simulators and/or models together and to perform cosimulation. Syn-

chronize the simulation process with a global time clock and manage data exchange through a socket connection between the simulators. These two features make it a suitable orchestrator for distributed simulations. In other words, Mosaik gives an opportunity to:

- run simulations across a computing cluster (such as several strung RasPis),
- independently develop models in any programming language
- use models already encapsulated within various simulation tools.

In other words, Mosaik facilitates blurring the line between a model and a simulator by integrating both into a unified simulation environment. Given that Mosaik is written in Python, this language has been chosen for developing the core libraries of The Illuminator.

The process of using and setting up The Illuminator is shown in Figure 5.3.

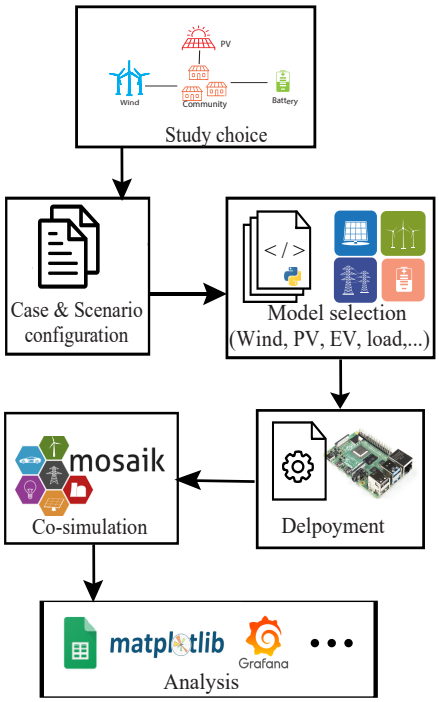

Figure 5.3: The simulation process of The Illuminator

Configuring simulation runs first requires specifying which models will run and in which configuration (see next section for details). Second, it must be specified which model will be deployed on which RasPi. Note that more than one model can run on a single RasPi since they are connected via socket connections. The deployment of the models across RasPi is achieved through the shell script (sh-file) via the leader RasPi,

leaving room for the creation of an automated software deployment architecture in the future.

Since the entire message exchange must pass through the leader RasPi due to the simulation synchronization needs, it is easy to set up monitoring and logging functionalities from this node. Users can select the model states to be monitored. The states and the simulation results are stored as *.csv files, while The Illuminator kit allows one to plot the data per simulation step or, alternatively, at the end of the simulation. The second approach allows faster simulation times. WANDB [118] is used as a dashboard for results visualization during the simulation and to compare results of different simulation runs.

5.3. LIBRARIES OF THE ILLUMINATOR

I distribute several libraries for the creation of energy transition case studies. The Illuminator comes with:

- a library of models,
- a library of cases, and
- a library of scenarios.

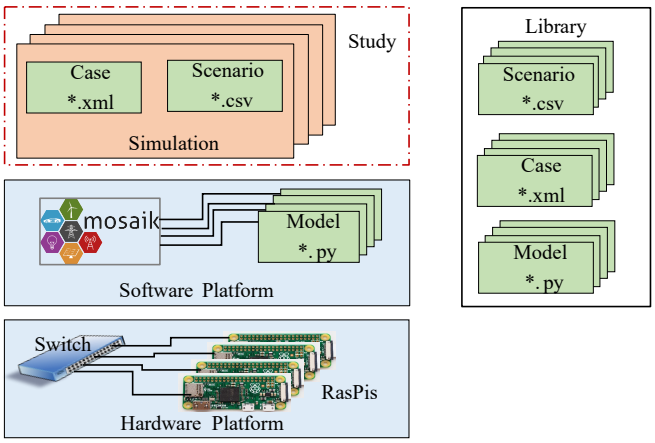

Figure 5.4: The Illuminator concept

The library of *models* contains the common power system models including PV systems, wind turbines, electric vehicles, households, etc. These models are combined into *cases*. Several typical cases relevant for power and energy systems are provided, spanning from household energy systems to national energy systems. Finally, the library of *scenarios* contains the relevant profiles of energy generation and consumption that can be used to investigate the case under different scenarios. The provided models are common and rather simplified academic models, but the open source nature of The Illuminator gives possibilities to extend and enhance them. The models, cases and scenarios

are populated with typical parameters and profiles giving a representative outlook of the energy system.

Most of the provided models are static models, comprised of algebraic equations. They are snapshot models which are strung together into cases. The storage models differ. They contain memory in terms of the SoC.

5.3.1. PV MODEL

To ascertain the output of a PV system, it's imperative to compute the irradiance incident on the module. The attenuation of solar radiation upon entering the Earth's atmosphere occurs due to scattering and absorption by dust particles, aerosols, and air molecules. Additionally, water vapor, oxygen, and carbon dioxide significantly contribute to radiation absorption. This attenuation segregates the incoming radiation into a diffused component—termed as Diffused Horizontal Irradiance (DHI), and a direct component, referred to as Direct Normal Irradiance (DNI). Furthermore, a reflected component exists arising from radiations reflected by surfaces surrounding the module, known as Global Horizontal Irradiance (GHI).

Meteorological stations typically record the DHI and DNI data, facilitating the computation of GHI using the following equation, where the α ranges from 0.05 - 0.20 for urban areas, 0.05 - 0.10 for forests, and 0.60 for snowy environments:

$$\begin{aligned} G_{\text{Direct}} &= \text{DNI} \cdot \cos(\text{AOI}), \\ G_{\text{Diffused}} &= \text{SVF} \cdot \text{DHI}, \\ G_{\text{Reflected}} &= \text{GHI} \cdot \alpha \cdot (1 - \text{SVF}). \end{aligned}$$

Here, SVF represents the Sky View Factor, delineating the fraction of the sky visible to the module, which is influenced by the module's inclination. AOI stands for "Angle of Incidence". In PV systems, the Angle of Incidence refers to the angle at which the sun's rays strike the surface of the solar panel. This angle is critical in determining how much sunlight falls directly onto the surface of the solar panel. The data of those weather parameters can get from weather API such as meteomatics [119].

The cumulative irradiance (G_{Module}) received by the module is the summation of the direct (G_{Direct}), diffused (G_{Diffused}), and reflected irradiance ($G_{\text{Reflected}}$), formulated as:

$$G_{\text{Module}} = G_{\text{Direct}} + G_{\text{Diffused}} + G_{\text{Reflected}} \tag{5.1}$$

Weather conditions significantly influence the PV module's performance, with the module temperature having a notable effect on its output. As the module output is vital for PV system modeling, the efficiency variation under fluctuating temperature and irradiance conditions is given by:

$$\eta(T_M, G_{\text{Module}}) = \eta(25^\circ\text{C}, G_{\text{Module}}) \cdot \left[1 + k(T_M - 25^\circ\text{C})\right] \tag{5.2}$$

Here, η signifies the module's efficiency, T_M denotes the module temperature, G_{Module} represents the irradiance falling on the module (calculated earlier). Note that the module's efficiency undergoes continuous alterations throughout the day, influenced by changes in temperature and irradiance levels.

5.3.2. WIND MODULE

The construction of a wind module centers on harnessing the kinetic energy present in wind to generate electrical energy. This is achieved by rotating turbine blades which, in turn, generate electrical energy.

The wind speed is a critical factor in the power generation capacity of a wind turbine. The power generated by a wind turbine is proportional to the cube of the wind speed and the square of the radius of the turbine rotor. The larger the rotor's radius, the greater the wind it can harness, thereby enhancing the power generation capacity. The equation representing this is given as:

$$P = \frac{1}{2}\rho A v^3 = \frac{1}{2}\rho \pi r^2 v^3 \tag{5.3}$$

where P is the power generated, ρ represents the air density, A is the area swept by the turbine blades, v is the wind speed, and r is the radius of the turbine rotor.

The wind turbine possesses inherent restrictions regarding the operational wind speeds. A designated range of wind speeds exists - from the cut-in to the cut-out wind speed - within which the turbine can generate electricity efficiently. The cut-in wind speed signifies the threshold at which the turbine blades initiate rotation. Below this threshold, the turbine incurs higher losses than the energy extracted from the wind, necessitating external energy input to maintain motion. Conversely, the cut-out wind speed defines the upper limit of wind speed for turbine operation, beyond which the turbine shuts down to prevent damage. The graphical representation of this phenomenon is depicted in Figure 5.5.

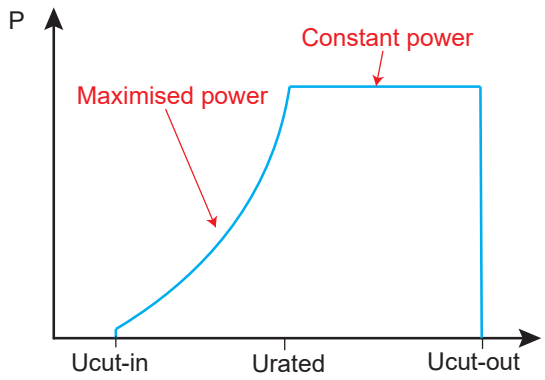

Figure 5.5: Power curve of the wind turbine[120]

5.3.3. BESS MODEL

The BESS plays a pivotal role in ensuring a smooth energy supply, especially during low renewable energy generation periods. The BESS capacity, often measured in kWh, defines the maximum amount of energy that can be stored and dispatched. The SOC rep-

resents the current energy content as a percentage of the BESS's total capacity. The dynamic SOC can be modeled using the following equation:

$$SoC_{BS}(t) = SoC_{BS}(t-1) + \frac{\eta_{ch} \cdot P_{ch}(t) - P_{dis}(t)/\eta_{dis}}{C_{\text{bat}}} \tag{5.4}$$

where $SoC_{BS}(t)$ is the state of charge at time t, C_{bat} is the battery capacity, $P_{\text{ch}}(t)$ and $P_{dis}(t)$ are the charging and discharging power at time t, η_{ch} is the charging efficiency.

5.3.4. HYDROGEN SYSTEM MODEL

The hydrogen system consists of an electrolyzer, which converts electricity into hydrogen gas through the process of water electrolysis. The generated hydrogen is stored in tanks and can be utilized to generate electricity through a fuel cell. The SOC of the hydrogen tank can be modeled as follows:

$$SoC_{HS}(t) = SoC_{HS}(t-1) + \frac{\eta_{ELE} \cdot P_{ELE}(t) - P_{FC}(t)/\eta_{FC}}{C_{HS}} \tag{5.5}$$

where $SoC_{HS}(t)$ is the state of charge at time t of hydrogen storage, C_{HS} is the hydrogen storage capacity, $P_{ELE}(t)$ and $P_{FC}(t)$ are the electrolyser and fuel cell power at time t, η_{ELE} and η_{FC} are the efficiency of the electorlyser and fuel cell system.

5.3.5. POWER GRID MODEL

The grid model in my study is developed based on pandapower, an open-source software package that enables the simulation and analysis of power grids [121]. Its robust platform integrates seamlessly with Python, offering functionalities for power flow analysis, optimal power flow, state estimation, and various other power system analyses. The software facilitates modeling various grid components such as generators, loads, transformers, and transmission lines with detailed parameterization.

```
import pandapower as pp
# create an empty network
net = pp.create_empty_network()

# add components (e.g., buses, lines, transformers)
pp.create_bus(net, vn_kv=20., name="Bus 1")
pp.create_bus(net, vn_kv=0.4, name="Bus 2")
pp.create_line(net, from_bus=0, to_bus=1, length_km=0.1,
               name="Line 1", std_type="NAYY 4x50 SE")

# perform power flow analysis
pp.runpp(net)
```

The above Python script snippet creates an elementary grid network using Pandapower, demonstrating the simplicity and efficiency of power grid modeling using this software.

Currently, no specific ontology is proposed for The Illuminator message exchange. The typical information that gets passed between models is power on the model inter-

face (either input or output power or both depending on which other models the model in question is connected to), but other internal states can also be shared. This can be useful when, for example, one wishes to devise a control logic of the charging point to react on the battery SoC. Defining ontology remains part of future work. The Illuminator runs in real and non-real time. The time step of The Illuminator is defined by the user in the whole multiples of one second. Therefore, one second is the finest resolution of The Illuminator kit.

5.4. USING THE ILLUMINATOR

Before explaining the utilization of The Illuminator, the notion of simulation and study is introduced. A combination of a case and scenario defines one *simulation* run. According to this simulation run, the models are deployed and simulated. A *study* comprises one or more simulation runs. Any phenomena under investigation would be first captured in the notion of study which would then be split into simulation runs specifying desired cases and scenarios.

Although the cases are possible to define by directly modifying *.xml case files, the user also has the option to interact more vividly with The Illuminator by drawing a configuration diagram on a touch screen or a smart board, such as shown in Figure 5.6. Based on the drawing, The Illuminator will automatically assemble the case file. Assignment of the models to specific RasPis in this manner will be enabled in the near future.

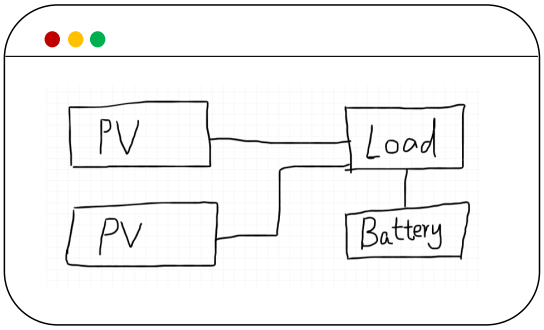

Figure 5.6: The Configuration diagram

- *Energy transition studies* - As already explained in the main motivation of my work, The Illuminator is intended to capture the relevant challenges and solutions to the energy transition, and therefore, the first domain of use of The Illuminator is as a table-top replica of the energy system for education and demonstration purposes. However, its design features allow two other interesting applications.

- *Sandbox for validation and verification* - The Illuminator can be used as a validation and verification platform for newly developed coordination and control algorithms. Python language, together with the distributed architecture and an abun-

dance of models, makes Illuminator perfectly suitable as a sandbox for testing of algorithms, in real and non-real time.

- *Digital twin* - Flexible nature and its ability to be easily reconfigured and deployed, make The Illuminator suitable to spawn a multitude of system variations in operational policies and/or system configuration, in this way informing future design and operational decisions.

Many researchers are contributing to new algorithms to support the energy network and prepare it for coming challenges. Testing them in an environment that can mimic real life is of benefit. Thus, Illuminator aims to provide this environment. Along with students, communities must be educated about the changing energy networks. It is essential to keep everyone informed about the ongoing transition and communicate an accurate picture. The toolkit aims at bridging that gap while generating curiosity among the youth to contribute towards further development. Educating consumers can also be a contributing step towards increasing consumer participation which can be of assistance for an effective transition to a clean future. Therefore, The Illuminator provides a friendly user interface for different groups to do education, research, or demonstration.

5.4.1. ILLUMINATOR SET UP

After installing the Raspberry pi OS into the RasPi, we need several steps to set up The Illuminator environment for all RasPis.

- Set the static IP address for the RasPi by changing the file "/etc/dhcpcd.conf" as below.

```
interface etho
static ip_address=192.168.0.1/24
```

- Set SSH keys to available for all RasPis.
- Install the required packages in Python [116].
- Run the 'buildcilentremoterun.py' file at each Client RasPi, and give all users execute permission to all the documents in the folder "runshfile".

And after those four steps, all RasPis are prepared well for The Illuminator box.

5.4.2. SIMULATION CONFIGURATION

I provide two options for the users to configure the simulation. One is through the "config.xml" and "connection.xml" files, such as below.

```
<index>0</index>
<model>Wind</model>
<method>connect</method>
<location>192.168.1.0:5123</location>
...
<index>15</index>
<send>wind[0]</send>
<receive>monitor</receive>
<message>wind_gen</message>
```

The configuration shows that the simulator wind turbine will be simulated at the RasPi with IP address 192.168.1.0, and the wind turbine will communicate with other simulators with Port 5123. By changing the IP and Port, we can point the simulator running in a specific RasPi and share its information with a particular Port. Moreover, we can build more than one wind turbine in the simulation. The second definition is to specify the message exchange. The message "wind_gen" of the first wind turbine will be sent to the monitor, as shown in the example code.

5.4.3. INTERFACING

The other way is through drawing a configuration diagram on a touch screen on the web, such as Figure 5.6. That means there will be two PV panels in the simulation system, one load and one Battery. The Illuminator will automatically build up a simulation system following the configuration diagram. And for the deployment of the simulator to the specific RasPi, we still need to configure it in the "config.xml" file.

5.4.4. SIMULATOR DEFINITION

The model parameters, simulation scheduling, and results in presentation format are defined in the file' buildmodelse.py'. The load set is used as an example for explanation. The `load_set` is the parameter to specify the residential load, and the `houses` means the number of typical houses included in the residential load. The parameter settings for other simulators are specified in that file, with notes added for each parameter in The Illuminator. The `RESULTS_SHOW_TYPE` is the dictionary used to define how to present the simulation results. A 'True' value for `write2csv` indicates that the results will be written to a '.csv' file during the simulation. A 'True' value for `dashboard_show` indicates that the results will be displayed on the Dashboard during the simulation. The Dashboard retains the simulation results and allows for the comparison of several different scenarios. In The Illuminator, the WANDB platform [118] is utilized for results visualization during the simulation. A 'True' value for `Finalresults_show` means that the results will be displayed in figures at the end of the simulation. The `realtimefactor` is the real-time factor set to adjust the simulation speed, which can range from a real-time simulation to a wall-clock time simulation. A real-time factor of 1 means that one simulation time unit (typically a simulation second) corresponds to 1 second of real-time. Setting it to 1/60 means that one simulated minute will take one real-time second. A zero setting indicates that the simulation will run as fast as possible.

```
load_set={'houses':1000}
...
RESULTS_SHOW_TYPE={
   'write2csv':True,
   'dashboard_show':True,
   'Finalresults_show':True}
realtimefactor=0
```

5.4.5. ENERGY SIMULATOR BUILD UP FOR DEVELOPERS

For each simulator, there are two python files. The first one is the model of the assets, and the developer can use their model no matter written by which language. The second one is the SimAPI file for the model, which connects the model with Mosaik. Implementing this file ensures the basic communication that needs to be done with Mosaik for data flow and simulation. It has a specific set of API calls which are shown as below.


```
class BatterySim(Mosaik_api.Simulator):
   def __init__(self):
       super().__init__(meta)
       self.entities = {}
       ...
   def init(self, ... ):
       ...
   def create(self, ...):
       ...
   def step(self, ...):
       ...
   def get_data(self, ...):
       ...
```

The **init** is used for assigning additional. When the simulator is started in the Scenario API file, this method will be called exactly once. **create** call instantiates the simulation model and creates a user-defined number of entities of that model. **step** This call helps proceed with the simulation by using the inputs. **get_data** returns the current values of all the attributes mentioned in the simulation model. In The Illuminator, the SimAPI file for all models is provided and packaged within the simulator, facilitating connection with Mosaik. Developers wishing to use their own models can easily modify the provided SimAPI file to match their specific requirements.

5.5. CASE VALIDATION

5.5.1. ENERGY MANAGEMENT SYSTEM SIMULATION

One trend to reduce energy bills and greenhouse gas emissions is by forming self-sufficient energy communities. Having sufficient renewable energy generation and storage could potentially make the community self-sufficient. An EMS is needed to manage the energy

flows.

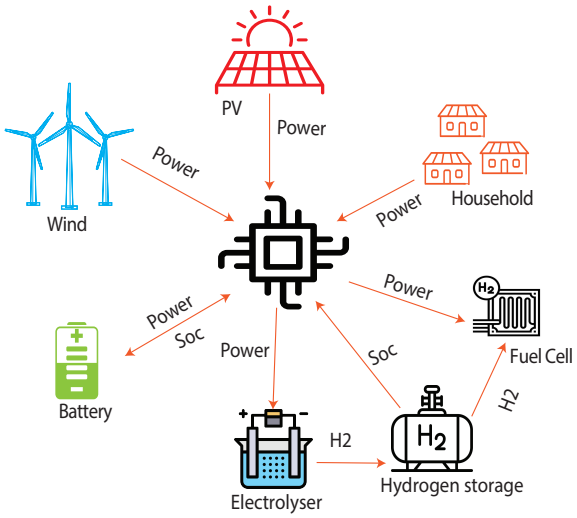

Figure 5.7: The schematic of the case

In this expansive case study, a deep analysis of a contemporary energy system tailored to meet the requirements of a self-sufficient community is conducted. A comprehensive approach is demonstrated to examine the feasibility of autonomous energy generation and consumption within a localized setting. Central to this investigation is the deployment and performance evaluation of the groundbreaking Illuminator kit. The heart of this system rests on various intricately designed models that portray different components of the modern energy ecosystem. These models encapsulate the dynamics of a small-scale wind turbine and a rooftop PV system, which act as the primary sources of renewable energy. Complementing these are models representing typical household consumption patterns and two distinct yet complementary storage assets that ensure a continuous energy supply. The first storage asset encompasses a fuel cell, a hydrogen storage tank, and an electrolyzer, establishing a long-term storage system capable of managing seasonal energy variations. On the other hand, the second asset, a lithium-ion BESS, facilitates short-term storage, adept at handling daily fluctuations in energy production and consumption.

A pivotal component in this ecosystem is the EMS, represented graphically as a central controller in the schematic depicted in Figure 5.7. This controller orchestrates the energy flow within the system, determining the charging and discharging rates of the storage assets based on the real-time data it receives. The EMS operates on a simple yet effective logic: initially, the battery is deployed to maintain the power balance, leveraging its capacity to handle daily energy fluctuations. However, if it reaches its capacity, the system activates either the electrolyzer or the fuel cell to manage the energy demand, thus ensuring a seamless energy supply at all times. The EMS algorithm is deployed on the leader RasPi, while the rest of the models are separately deployed in different follower

RasPis.

A realistic scenario using typical June profiles for household power consumption and power generation from the wind and PV systems was devised to gauge the system's performance. These profiles are graphically demonstrated in Figure Figure 5.8. The simulation observes a time step of 15 minutes, providing a granular insight into the system's behavior over a month.

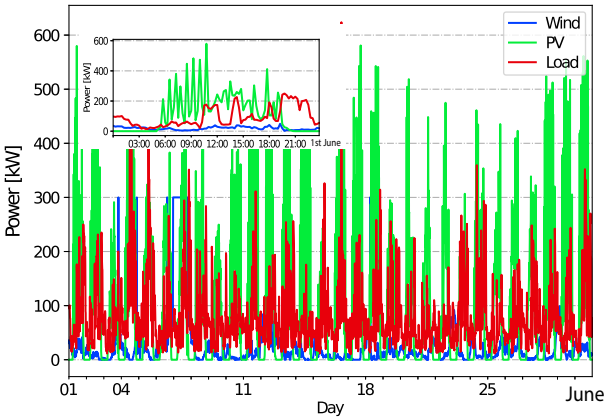

Figure 5.8: The Load and generated power from PV and wind in June

The resulting data showcases the fluctuating power dynamics of the BESS and the hydrogen storage, displayed in Figure 5.9, Figure 5.10 and Figure 5.11. Figure 5.9 and Figure 5.11 show that the BESS is mainly used to balance the fluctuation of solar and wind in the daily cycle. The BESS is sized well to accommodate almost the entire daily variability. In contrast, hydrogen storage is mainly used to balance seasonal variations. While the SOC of BESS cycles once daily, the hydrogen accumulates in June and will be consumed in season when renewable power is low, i.e., in winter. And from Figure 5.10, the fuel cell works much less time than electrolyser.

The simulation on a RasPi cluster takes 1035 seconds. The same simulation, if deployed on a desktop PC with Intel(R) Xeon(R) W-2123 CPU @ 3.60GHz takes 493 seconds.

5.5.2. VOLTAGE REGULATION IN DISTRIBUTION NETWORK SIMULATION

In the evolving landscape of power distribution networks, maintaining optimal voltage profiles is critical to ensure the reliable and efficient operation of the system. As the integration of renewable energy sources into the power grid increases, so does the complexity of managing voltage levels within the network. In this case, my investigation focused on understanding and addressing the voltage fluctuations that occur primarily during winter. To provide deeper insight into the platform's potential in managing these challenges, a case study centered around the CIGRE distribution network was developed, as depicted in Figure 3.5 in Section 3.2.

A one-day real-time simulation was orchestrated to establish a realistic yet challenging test scenario that closely mirrors the energy demands and generation patterns typ-

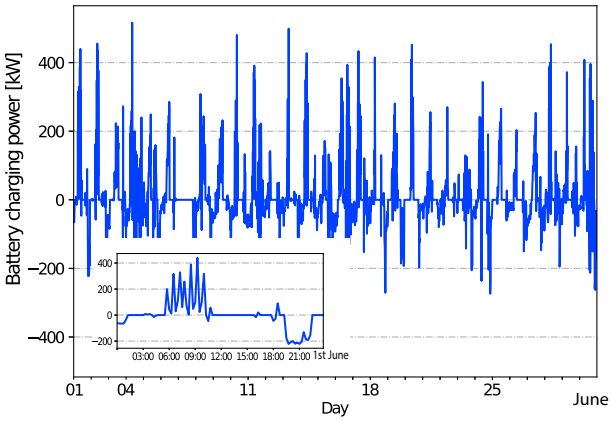

Figure 5.9: BESS charging (positive values) and discharging (negative values) power in June

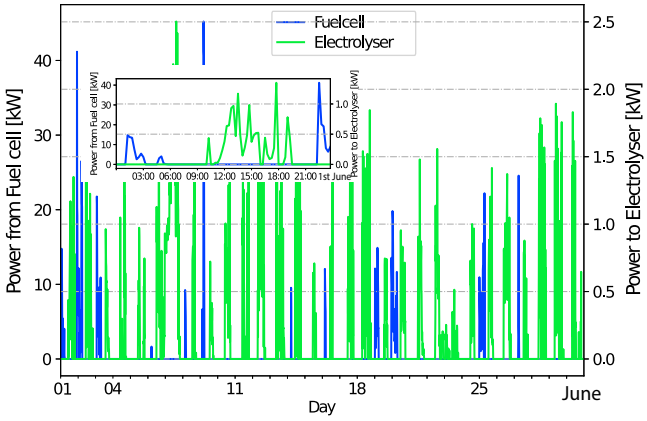

Figure 5.10: Electrical power injection from the fuel cell and electrical power taken by the electrolyser in June

ical of a January day (1st January) in a residential area. This choice of timeframe is significant, considering the diminished power output from residential rooftop PV panels due to the reduced sunlight hours during winter, which exacerbates the network's potential for voltage drop issues. Specific simulation data is displayed on the Github of The Illuminator[122].

I chose to employ the centralized control method, a popular approach known for its effectiveness in maintaining voltage regulation in complex networks. This method, as detailed in Section 3.2.1, provides a framework for precise control and management of voltage levels throughout the network, thereby ensuring stability and minimizing losses.

My analysis brought to the fore a significant issue - a noticeable voltage drop resulting from the imbalance between the power generated by the residential PV panels and

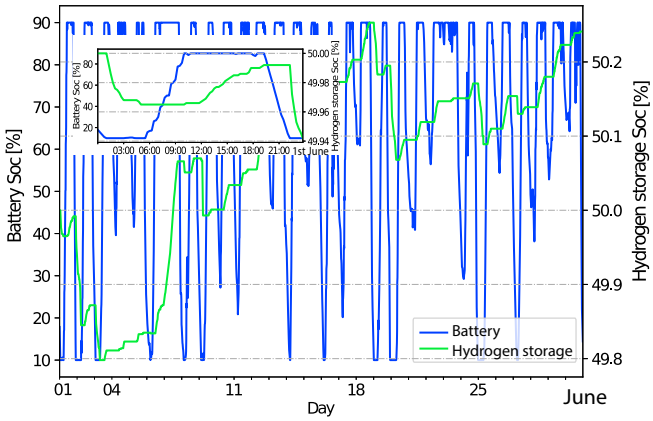

Figure 5.11: The SOC of the BESS and the hydrogen storage in June

the power consumption during the winter. This voltage drop, if unaddressed, can potentially lead to inefficiencies and disruptions in the power distribution network.

However, my simulation showcased the effectiveness of the centralized control method in mitigating this issue. As illustrated in Figure 5.12 and Figure 5.13, the implementation of voltage regulation strategies successfully rectified the voltage drop problem. Notably, the post-regulation voltage profile indicated that the lowest voltage level within the network was maintained above 0.95 pu, thereby ensuring a stable and reliable power supply.

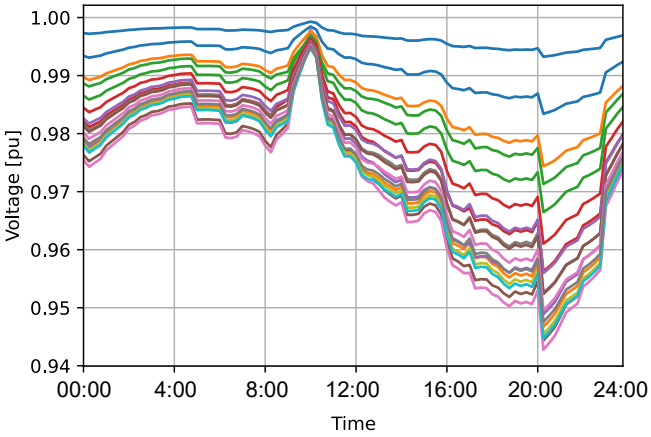

Figure 5.12: The voltage profile before voltage regulation

These are two simple cases with simple control logic that illustrate how The Illuminator works. The developers can add other models to the library, build their own control logic, link the models in different configurations, and change the time step of the simu-

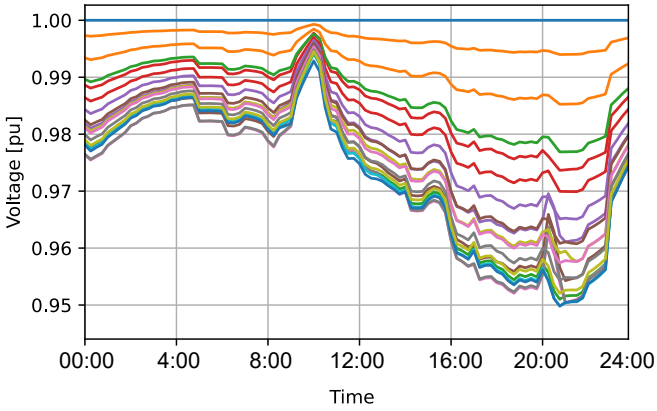

Figure 5.13: The voltage profile after voltage regulation

lation. Each variation could lead to innovative studies and insights.

5.6. CONCLUSION

This chapter sets out to address the crucial question: How can a flexible and extendable kit be developed to enable intelligent grid control algorithms from digital test fields to real-world applications? Firstly, the architectural design and software-hardware integration of The Illuminator are key responses to the demand for a flexible and extendable energy system integration development kit. By utilizing a modular software platform that operates on Raspberry Pi clusters or personal computers, The Illuminator demonstrates adaptability and scalability, which are crucial for real-world applications. The Illuminator's open-source nature and its user-friendly design significantly contribute to making the development kit accessible to a broad range of users. The Mosaik co-simulation platform is used to address tasks such as time synchronization and interactions across the integrated energy assets. The successful application of The Illuminator in a residential case study, focusing on voltage regulation method testing, further validates its effectiveness. This practical demonstration underscores the kit's capability to address real-world challenges in energy transition and intelligent grid control, thus providing a tangible solution to the posed research question. Although the platform supports HIL testing, the case study did not evaluate this feature. This is an aspect that requires further exploration in the future.

6

CONCLUSION AND DISCUSSION

This research was initiated with the intent to understand the challenges of integrating DRES into DNs and pave the way for renewable energy transition. This thesis aims to identify the main barriers limiting the integration of DRES and develop and verify self-organizing optimal voltage regulation strategies in future DNs to achieve high DRES penetration levels in power grids. This thesis provides a solution for three critical phases for self-organizing voltage regulation in smart power grids: planning, operations, and validation. The chapter begins by revisiting the research questions from Chapter 1, providing a comprehensive overview of the solutions and methods discussed in this thesis. Additionally, potential future research directions are explored, highlighting the development of self-organized, efficient, and resilient power grids.

This thesis thoroughly investigates the complex challenges of integrating DRES into the power grid. As we move towards a more sustainable future, integrating DRES becomes even more crucial. It is not just about being environmentally responsible; it also opens doors to new ideas and improvements in our power systems. This final chapter provides a review of the research's main points, along with a discussion of its implications for building self-organizing power grids and suggestions for areas of future study.

6.1. RESEARCH CONTRIBUTIONS TO RESEARCH QUESTIONS

In this section, the research questions presented in Chapter 1 are addressed.

- **Research Question 1: How to integrate a large number of DRES into DNs?**

  To answer the initial research question, a stochastic simulation-based approach is proposed for assessing and determining the DRES penetration level and BESS capacity for power smoothing, as detailed in Chapter 2. First, various stochastic scenarios are generated based on existing grid conditions. Then, through the analysis of a variety of simulation results based on each generated scenario, the maximum allowable penetration level of DRES for the DN is determined. Finally, an incremental approach to size the BESS capacity is implemented with different power smoothing logic to mitigate the influence of power fluctuations on the external grid. Case studies incorporating four voltage control algorithms and three power smoothing methods demonstrate the universality and effectiveness of the proposed approach.

  My analysis demonstrated that the Q(V) control method yielded superior results compared to other control methods, and an increased number of DRES installations resulted in a tighter distribution of DRES maximum installed capacity. A one-year simulation indicated that the risk of voltage violations could be minimized to 5.68% with an appropriately designed DRES installation and control strategy. The case study to determine the BESS capacity for power smoothing revealed that the Step Ramp-rate Control Strategy required significantly lower BESS capacity compared to other methods while preserving power quality. These findings can assist network operators and planners in efficiently integrating renewable energy sources and storage systems for a reliable and sustainable power grid.

  The main contributions are three points by answering Q1. Firstly, by providing a variety of conditions and control logic, numerous stochastic scenarios can be automatically generated. A comparative analysis of voltage control and BESS power smoothing methods is performed. Second, the risk of technical violation and power smoothing target failure can be analyzed by examining a long period of simulation results. Third, the primary advantage is that DSOs can assess their preferred voltage regulation and power smoothing methods and decide which one to use based on their network and needs.

  you can highlight that with the power smoothing control performed by the BESS located at the substation level, the DSOs can provide the power smoothing as a service to the upstream voltage levels either to help the frequency stability or the voltage quality

- **Research Question 2: How can voltage regulation in future DNs be effectively managed to accommodate the increasing DRES penetration levels from the DSO side?**

  The findings in Q1 indicate that as the penetration of DRES increases in DNs, voltage regulation becomes a significant hurdle. Although the proposed local voltage control method improves the maximum DRES penetration level of the power grid, it still falls short of the expected levels for future DNs. Innovative approaches are imperative to transition to a renewable power grid truly.

  In response to Q2, a novel distributed cooperation voltage regulation method for future DNs was developed. The proposed method can minimize the number of agents involved in the voltage regulation and minimize the change of required power for voltage regulation, which together minimizes the need for re-dispatching, i.e. the impact of voltage regulation on the exchange of energy. Moreover, the proposed method performs online optimization, i.e., the value of the decision variable is physically implemented as a controller set-point at each iteration, reducing the response time. The algorithm presented is benchmarked against the ADMM and centralized optimization. The results show the voltage regulation effectiveness. Compared to the ADMM method, the proposed method dramatically reduces the action time and does not require retuning if the network topology or agent participation changes.

  The main contributions can be summarized by answering this research question in two main points. First, the proposed method uses the minimal number of agents and the minimal amount of contributed power to regulate voltage. By reducing the number of agents and their power contribution, the need for re-dispatching is minimized, i.e., the deviations from the nominal power exchange are minimized. The nominal power exchange is associated with comfort levels and financial transactions; therefore, it is essential to minimize deviations from it. The proposed algorithm relies on voltage sensitivity to engage only the agents with the highest potential to regulate voltage. Second, the proposed method implements the set points in each iteration in the spirit of online optimization. Hence, the response time of the algorithm is minimal and the voltage violations are acted upon quickly, much faster than with ADMM and similar algorithms.

- **Research Question 3: How to develop an EMS system for energy communities that optimally synchronizes energy consumption and generation, facilitating self-organizing voltage regulation?**

  A novel four-stage energy management strategy is introduced to answer this research question, harnessing receding horizon optimization to manage energy consumption within a PV-BESS-electrolyzer-fuel cell residential energy community setup. My approach uniquely sequences four optimization stages: yearly, monthly, day-ahead, and intra-day. This integration blends both long-term and short-term strategies in EMS development, positioning hydrogen produced by electrolyzers as seasonal storage and batteries for daily utilization. The algorithm presents three modes, each defined by a distinct objective function, catering to different user

preferences: self-sufficiency, profit maximization in the energy market, and provision of balancing services to grid operators and external entities. The method's effectiveness is validated through simulations and a detailed analysis of a real-world PV-BESS-electrolyzer-fuel cell lab setup, including an assessment of algorithm efficiency and a performance comparison across the various operational modes. Additionally, the robustness of the proposed distributed control algorithm answering Q2, especially concerning the failure of a single agent, is explored, revealing the advantages of the proposed distributed control algorithm over a centralized control mechanism, and demonstrating the cooperation of four-stage energy management strategy and distributed control algorithm to achieve self-organizing voltage regulation.

By answering this research question, the main contributions can be summarized in two main points. Firstly, the proposed algorithms can help energy communities achieve self-sufficiency, flexibility, and reliable energy supply with user preferences and priorities. Then, the proposed strategy also collaborates with the DSO to facilitate self-organizing voltage regulation, thereby playing a pivotal role in advancing the sustainable evolution of our energy systems.

- **Research Question 4: How can a flexible and extendable kit be developed to enable intelligent grid control algorithms from digital test fields to real-world applications?**

  In response to the research question, a do-it-yourself kit was developed to demonstrate the energy transition challenges and solutions. The kit called The Illuminator is flexible and modular, allowing a variety of cases to be explored. The kit is available on GitHub under the LGPL license. The Illuminator comes with models, case studies and scenarios to represent a variety of possible contexts relevant to the energy transition. The architecture of the hardware and software of The Illuminator is first explained, then the libraries of The Illuminator and its user manual are presented. At its core, The Illuminator leverages the capabilities of Mosaik, a dynamic platform that orchestrates seamless data flows and scheduling functionalities. This makes The Illuminator a testing environment not only for demonstrating the energy transition pathways to a broad user base but also for assessing the performance metrics of intelligent control algorithms. Moreover, The Illuminator supports various communication protocols and techniques, allowing for comprehensive hardware-in-the-loop testing. This enriched platform amplifies the authenticity of the simulations, creating a potent nexus between the virtual and physical realms.

  The main contributions can be summarized in two main points by answering this research question. First, as an open-source, replicable, and scalable kit, The Illuminator can outline and address the relevant challenges and solutions inherent in the energy transition and evaluate the on-site deployment of intelligent control algorithms. Second, the inherent flexibility of The Illuminator, coupled with the ability to be easily reconfigured and deployed, makes it a powerful tool capable of generating a wide range of system changes in operational strategies and/or configurations that can generate many scenarios to assess the reliability of the algorithm

in the deployment on-site.

6.2. DISCUSSION AND FUTURE WORK

The study of self-organizing smart grids is an emerging field with a wide array of research possibilities and applications across disciplines. This thesis focuses on voltage regulation within DNs in three phases: planning, operations, and validation. The findings of this thesis and limitations in the scope of the research suggest several interesting topics for future research. Detailed discussions of future work are provided in the following.

- **Self-organizing voltage regulation integration with the transformer:** With the distributed cooperation voltage regulation algorithm proposed in Chapter 3 and the four-stage energy management strategy in Chapter 4, Self-organizing voltage regulation can be addressed within the scope between DSO and energy communities. However, the integration of the transformer and the upstream network is still an open challenge. Transformers play an important role in voltage management. Their ability to adjust voltage levels through tap-changing mechanisms is fundamental to grid stability. Therefore, a self-organizing voltage regulation integration transformer is the next potential research step. However, the tap-changing ability of the transformer is not continuous but quantized, allowing for voltage adjustments only at specific set points. This characteristic introduces mixed-integer variables into the optimization problem. Addressing this in a self-organizing context is a complex research challenge.

- **Control Algorithm Discovery and Integration:** The local, distributed, and centralized control algorithm has its application area to its best efficiency. Local control is fast and easy to apply; centralized control has a global perspective in decision-making and distributed control scalability and efficiency in parallel tasks. Therefore, choosing the right control algorithm depending on the specific characteristics and needs of the energy system with high DRES penetration levels is essential. As the penetration level of DRES increases, we must ensure the balance and integration of local, distributed, and centralized control for optimal operations of the electricity system.

- **Self-organizing power grid:** While voltage regulation remains a crucial pillar of grid stability, it is not the sole factor that dictates grid health. Achieving a true self-organizing grid requires an integrated energy management approach to operate the power grid, which requires respecting the voltage, frequency stability, and technical constraints of the power grid. The dynamics between voltage, congestion, and frequency are intricate. A surge in power, for instance, from high DRES output, can lead to voltage rise, increased line congestion, and frequency variations. Conversely, a sudden drop can depress voltage levels and reduce congestion but disturb frequency. By understanding and harnessing the synergies between voltage, congestion, and frequency, we can usher in an era of grids that are not mere conduits but intelligent entities, dynamically orchestrating the energy dance of supply and demand.

- **Develop The Illuminator for self-organizing multi-carrier energy systems:** The evolving energy landscape today is becoming increasingly interconnected. The concept of energy islands, where the grid operates independently of the rest of the energy sector, is becoming obsolete. To truly drive the energy transition, multi-carrier energy systems that weave electricity, heat, natural gas and other forms of energy into a cohesive, synergistic tapestry must be explored and understood. These systems are no longer static entities but are expected to participate in self-organization, adapting and responding in real-time to changing conditions. This shift underscores the need for advanced tools like the Illuminator.

  The Illuminator, with its modular and flexible design, is pivotal in exploring these complex, interconnected systems. Its open-source nature and comprehensive libraries allow for the integration of diverse energy models. However, the challenge lies in the seamless incorporation of agent intelligence within these environments. This integration is crucial for simulating the dynamic behavior of components like heat pumps and natural gas flows, as well as understanding the charging patterns of electric vehicles. Another significant challenge is the hardware-in-the-loop testing capabilities of the Illuminator. While this feature enhances simulation realism by incorporating physical hardware components, it also introduces complexities in understanding how these components interact within a larger, self-organizing system. The ability to predict system behavior, identify potential bottlenecks, and devise strategies for smooth integration requires advanced analytical tools and a deep understanding of the interplay between different energy carriers.

  As researchers, policymakers, and industry professionals delve deeper into multi-carrier energy systems, tools like the Illuminator become indispensable. They provide critical insights into system behaviors and help in developing robust, adaptable, and efficient energy systems. Yet, the path is fraught with research challenges, particularly in integrating and managing the intelligence of autonomous agents within these complex networks.

BIBLIOGRAPHY

[1] Valérie Masson-Delmotte et al. “Climate change 2021: the physical science basis”. In: *Contribution of working group I to the sixth assessment report of the intergovernmental panel on climate change* 2.1 (2021), p. 2391.

[2] Dolf Gielen et al. “Global energy transformation: a roadmap to 2050”. In: (2019).

[3] Stéphanie Bouckaert et al. “Net zero by 2050: A roadmap for the global energy sector”. In: (2021).

[4] Paris IEA. “World Energy Balances”. In: (). URL: https://www.iea.org/data-and-statistics/data-product/world-energy-balances.

[5] Dolf Gielen et al. “World energy transitions outlook: 1.5° C pathway”. In: (2021).

[6] Hans-Otto Pörtner et al. “Climate change 2022: impacts, adaptation and vulnerability”. In: *IPCC Sixth Assessment Report* (2022).

[7] Gautam Gowrisankaran, Stanley S Reynolds, and Mario Samano. “Intermittency and the value of renewable energy”. In: *Journal of Political Economy* 124.4 (2016), pp. 1187–1234.

[8] Sara Eftekharnejad et al. “Impact of increased penetration of photovoltaic generation on power systems”. In: *IEEE Transactions on Power Systems* 28.2 (2013), pp. 893–901. DOI: 10.1109/TPWRS.2012.2216294.

[9] Ghimar Merhy, Ahmed Nait-Sidi-Moh, and Nazih Moubayed. “Control, regulation and optimization of bidirectional energy flows for electric vehicles’ charging and discharging”. In: *Sustainable Cities and Society* 57 (2020), p. 102129. DOI: 10.1016/j.scs.2020.102129.

[10] Alliander N.V. “Alliander N.V. Results 2021”. In: (2021). URL: https://www.alliander.com/content/uploads/dotcom/Alliander-Results-2021-def.pdf.

[11] “Capaciteitskaart invoeding elektriciteitsnet”. In: (2021). URL: https://https://capaciteitskaart.netbeheernederland.nl/.

[12] Bahareh Oryani et al. “Barriers to renewable energy technologies penetration: Perspective in Iran”. In: *Renewable Energy* 174 (2021), pp. 971–983. DOI: 10.1016/j.renene.2021.04.052.

[13] Chu Donatus Iweh et al. “Distributed generation and renewable energy integration into the grid: Prerequisites, push factors, practical options, issues and merits”. In: *Energies* 14.17 (2021), p. 5375. DOI: 10.3390/en14175375.

[14] Fco Javier Zarco-Soto, Pedro J Zarco-Periñán, and Jose L Martınez-Ramos. “Centralized control of distribution networks with high penetration of renewable energies”. In: *Energies* 14.14 (2021), p. 4283. DOI: 10.3390/en14144283.

[15] Yesbol Gabdullin and Brian Azzopardi. “Impacts of photovoltaics in low-voltage distribution networks: a case study in Malta”. In: *Energies* 15.18 (2022), p. 6731. DOI: 10.3390/en15186731.

[16] Anestis G Anastasiadis et al. “Effects of increased electric vehicles into a distribution network”. In: *Energy Procedia* 157 (2019), pp. 586–593. DOI: 10.1016/j.egypro.2018.11.223.

[17] National Electrical Manufacturers Association and others. “American National Standards Institute (ANSI) C84. 1-2006, Voltage Ratings for Electric Power Systems and Equipment”. In: *Rosslyn, VA* (2006).

[18] Thomas Stetz, Frank Marten, and Martin Braun. “Improved low voltage grid-integration of photovoltaic systems in Germany”. In: *IEEE Transactions on Sustainable Energy* 4.2 (2013), pp. 534–542. DOI: 10.1109/TSTE.2012.2198925.

[19] “IEEE Standard for Interconnection and Interoperability of Distributed Energy Resources with Associated Electric Power Systems Interfaces”. In: *IEEE Std 1547-2018 (Revision of IEEE Std 1547-2003)* (2018), pp. 1–138. DOI: 10.1109/IEEESTD.2018.8332112.

[20] Yuan-Kang Wu, Shih-Ming Chang, and Paras Mandal. “Grid-connected wind power plants: a survey on the integration requirements in modern grid codes”. In: *IEEE Transactions on Industry Applications* 55.6 (2019), pp. 5584–5593. DOI: 10.1109/TIA.2019.2934081.

[21] Australia AEMO. “AS/NZS 4777.2 – Inverter Requirements standard”. In: (2020). URL: https://aemo.com.au/en/initiatives/major-programs/nem-distributed-energy-resources-der-program/standards-and-connections/as-nzs-4777-2-inverter-requirements-standard.

[22] Basil H Jasim et al. “A heuristic optimization approach for the scheduling home appliances”. In: *Bulletin of Electrical Engineering and Informatics* 12.3 (2023), pp. 1256–1266. DOI: 10.11591/eei.v12i3.3989.

[23] UK Power Networks. “Quicker and more cost-effective connections of renewable generation to the distribution network using a flexible approach SDRC 9.7”. In: (2014). URL: https://innovation.ukpowernetworks.co.uk/wp-content/uploads/2019/06/SDRC-9.7-Quicker-and-More-Cost-Effective-Connections-of-Renewable-Generation-to-the-Distribution-Network-Using-Flexible-Approach.pdf.

[24] Chunyu Zhang et al. “FLECH: A Danish market solution for DSO congestion management through DER flexibility services”. In: *Journal of Modern Power Systems and Clean Energy* 2.2 (2014), pp. 126–133. DOI: 10.1007/s40565-014-0048-0.

[25] Cédric Clastres et al. “Ancillary services and optimal household energy management with photovoltaic production”. In: *Energy* 35.1 (2010), pp. 55–64. DOI: 10.1016/j.energy.2009.08.025.

[26] Luanna Maria Silva de Siqueira and Wei Peng. “Control strategy to smooth wind power output using battery energy storage system: A review”. In: *Journal of Energy Storage* 35 (2021), p. 102252.

[27] Hoa Minh Nguyen et al. “MPC based centralized voltage and reactive power control for active distribution networks”. In: *IEEE Transactions on Energy Conversion* 36.2 (2021), pp. 1537–1547. DOI: 10.1109/TEC.2021.3054844.

[28] Wei Ma et al. “A centralized voltage regulation method for distribution networks containing high penetrations of photovoltaic power”. In: *International Journal of Electrical Power & Energy Systems* 129 (2021), p. 106852. DOI: 10.1016/j.ijepes.2021.106852.

[29] Haik Silm et al. “Comparison of the time-delay margin of a distributed and centralized observer”. In: *2018 European Control Conference (ECC)*. 2018, pp. 1963–1968. DOI: 10.23919/ECC.2018.8550324.

[30] Xiaohua Ge et al. “Dynamic event-triggered distributed coordination control and its applications: a survey of trends and techniques”. In: *IEEE Transactions on Systems, Man, and Cybernetics: Systems* 50.9 (2020), pp. 3112–3125. DOI: 10.1109/TSMC.2020.3010825.

[31] Adriana C. Luna et al. “Mixed-integer-linear-programming-based energy management system for hybrid PV-wind-battery microgrids: modeling, design, and experimental verification”. In: *IEEE Transactions on Power Electronics* 32.4 (2017), pp. 2769–2783. DOI: 10.1109/TPEL.2016.2581021.

[32] Lukas Engbroks et al. “Applying forward dynamic programming to combined energy and thermal management optimization of hybrid electric vehicles”. In: *IFAC-PapersOnLine* 51.31 (2018), pp. 383–389. DOI: 10.1016/j.ifacol.2018.10.078.

[33] S. Kusagawa et al. “Multipurpose design optimization of EMS-type magnetically levitated vehicle based on genetic algorithm”. In: *IEEE Transactions on Applied Superconductivity* 14.2 (2004), pp. 1922–1925. DOI: 10.1109/TASC.2004.830933.

[34] Pablo Garcıa-Triviño et al. “Long-term optimization based on PSO of a grid-connected renewable energy/battery/hydrogen hybrid system”. In: *International journal of hydrogen energy* 39.21 (2014), pp. 10805–10816. DOI: 10.1016/j.ijhydene.2014.05.064.

[35] Robert Luca et al. “Comparative study of energy management systems for a hybrid fuel cell electric vehicle-A novel mutative fuzzy logic controller to prolong fuel cell lifetime”. In: *International Journal of Hydrogen Energy* 47.57 (2022), pp. 24042–24058. DOI: 10.1016/j.ijhydene.2022.05.192.

[36] Hou Shengren et al. “Performance comparison of deep RL algorithms for energy systems optimal scheduling”. In: *2022 IEEE PES Innovative Smart Grid Technologies Conference Europe (ISGT-Europe)*. 2022, pp. 1–6. DOI: 10.1109/ISGT-Europe54678.2022.9960642.

[37] Mohamad-Amin Nasr, Abbas Rabiee, and Innocent Kamwa. “MPC and robustness optimisation-based EMS for microgrids with high penetration of intermittent renewable energy”. In: *IET Generation, Transmission & Distribution* 14.22 (2020), pp. 5239–5248. DOI: 10.1049/iet-gtd.2020.0460.

[38] Feng Zhang et al. “MPC based control strategy for battery energy storage station in a grid with high photovoltaic power penetration”. In: *International Journal of Electrical Power & Energy Systems* 115 (2020), p. 105448. DOI: 10.1016/j.ijepes.2019.105448.

[39] Cornelius Steinbrink et al. “CPES testing with mosaik: co-simulation planning, execution and analysis”. In: *Applied Sciences* 9.5 (2019). ISSN: 2076-3417. DOI: 10.3390/app9050923. URL: https://www.mdpi.com/2076-3417/9/5/923.

[40] Ahmed Bedawy et al. “Optimal voltage control strategy for voltage regulators in active unbalanced distribution systems using multi-agents”. In: *IEEE Transactions on Power Systems* 35.2 (2020), pp. 1023–1035. DOI: 10.1109/TPWRS.2019.2942583.

[41] Aihui Fu, Miloš Cvetković, and Peter Palensky. “Distributed cooperation for voltage regulation in future distribution networks”. In: *IEEE Transactions on Smart Grid* 13.6 (2022), pp. 4483–4493. DOI: 10.1109/TSG.2022.3191389.

[42] Charis S. Demoulias et al. “Ancillary services offered by distributed renewable energy sources at the distribution grid level: an attempt at proper definition and quantification”. In: *Applied Sciences* 10.20 (2020). ISSN: 2076-3417. DOI: 10.3390/app10207106. URL: https://www.mdpi.com/2076-3417/10/20/7106.

[43] Kyriaki-Nefeli D. Malamaki et al. “Ramp-rate control of DRES employing supercapacitors in distribution systems”. In: *2021 International Conference on Smart Energy Systems and Technologies (SEST)*. 2021, pp. 1–6. DOI: 10.1109/SEST50973.2021.9543116.

[44] M. J. E. Alam, K. M. Muttaqi, and D. Sutanto. “A novel approach for ramp-rate control of solar PV using energy storage to mitigate output fluctuations caused by cloud passing”. In: *IEEE Transactions on Energy Conversion* 29.2 (2014), pp. 507–518. DOI: 10.1109/TEC.2014.2304951.

[45] Miswar A Syed and Muhammad Khalid. “Neural network predictive control for smoothing of solar power fluctuations with battery energy storage”. In: *Journal of Energy Storage* 42 (2021), p. 103014. DOI: 10.1016/j.est.2021.103014.

[46] João Martins et al. “Comparative study of ramp-rate control algorithms for PV with energy storage systems”. In: *Energies* 12.7 (2019). ISSN: 1996-1073. DOI: 10.3390/en12071342. URL: https://www.mdpi.com/1996-1073/12/7/1342.

[47] Hira Tahir et al. “Optimal ESS size calculation for ramp rate control of grid-connected microgrid based on the selection of accurate representative days”. In: *International Journal of Electrical Power & Energy Systems* 139 (2022), p. 108000. ISSN: 0142-0615. DOI: 10.1016/j.ijepes.2022.108000. URL: https://www.sciencedirect.com/science/article/pii/S014206152200045X.

[48] DIgSILENT PowerFactory. “Digsilent powerfactory 2021 user manual”. In: *DIgSILENT GmbH, 2021* (2021).

[49] European Committee for Electrotechnical Standardization (CENELEC). “Requirements for generating plants to be connected in parallel with distribution networks - Part 1: Connection to a LV distribution network - Generating plants up to and including Type B”. In: *EN 50549-1:2019 Standard* (2019).

[50] European Committee for Electrotechnical Standardization (CENELEC). “Requirements for generating plants to be connected in parallel with distribution networks - Part 2: Connection to a MV distribution network - Generating plants up to and including Type B”. In: *EN 50549-2:2019 Standard* (2019).

[51] Haoming Liu et al. “Control strategy of energy storage for smoothing photovoltaic power fluctuations”. In: *IFAC-PapersOnLine* 48.28 (2015), pp. 162–165. DOI: 10.1016/j.ifacol.2015.12.118.

[52] Kyriaki-Nefeli D. Malamaki et al. “D1.3 1st Report on the Reactive Power Control Algorithm for Converter-Interfaced DRES/BESS and Analytical Tool for Parametric BESS Sizing for low-frequency Power Smoothing”. In: *H2020 EASY-RES Project Deliverable* (Jul. 2019). URL: https://ec.europa.eu/research/participants/documents/downloadPublic?documentIds=080166e5c59fdedc&appId=PPGMS.

[53] TF CIGRE. “Benchmark systems for network integration of renewable and distributed energy resources”. In: *Benchmark systems for network integration of renewable and distributed energy resources", technical brochure, version* 21 (2014).

[54] Maman Ahmad Khan and Barry Hayes. *For paper "A Reduced Electrically-Equivalent Model of the IEEE European Low Voltage Test Feeder"*. 2020. DOI: 10.21227/0d2n-j565. URL: https://dx.doi.org/10.21227/0d2n-j565.

[55] Liander Open Dates. URL: https://www.liander.nl/partners/datadiensten/open-data.

[56] British Standard et al. “Voltage characteristics of electricity supplied by public distribution networks”. In: *BS EN* (2007). URL: https://fs.gongkong.com/files/technicalData/201110/20111009223856000001.pdf.

[57] National Renewable Energy Laboratory. *Puerto Rico Electric Power Authority’s minimum technical renewables interconnection requirements*. 2012. URL: https://www.esig.energy/wiki-main-page/puerto-rico-electric-power-authority-s-minimum-technical-renewables-interconnection-requirements/.

[58] Xiaomeng Ai et al. “Multi-time-scale coordinated ramp-rate control for photovoltaic plants and battery energy storage”. In: *IET Renewable Power Generation* 12.12 (2018), pp. 1390–1397. DOI: 10.1049/iet-rpg.2018.5190.

[59] Kyriaki E. Antoniadou-Plytaria et al. “Distributed and decentralized voltage control of smart distribution networks: models, methods, and future research”. In: *IEEE Transactions on Smart Grid* 8.6 (2017), pp. 2999–3008. DOI: 10.1109/TSG.2017.2679238.

[60] Maher Abdelkhalek Azzouz, Mostafa F. Shaaban, and Ehab F. El-Saadany. “Real-time optimal voltage regulation for distribution networks incorporating high penetration of PEVs”. In: *IEEE Transactions on Power Systems* 30.6 (2015), pp. 3234–3245. DOI: 10.1109/TPWRS.2014.2385834.

[61] A Cagnano and E De Tuglie. “Centralized voltage control for distribution networks with embedded PV systems”. In: *Renewable Energy* 76 (2015), pp. 173–185. DOI: 10.1016/j.renene.2014.11.015.

[62] Kalpesh Joshi and Naran Pindoriya. “Advances in distribution system analysis with distributed resources: Survey with a case study”. In: *Sustainable Energy, Grids and Networks* 15 (2018), pp. 86–100. DOI: 10.1016/j.segan.2017.12.004.

[63] Bo Zhao et al. “Network partition-based zonal voltage control for distribution networks with distributed PV systems”. In: *IEEE Transactions on Smart Grid* 9.5 (2018), pp. 4087–4098. DOI: 10.1109/TSG.2017.2648779.

[64] D. Ranamuka, A. P. Agalgaonkar, and K. M. Muttaqi. “Online voltage control in distribution systems with multiple voltage regulating devices”. In: *IEEE Transactions on Sustainable Energy* 5.2 (2014), pp. 617–628. DOI: 10.1109/TSTE.2013.2277719.

[65] Giuseppe Fusco, Mario Russo, and Michele De Santis. “Decentralized voltage control in active distribution systems: features and open issues”. In: *Energies* 14.9 (2021), p. 2563. DOI: 10.3390/en14092563.

[66] Stephen Boyd, Neal Parikh, and Eric Chu. *Distributed optimization and statistical learning via the alternating direction method of multipliers*. Now Publishers Inc, 2011. DOI: 10.1561/2200000016.

[67] Daniel K. Molzahn et al. “A survey of distributed optimization and control algorithms for electric power systems”. In: *IEEE Transactions on Smart Grid* 8.6 (2017), pp. 2941–2962. DOI: 10.1109/TSG.2017.2720471.

[68] Tao Yang et al. “A survey of distributed optimization”. In: *Annual Reviews in Control* 47 (2019), pp. 278–305. DOI: 10.1016/j.arcontrol.2019.05.006.

[69] Petr Šulc, Scott Backhaus, and Michael Chertkov. “Optimal distributed control of reactive power via the alternating direction method of multipliers”. In: *IEEE Transactions on Energy Conversion* 29.4 (2014), pp. 968–977. DOI: 10.1109/TEC.2014.2363196.

[70] Qianzhi Zhang, Kaveh Dehghanpour, and Zhaoyu Wang. “Distributed CVR in unbalanced distribution systems with PV penetration”. In: *IEEE Transactions on Smart Grid* 10.5 (2019), pp. 5308–5319. DOI: 10.1109/TSG.2018.2880419.

[71] Rahul Ranjan Jha et al. “Distributed algorithm for Volt - VAr optimization in unbalanced distribution system”. In: *2020 IEEE Power Energy Society Innovative Smart Grid Technologies Conference (ISGT)*. 2020, pp. 1–5. DOI: 10.1109/ISGT45199.2020.9087698.

[72] Niloy Patari et al. “Distributed voltage control for three-phase unbalanced distribution systems with DERs and practical constraints”. In: *IEEE Transactions on Industry Applications* 57.6 (2021), pp. 6622–6633. DOI: 10.1109/TIA.2021.3114388.

[73] Mehdi Zeraati, Mohamad Esmail Hamedani Golshan, and Josep M. Guerrero. "A consensus-based cooperative control of PEV battery and PV active power curtailment for voltage regulation in distribution networks". In: *IEEE Transactions on Smart Grid* 10.1 (2019), pp. 670–680. DOI: 10.1109/TSG.2017.2749623.

[74] Yifei Guo, Houlei Gao, and Qiuwei Wu. "Distributed cooperative voltage control of wind farms based on consensus protocol". In: *International Journal of Electrical Power & Energy Systems* 104 (2019), pp. 593–602. DOI: 10.1016/j.ijepes.2018.07.030.

[75] Yasin Zabihinia Gerdroodbari, Reza Razzaghi, and Farhad Shahnia. "Decentralized control strategy to improve fairness in active power curtailment of PV inverters in low-voltage distribution networks". In: *IEEE Transactions on Sustainable Energy* 12.4 (2021), pp. 2282–2292. DOI: 10.1109/TSTE.2021.3088873.

[76] Jiayong Li et al. "Distributed online voltage control in active distribution networks considering PV curtailment". In: *IEEE Transactions on Industrial Informatics* 15.10 (2019), pp. 5519–5530. DOI: 10.1109/TII.2019.2903888.

[77] M. E. Baran and F. F. Wu. "Network reconfiguration in distribution systems for loss reduction and load balancing". In: *IEEE Transactions on Power Delivery* 4.2 (1989), pp. 1401–1407. DOI: 10.1109/61.25627.

[78] Fabian Tamp and Phil Ciufo. "A sensitivity analysis toolkit for the simplification of MV distribution network voltage management". In: *IEEE Transactions on Smart Grid* 5.2 (2014), pp. 559–568. DOI: 10.1109/TSG.2014.2300146.

[79] Michael Jack and Kiti Suomalainen. "Potential future changes to residential electricity load profiles – findings from the GridSpy dataset (Project Report)". In: (2018). URL: http://hdl.handle.net/10523/8074.

[80] Arthur R Bergen. *Power systems analysis*. Pearson Education India, 2009.

[81] Eric Woittiez. "Flexibility from residential power consumption: a new market filled with opportunities". In: (2016). URL: https://www.usef.energy/app/uploads/2016/12/EnergieKoplopersEngels_FinalReport_2016_vs4-1.pdf.

[82] Mohamad K Daryabari, Reza Keypour, and Hessam Golmohamadi. "Stochastic energy management of responsive plug-in electric vehicles characterizing parking lot aggregators". In: *Applied Energy* 279 (2020), p. 115751. DOI: 10.1016/j.apenergy.2020.115751.

[83] Vahid Hosseinnezhad et al. "Optimal home energy management for electric flexibility provision". In: *2019 IEEE PES Innovative Smart Grid Technologies Europe (ISGT-Europe)*. 2019, pp. 1–6. DOI: 10.1109/ISGTEurope.2019.8905468.

[84] Tiago Sousa et al. "A flexibility home energy management system to support aggregator requests in smart grids". In: *2018 IEEE Symposium Series on Computational Intelligence (SSCI)*. 2018, pp. 1830–1836. DOI: 10.1109/SSCI.2018.8628918.

[85] Sheraz Aslam, Adia Khalid, and Nadeem Javaid. “Towards efficient energy management in smart grids considering microgrids with day-ahead energy forecasting”. In: *Electric Power Systems Research* 182 (2020), p. 106232. DOI: 10.1016/j.epsr.2020.106232.

[86] Hasan Mehrjerdi and Reza Hemmati. “Energy and uncertainty management through domestic demand response in the residential building”. In: *Energy* 192 (2020), p. 116647. DOI: 10.1016/j.energy.2019.116647.

[87] Abdullah Al Hadi et al. “Algorithm for demand response to maximize the penetration of renewable energy”. In: *IEEE Access* 8 (2020), pp. 55279–55288. DOI: 10.1109/ACCESS.2020.2981877.

[88] Liang Yu et al. “Deep reinforcement learning for smart home energy management”. In: *IEEE Internet of Things Journal* 7.4 (2020), pp. 2751–2762. DOI: 10.1109/JIOT.2019.2957289.

[89] Hou Shengren et al. “Optimal energy system scheduling using a constraint-aware reinforcement learning algorithm”. In: *International Journal of Electrical Power & Energy Systems* 152 (2023), p. 109230. DOI: 10.1016/j.ijepes.2023.109230.

[90] Haris Ishaq, Ibrahim Dincer, and Curran Crawford. “A review on hydrogen production and utilization: Challenges and opportunities”. In: *International Journal of Hydrogen Energy* 47.62 (2022), pp. 26238–26264. DOI: 10.1016/j.ijhydene.2021.11.149.

[91] A Kafetzis et al. “Energy management strategies based on hybrid automata for islanded microgrids with renewable sources, batteries and hydrogen”. In: *Renewable and Sustainable Energy Reviews* 134 (2020), p. 110118. DOI: 10.1016/j.rser.2020.110118.

[92] Abdulrahman M. Abomazid, Nader A. El-Taweel, and Hany E. Z. Farag. “Optimal energy management of hydrogen energy facility using integrated battery energy storage and solar photovoltaic systems”. In: *IEEE Transactions on Sustainable Energy* 13.3 (2022), pp. 1457–1468. DOI: 10.1109/TSTE.2022.3161891.

[93] Nourredine Zidane and Sofia-Lalouni Belaid. “A new fuzzy logic solution for energy management of hybrid photovoltaic/battery/hydrogen system”. In: *REVUE ROUMAINE DES SCIENCES TECHNIQUES—SÉRIE ÉLECTROTECHNIQUE ET ÉNERGÉTIQUE* 67.1 (2022), pp. 21–26.

[94] Mingli Zhang et al. “Optimal design and operation of regional multi-energy systems with high renewable penetration considering reliability constraints”. In: *IEEE Access* 8 (2020), pp. 205307–205315. DOI: 10.1109/ACCESS.2020.3036640.

[95] TU Delft. *24/7 Energy Lab*. URL: https://www.thegreenvillage.org/en/24-7-energy-lab/.

[96] Na Li, Zofia Lukszo, and John Schmitz. “An approach for sizing a PV–battery–electrolyzer–fuel cell energy system: A case study at a field lab”. In: *Renewable and Sustainable Energy Reviews* 181 (2023), p. 113308. ISSN: 1364-0321. DOI: 10.1016/j.rser.2023.113308.

[97] Digvijay Gusain, Milos Cvetković, and Peter Palensky. “Quantification of operational flexibility from a portfolio of flexible energy resources”. In: *International Journal of Electrical Power & Energy Systems* 141 (2022), p. 107466. DOI: 10.1016/j.ijepes.2021.107466.

[98] *Open Power System Data*. URL: https://data.open-power-system-data.org/time_series/2020-10-06 (visited on 02/21/2023).

[99] Aihui Fu et al. “The Illuminator: an open source energy system integration development kit”. In: *2023 IEEE Belgrade PowerTech*. 2023, pp. 01–05. DOI: 10.1109/PowerTech55446.2023.10202816.

[100] Europen Union. *O2050 long-term strategy*. 2020.

[101] Ray Daniel Zimmerman, Carlos Edmundo Murillo-Sánchez, and Robert John Thomas. “MATPOWER: steady-state operations, planning, and analysis tools for power systems research and education”. In: *IEEE Transactions on Power Systems* 26.1 (2011), pp. 12–19. DOI: 10.1109/TPWRS.2010.2051168.

[102] Tom Brown, Jonas Hörsch, and David Schlachtberger. “PyPSA: Python for power system analysis”. In: *arXiv preprint arXiv:1707.09913* (2017).

[103] Leon Thurner et al. “Pandapower—An open-source Python tool for convenient modeling, analysis, and optimization of electric power systems”. In: *IEEE Transactions on Power Systems* 33.6 (2018), pp. 6510–6521. DOI: 10.1109/TPWRS.2018.2829021.

[104] Taco Niet et al. “Developing a community of practice around an open source energy modelling tool”. In: *Energy Strategy Reviews* 35 (2021), p. 100650. DOI: 10.1016/j.esr.2021.100650.

[105] Marco Wirtz, Peter Remmen, and Dirk Müller. “EHDO: A free and open-source webtool for designing and optimizing multi-energy systems based on MILP”. In: *Computer Applications in Engineering Education* 29.5 (2021), pp. 983–993. DOI: 10.1002/cae.22352.

[106] Clemente Capasso Capasso, Dario Assante Assante, and Ottorino Veneri Veneri. “Internet of energy training through remote laboratory demonstrator”. In: *Technologies* 7.3 (2019). DOI: 10.3390/technologies7030047.

[107] Martin Pajpach et al. “Low-cost education kit for teaching basic skills for Industry 4.0 using deep learning in quality control tasks”. In: *Electronics* 11.2 (2022), p. 230. DOI: 10.3390/electronics11020230.

[108] Peter van Duijsen, Johan Woudstra, and Pepijn van Willigenburg. “Educational setup for Power Electronics and IoT”. In: *2018 19th International Conference on Research and Education in Mechatronics (REM)*. 2018, pp. 147–152. DOI: 10.1109/REM.2018.8421802.

[109] Henrik Lund et al. “EnergyPLAN–Advanced analysis of smart energy systems”. In: *Smart Energy* 1 (2021), p. 100007.

[110] Gerwin Hoogsteen, Johann L. Hurink, and Gerard J. M. Smit. "DEMKit: a decentralized energy management simulation and demonstration toolkit". In: *2019 IEEE PES Innovative Smart Grid Technologies Europe (ISGT-Europe)*. 2019, pp. 1–5. DOI: 10.1109/ISGTEurope.2019.8905439.

[111] JK Kok. "The powermatcher: Smart coordination for the smart electricity grid". In: (2013).

[112] Vahid Salehi et al. "Laboratory-based smart power system, Part I: design and system development". In: *IEEE Transactions on Smart Grid* 3.3 (2012), pp. 1394–1404. DOI: 10.1109/TSG.2012.2194518.

[113] José María Maza-Ortega et al. "A multi-platform lab for teaching and research in active distribution networks". In: *IEEE Transactions on Power Systems* 32.6 (2017), pp. 4861–4870. DOI: 10.1109/TPWRS.2017.2681182.

[114] PowSyBI. "Power System Blocks". In: (2020). URL: https://www.lfenergy.org/projects/powsybl/.

[115] LF Energy. "Linux Foundation Energy open source initiatives". In: (2019). URL: https://www.lfenergy.org.

[116] Illuminator-TUDelft-IEPG. 2024. URL: https://github.com/Illuminator-TUDelft-IEPG/Illminator-Local/.

[117] Steffen Schütte, Stefan Scherfke, and Martin Tröschel. "Mosaik: A framework for modular simulation of active components in Smart Grids". In: *2011 IEEE First International Workshop on Smart Grid Modeling and Simulation (SGMS)*. 2011, pp. 55–60. DOI: 10.1109/SGMS.2011.6089027.

[118] WANDB platform. URL: https://wandb.ai/home.

[119] Julie Thérèse Pasquier et al. "EURO1k: A high-resolution European weather model developed by Meteomatics". In: *EGU General Assembly Conference Abstracts*. 2023, EGU–16670.

[120] C Carrillo et al. "Review of power curve modelling for wind turbines". In: *Renewable and Sustainable Energy Reviews* 21 (2013), pp. 572–581. DOI: 10.1016/j.rser.2013.01.012.

[121] L. Thurner et al. "Pandapower — an open-source Python tool for convenient modeling, analysis, and optimization of electric power systems". In: *IEEE Transactions on Power Systems* 33.6 (Nov. 2018), pp. 6510–6521. ISSN: 0885-8950. DOI: 10.1109/TPWRS.2018.2829021.

[122] Illuminator-TUDelft-IEPG. 2024. URL: https://github.com/Illuminator-team/Illuminator/blob/main/Scenarios.

List of Publications

First Author Publications

- **A. Fu**, M. Cvetković and P. Palensky, *Distributed Cooperation for Voltage Regulation in Future Distribution Networks* IEEE Transactions on Smart Grid, vol. 13, no. 6, pp. 4483-4493, Nov. 2022, doi: 10.1109/TSG.2022.3191389.

- **A. Fu**, R. Saini, R. Koornneef, A. van der Meer, P. Palensky and M. Cvetković, *The Illuminator: An Open Source Energy System Integration Development Kit*, 2023 IEEE Belgrade PowerTech, Belgrade, Serbia, 2023, pp. 01-05, doi: 10.1109/PowerTech 55446.2023.10202816.

- **A. Fu**, A. Lekić, E.O. Kontis, K. -N. D. Malamaki, G. C. Kryonidis, J. M. Mauricio, C. S. Demoulias and M. Cvetković, *Impact of Virtual Synchronous Generators on Power System Frequency Dynamics*, 2023 International Conference on Smart Energy Systems and Technologies (SEST), Mugla, Turkiye, 2023, pp. 1-6, doi: 10.1109/SEST 57387.2023.10257357.

- **A. Fu**, A. Lekić, K. -N. D. Malamaki, G. C. Kryonidis, J. M. Mauricio, C. S. Demoulias, P. Palensky and M. Cvetković, *A stochastic simulation-based approach for sizing DRES penetration level and BESS capacity in distribution grids*, International Journal of Electrical Power & Energy Systems, Submitted.

- **A. Fu**, A. Lekić, E.O. Kontis, K. -N. D. Malamaki, G. C. Kryonidis, J. M. Mauricio, C. S. Demoulias and M. Cvetković, *Performance Assessment of Virtual Synchronous Generators on Power System Frequency Dynamics*, Sustainable Energy, Grids and Networks, Submitted.

- **A. Fu** and M. Cvetković, *A Multi-Stage Energy Management Approach Incorporating Seasonal Hydrogen Storage in a PV-Battery-Electrolyzer-Fuel Cell System*, ISGT 2024, Submitted.

- **A. Fu**, J. Bosrup, S. Renzaglia, M. Cvetković, M. Kreijns and M. Zeman *Design and Implementation a Local Energy Hub for Urban Environment*, 52nd IEEE Photovoltaic Specialists Conference, Accepted.

- **A. Fu**, J. Bosrup, S. Renzaglia, M. Cvetković, M. Kreijns and M. Zeman *Local Energy Hub for Urban Environment: Role of Energy Management System*, 41st European Photovoltaic Solar Energy Conference and Exhibition, Accepted.

OTHER PUBLICATIONS

- J. Wu and S. Li, **A. Fu**, M. Cvetković, P. Palensky, J. C. Vasquez and J. M. Guerrero, *Hierarchical online energy management for residential microgrids with Hybrid hydrogen–electricity Storage System*, Applied Energy, vol. 363, no. 6, pp. 123020, Jun. 2024, doi:10.1016/j.apenergy.2024.123020.

- K. -N. D. Malamaki, **A. Fu**, J. M. Mauricio, M. Cvetković and C. S. Demoulias, *Evaluation of Ramp-Rate Limitation at Distribution Transformer Level via Central and Distributed Storage Systems*, 2023 IEEE Belgrade PowerTech, Belgrade, Serbia, 2023, pp. 1-6, doi: 10.1109/PowerTech55446.2023.10202995.

- F. Zhang, **A. Fu**, L. Ding, and Q. Wu*MPC based control strategy for battery energy storage station in a grid with high photovoltaic power penetration.*, International journal of electrical power & energy systems 115 (2020): 105448.

- S. Janssen, **A. Fu**, M. Cvetković and P. Palensky, *Relocatable Energy Storage Systems for Congestion Management*, 2020 IEEE PES Innovative Smart Grid Technologies Europe (ISGT-Europe), The Hague, Netherlands, 2020, pp. 1166-1170, doi: 10.1109/ISGT-Europe47291.2020.9248849.

- F. Zhang, **A. Fu**, L. Ding, Q. Wu, B. Zhao, and P. Zi. *Optimal sizing of ESS for reducing AGC payment in a power system with high PV penetration*, International journal of electrical power & energy systems 110 (2019): 809-818.

- J. Alpízar-Castillo, **A. Fu** L. Ramírez-Elizondo, M. Cvetković and P. Bauer. *Multi-Carrier Home Energy Management System Using Genetic Algorithms and Random Forest Regression Predictions*, IEEE Energy Conversion Conference and Expo 2024, Submitted.

List of Projects Involved

Current Projects

- **SHPLES: Smart Hydrogen Powered Local Energy System**
  The aim of the 'SHPLES project' is to develop a local and CO2-free energy system based on renewable energy sources that autonomously and real-time optimizes its performance and offers the desired control options to operators of the system. The intended deliverables are an improved configuration of a local energy system using hydrogen and an Open-source energy management system.

- **Synergys(II): Smart Multi-Commodity Energy Systems**
  The aim of the SynergyS project is to develop and test a smart control system for multi-commodity energy systems (MCES). The intended deliverables are a digital twin of MCES and specification and implementation of the IT system in a residential experiments environment.

Finished Projects

- **The Illuminator: An Open Source Energy System Integration Development Kit**
  The Illuminator is a development kit demonstrating the energy transition challenges and the benefits of intelligent multi-energy systems. It aims at helping students, policymakers and energy stakeholders to understand the complexity of the energy transition better. The developed kit is published on Github: https://github.com/Illuminator-team/Illuminator.

- **EASY-RES: Enable Ancillary Services by Renewable Energy Sources**
  The key objective of this project is to increase the robustness of the power system towards abrupt frequency changes by introducing virtual inertia and damping in DRES. I participate in deliverables D6.5 Report on the evaluation of project KPIs and D1.8 Voltage regulation algorithms within the LV G and MV ICA.

- **Solution for Amsterdam Buiksloterham-Zuid Distribution Network Congestion Issue**
  Amsterdam Buiksloterham-Zuid/Overhoeks area power grid faces congestion challenges as the demand for electricity continuously rises. Using the electricity grid of one of Amsterdam's fast-growing areas as a case study, the main objective is to find promising solutions to optimize the existing grid capacity. The entire research outcome of this study can be found https://doi.org/10.13140/RG.2.2.11476.68481.

ACKNOWLEDGEMENTS

Embarking on my PhD journey has been both an academic adventure and a profound personal transformation. Reflecting on this period, I am deeply grateful for the encouragement, support, and advice from an incredible group of people who have significantly shaped my path.

Family: The role of my family is immeasurable. My parents Bingxin Fu and Qiulian Li, my first teachers, have been steadfast in their support, making financial and emotional sacrifices to help me pursue my dreams. Their teachings have shaped my character, instilling determination and love. My sister Aihua Fu, more than just a sibling, has been a confidant and friend, offering kindness and comfort during challenging times. My life partner, Yuexiang Chen, has been my constant support. Along the way, he has walked side by side with me through every high mountain and every low valley, providing me with solace, cheering for my every victory, and giving me a shoulder to lean on in tough times. And in this academic pursuit, my daughter Fuqi Chen brought a new purpose and brightness. Her every smile and moment of laughter reminds me of the joys of life and motherhood. My little son Robert Chen, although he was born a few months ago, brings a lot of happiness to my family and me. Mother-in-law Qiumei Tian I also want to thank her; she helped me care for my son and gave me time to finalize my thesis in the last month of my PhD journey. All in all give a lot of my thanks to the support of my family.

Academic Guidance: Dr. Milos Cvetkovic's guidance has been a cornerstone of my PhD experience. His meticulous attention to detail, deep insights, and unwavering patience have immensely contributed to my academic development. Dr. Milos Cvetkovic has nurtured my academic thinking, fostered my experience with diverse collaborative partners, and guided me in proposal applications. His support has been pivotal in my academic growth and in providing opportunities for me to challenge myself. I am deeply grateful for all his support. Prof. Peter Palensky played a crucial role in the early stages of my PhD, guiding me through a myriad of ideas. He granted me the freedom to explore self-organizing power systems and was always available for support when needed. His invaluable advice has been instrumental in charting my academic path. Both mentors have offered kindness and support throughout my journey, for which I am deeply thankful.

Collaborative Research: I am deeply grateful to my co-authors, including Aleksandra Lekic, Kyriaki-Nefeli D. Malamaki, Georgios C. Kryonidis, Juan M. Mauricio, Charis S. Demoulias, Eleftherios O. Kontis, Raghav Saini, Remko Koornneef, Arjen van der Meer, Simona Renzaglia, Jingxuan Wu, Joel Bosrup, Marjan Kreijns, Miro Zeman and Suzanne Janssen. Each has enriched my work with their unique perspectives. A special acknowledgment to Aleksandra for her constant support and guidance. I also extend my gratitude to Dr. Simon Tindemans, Dr. Pedro P. Vergara, Dr. Alex Stefanov, and Prof. Marjan Popov for their invaluable advice and encouragement. My heartfelt thanks to all col-

leagues in the IEPG group, including Chenguang Wang, Le Liu, Haiwei Xie, Yigu Liu, Shengren Hou, Na Li, Kaikai Pan, Siyuan Liu, Lian Liu, Aleksandar Boricic, Ensieh Sharifnia, Nanda Kishor Panda, Neda Vahabzad, Shuyi Gao, and others. Our times together have been both refreshing and enlightening. The collaborations and shared knowledge in projects like Horizon EU 2020 EASY-RES, AMS congestion, Synergys, and SHPLES have been crucial to my research. I am particularly thankful to Marjan Kreijns, Arnoud van der Zee, Joel Bosru, Roby van Praag, Lidewij van Trigt, and Joep van der Weijden from The Green Village, as well as Ewoud Vos and Aly Brandenburg from Hanze Hogeschool Groningen, for their collaborative efforts and insights.

Friends: My time in the Netherlands has been greatly enriched by the deep connections and memorable moments shared with friends. Bowen Li& Yang Jin, Monica Zhang& Runzhang Hong, Ting Hu& Chenguang Wang, Xuan Chen& Zhengwei Wu, Qing Yong& Erqian Tang, and Xin Wang& Lei Zheng, and Ruochen Guo & Zhen Wang, your presence has been a constant source of joy and support. Our weekends together have been full of wonderful moments, and during challenging times, you have always been there. I am immensely grateful for your companionship and support throughout this journey.

In conclusion, I am filled with gratitude. Everyone mentioned, and those not listed, has played a significant role in this journey. I hope our paths cross again, creating more cherished memories. Here is to a future brimming with promise, achievements, and joy!